

METASTATIC BEHAVIOUR OF DOXORUBICIN RESISTANT MCF-7 BREAST CANCER
CELLS AFTER VIMENTIN SILENCING

A THESIS SUBMITTED TO
THE GRADUATE SCHOOL OF NATURAL AND APPLIED SCIENCES
OF
MIDDLE EAST TECHNICAL UNIVERSITY

BY

OKAN TEZCAN

IN PARTIAL FULFILLMENT OF THE REQUIREMENTS
FOR
THE DEGREE OF MASTER OF SCIENCE
IN
BIOLOGY

JANUARY 2013

Approval of the thesis:

**METASTATIC BEHAVIOUR OF DOXORUBICIN RESISTANT MCF-7 BREAST
CANCER CELLS AFTER VIMENTIN SILENCING**

submitted by **OKAN TEZCAN** in partial fulfillment of the requirements for the degree of **Master
of Science in Biology Department, Middle East Technical University** by,

Prof. Dr. Canan Özgen
Dean, Graduate School of **Natural and Applied Sciences**

Prof. Dr. Gülay Özcengiz
Head of Department, **Biological Sciences**

Prof. Dr. Ufuk Gündüz
Supervisor, **Biological Sciences Dept., METU**

Examining Committee Members:

Assoc. Prof. Dr. Mayda Gürsel
Biological Sciences Dept., METU

Prof. Dr. Ufuk Gündüz
Biological Sciences Dept., METU

Assoc. Prof. Dr. Çağdaş Son
Biological Sciences Dept., METU

Dr. Özlem Darcansoy İşeri
Transplantation and Gene Sciences Inst.,
Başkent University

Dr. Pelin Mutlu
Central Lab., METU

Date: 30.01.2013

I hereby declare that all information in this document has been obtained and presented in accordance with academic rules and ethical conduct. I also declare that, as required by these rules and conduct, I have fully cited and referenced all material and results that are not original to this work.

Name, Last Name : OKAN TEZCAN
Signature :

ABSTRACT

METASTATIC BEHAVIOUR OF DOXORUBICIN RESISTANT MCF-7 BREAST CANCER CELLS AFTER VIMENTIN SILENCING

TEZCAN, Okan
M.Sc., Department of Biology
Supervisor: Prof. Dr. Ufuk Gündüz

January 2013, 78 pages

Chemotherapy is one of the common treatments in cancer therapy. The effectiveness of chemotherapy is limited by several factors one of which is the emergence of multidrug resistance (MDR). MDR is caused by the activity of diverse ATP binding cassette (ABC) transporters that pump drugs out of the cells. There are several drugs which have been used in treatment of cancer. One of them is doxorubicin that intercalates and inhibits DNA replication. However, doxorubicin has been found to cause development of MDR in tumors. It has been reported that there is a correlation between multidrug resistance and invasiveness of cancer cells. Vimentin is a type III intermediate filament protein that is expressed frequently in epithelial carcinomas correlating with invasiveness and also poor prognosis of cancer. There are several studies that have shown the connection between expression level of vimentin and invasiveness. In this study, MCF-7 cell line (MCF-7/S), which is a model cell line for human mammary carcinoma, and doxorubicin resistant MCF-7 cell line (MCF-7/Dox) were used. The resistant cell line was previously obtained by stepwise selection in our laboratory. The main purpose of this study was to investigate changes of metastatic behaviour in MCF-7/Dox cell line, after transient silencing of vimentin gene by siRNA. In conclusion, down-regulation of vimentin gene expression in MCF-7/Dox cell lines was expected to change the characteristics in migration and invasiveness shown by migration and invasion assays.

Key words: Cancer, Breast cancer, MCF-7, Doxorubicin, Vimentin, Metastasis, Gene silencing, MDR

ÖZ

DOKSORUBİSİN DİRENÇLİ MCF-7 MEME KANSERİ HÜCRE HATLARINDA VİMENTİN SUSTURULMASININ METASTATİK ÖZELLİKLERE ETKİSİ

TEZCAN, Okan
Yüksek Lisans, Biyoloji Bölümü
Tez Yöneticisi: Prof. Dr. Ufuk Gündüz

Ocak 2013, 78 sayfa

Kemoterapi kanser tedavisinde yaygın olarak kullanılan terapi yöntemlerinden biridir. Kemoterapinin etkinliği çoklu ilaç dirençliliği gibi bazı faktörler tarafından sınırlanmaktadır. Çoklu ilaç dirençliliği, çeşitli ATP bağlanma kaseti taşıyıcı proteinlerinin ilaçları hücre dışına atmaları ile ortaya çıkar. Kanser tedavisinde birçok ilaç kullanılmaktadır. Bu ilaçlardan biri de doksorubisindir ve bu ilaç DNA molekülüne eklenerek onu eşlenmesini inhibe eder. Ancak doksorubisinin tümörlerde çoklu ilaç dirençliliğine sebep olduğu saptanmıştır. Çoklu ilaç dirençliliği ile kanser hücrelerinin yayılma yeteneği arasında bir bağlantı olduğu bildirilmiştir. Vimentin, tip III ara filaman proteinlerinden biridir ve epitel karsinomalarında sıklıkla sentezlenmekte olup hücre yayılması ile ilişkilendirilmektedir. Ayrıca kanser prognozu ile de ilişkisi olduğu bilinmektedir. Vimentin geninin ifade düzeyi ile hücre yayılması arasındaki bağlantı birçok çalışmada gösterilmiştir. Bu çalışmada insan meme karsinoması için bir çeşit model hücre hattı olan MCF-7(MCF-7/S) ve doksorubisine dirençli MCF-7 (MCF-7/Dox) hücre hatları kullanılmıştır. Doksorubisine dirençli MCF-7 hücre hattı laboratuvarımızda daha önce adım adım yapılan seçimler sonucu elde edilmiştir. Bu çalışmanın ana amacı; MCF-7/Dox hücre hattında, vimentin geninin siRNA kullanılarak geçici olarak susturulması sonucu metastatik değişikliklerin gözlenmesidir. Sonuç olarak; vimentin geni ifadesinin, doksorubisine dirençli MCF-7 hücre hattında azaltılması, hücre göçücülüğü ve yayılmacılığı üzerinde değişiklik yapması beklenmektedir.

Anahtar Kelimeler: Kanser, Meme kanseri, MCF-7, Doksorubisin, Vimentin, Metastas, Gen susturulması, Çoklu ilaç dirençliliği

To my Love,

ACKNOWLEDGEMENTS

I would like to express my deepest gratitude to my supervisor Prof. Dr. Ufuk Gündüz for her valuable support, guidance, encouragement and supervision during this thesis study.

I feel great appreciation to Dr. Özlem Darcansoy İşeri and Dr. Pelin Mutlu for their helpful advices, support and encouragement.

The examining committee members are greatly acknowledged for their participation, comments and suggestions.

I would compassionately express my deepest thanks to Murat Erdem, Aktan Alpsoy, Çağrı Urfalı, Neşe Çakmak, Tuğba Keskin, Zelha Nil, Tuğba Keskin, Yaprak Dönmez, Burcu Özsoy, Gülşah Pekgöz, and to other Lab 206 members for their precious help and lovely attitude both in the course of experimental period and in the course of writing this thesis.

I would like to extend my thanks to my close friends İlke Şen, Dr. Özlem Bozkurt, and Serkan Tuna for their friendship, care and endless support. With them, everything became tolerable.

I would also thank to Özlem Mavi, for her motherly attitude and sincere friendship.

I would also thank to Aysel Pekel for her kindly supports to my studies.

I am deeply thankful to my friends Aslı Sade Memişoğlu, Seda Tuncay and Dr. Tufan Öz for their encouragement, support and suggestions throughout this study, which are very precious to me.

I would like to send my ultimate appreciation to my mother Saliha Tezcan, my father Bahri Tezcan, and my brother Gökhan Tezcan.

My deepest thanks are extended to Ebru Aras, who made life worth and easier with her endless trust, encouragement, understanding, moral support, care, patience and love at every stage of this thesis.

TABLE OF CONTENTS

ABSTRACT	v
ÖZ	vi
ACKNOWLEDGEMENTS	viii
TABLE OF CONTENTS	ix
LIST OF TABLES	xi
LIST OF FIGURES	xii
LIST OF ABBREVIATIONS	xii
CHAPTERS	
1. INTRODUCTION.....	1
1.1. Cancer Biology	1
1.2. Breast Cancer	1
1.3. Treatment of Breast Cancer	2
1.3.1. Surgery.....	2
1.3.2. Hormonal Therapy.....	2
1.3.3. Targeted Therapy.....	3
1.3.4. Radiation Therapy	3
1.3.5. Chemothreapy.....	4
1.3.5.1. Doxorubicin (Adriamycin®).....	5
1.4. Multidrug Resistance (MDR).....	8
1.5. Metastasis and Invasiveness.....	9
1.6. Vimentin	10
1.6.1. Vimentin in Breast Cancer.....	11
1.6.1.1. RNA Interference Strategy	12
1.7. Aim of the Study	15
2. MATERIALS AND METHODS	17
2.1 Materials	17
2.1.1 Cell Lines.....	17
2.1.2 Chemicals and Reagents	17
2.1.3 siRNA	18
2.1.4 Primers.....	18
2.2 Methods	19
2.2.1 Cell Culture.....	19
2.2.1.1 Cell Line and Culture Conditions	19
2.2.1.2 Subculturing (Cell Passaging)	19
2.2.1.3 Cell Freezing	19
2.2.1.4 Thawing Frozen Cells	19
2.2.1.5 Viable Cell Counting by Trypan Blue Exclusion Method.....	20
2.2.2 siRNA and Transfection	20
2.2.2.1 FlexiTube <i>VIM</i> siRNA and <i>Mock</i> siRNA.....	20
2.2.2.2 Transfection.....	20
2.2.3 Reverse Transcription-Quantitative Polymerase Chain Reaction (RT-qPCR)	21

2.2.3.1 Isolation of Total RNA.....	21
2.2.3.2 Quantifying RNA by Spectral Absorption	21
2.2.3.3 Agarose Gel Electrophoresis for Monitoring RNA Samples	22
2.2.3.4 cDNA Synthesis	22
2.2.3.5 Quantitative Real-Time Polymerase Chain Reaction (RT-qPCR)	22
2.2.3.6 Quantitation of RT-qPCR Products.....	23
2.2.3.7 Statistical Analysis	23
2.2.4 Determination of siRNA Efficiency	24
2.2.4.1 Flow Cytometry Analysis.....	24
2.2.4.2 Fluorescence Microscopy after Control siRNA Treatment	25
2.2.4.3 Statistical Analysis	25
2.2.5 VIM Expression Analyses by Immunocytochemistry	25
2.2.6 VIM Protein Expression Analyses.....	26
2.2.6.2 Protein isolation and quantification.....	26
2.2.6.3 Vimentin Western blot analyses	26
2.2.6.4 Statistical Analyses	26
2.2.7 Cell Migration and Invasion Assays and Image Analysis	27
2.2.7.1 Boyden Chamber Cell Migration Assay.....	27
2.2.7.2 Boyden Chamber Cell Invasion Assay with Matrigel	27
2.2.7.3 Statistical Analysis	28
3. RESULTS AND DISCUSSION	29
3.1 Total RNA Isolation.....	29
3.2 Determination of Transfection Efficiency	30
3.3 Quantitative Real-Time Polymerase Chain Reaction (qPCR): Expression analysis of <i>VIM</i> and β - <i>actin</i> genes	35
3.3 Immunocytochemistry Analyses: Determination of VIM expression level in MCF-7/S and MCF-7/Dox cell lines	42
3.4 Western Blot Analyses: Detection of decline of vimentin after transient transfection with <i>VIM</i> siRNA	43
3.5 Boyden Chamber and Matrigel Assays: Visualization of changes in metastatic and invasive characteristics	44
4. CONCLUSION	53
REFERENCES.....	55
APPENDICES	
A. CELL CULTURE MEDIUM	65
B. BUFFERS AND SOLUTIONS	67
C. TRESHOLD CYCLE VALUES.....	69
D. MIGRATED AND INVADDED CELL NUMBERS	71
E. FLOW CYTOMETRY HISTOGRAM GRAPHS	71

LIST OF TABLES

TABLES

Table 2.1 Primers used in quantitative real-time polymerase chain reaction (qPCR) and the amplicon sizes.	18
Table 2.2 The sequences of <i>VIM</i> siRNA.	20
Table 2.3 Amplification Conditions for <i>VIM</i> and β -actin Genes.	23
Table 2.4 Transfection Solutions	24
Table A. 1 RPMI 1640 Medium formulation (in mg/L) (Thermo Scientific HyCLone).	65
Table C. 1 Threshold cycle values (C_T) of qPCR	69
Table D. 1 Number of migrated and invaded cell.	71

LIST OF FIGURES

FIGURES

Figure 1.1 The HER2/neu Tyrosine Kinase Receptor (Ross et al, 2004).	3
Figure 1.2 Doxorubicin is an anthracycline antibiotic (Pajeva et al, 2004).	5
Figure 1.3 Doxorubicin pathways in cancer cell lines, showing the cell death mechanism. (Thorn et al, 2011).	6
Figure 1.4 Doxorubicin pathways in cancer cell lines, showing the cardiotoxicity mechanism. (Thorn et al, 2011).	7
Figure 1.5 Cellular factors that induce drug resistance (Gottesman et al, 2002).	9
Figure 1.6 Vimentin's role in cancer and some related pathways (Satelli & Li, 2011).	12
Figure 1.7 Schematic overview of short interfering RNA (siRNA) molecule (Lage, 2005).	13
Figure 1.8 Mechanism of RNA interference (Dillin, 2003).	14
Figure 2.1 The Boyden Chamber assay is shown as two compartments separated with a porous membrane in which cells can pass through. The lower compartment has the medium containing serum or several chemoattractant solutions like fibronectin. Therefore, cells can be forced to pass through to lower compartment. These migratory cells get stuck in porous membrane of Transwell and then is counted to determination of migration ability (Toetsch et al, 2009).	28
Figure 3.1 Lane 1 and Lane 8. RNA ladder/Lanes 2 to 6. Total RNAs isolated from untreated MCF-7/Dox, mock siRNA treated MCF-7/Dox, <i>VIM</i> siRNA treated MCF-7/Dox and untreated MCF-7/S cell lines respectively on 1.2 % agarose gel.	29
Figure 3.2 MCF-7/Dox cells transfected with fluorescein conjugated SignalSline [®] control siRNA oligo (5nM). The image was taken by Nikon Eclipse 80i fluorescence microscope and with FITC channel (10X).	30
Figure 3.3 A. Side scatter area versus forward scatter graph for cell control (untreated MCF-7/Dox cell line) and gated area was shown on it. B. FITC height versus side scatter area graph showing the gated plots and these plots indicated the fluorescence signal of untreated MCF-7/Dox cell line.	31
Figure 3.4 A. Side scatter area versus forward scatter graph for the concentration of 1nM fluorescein conjugated control siRNA treated MCF-7/Dox cells and gated area was shown on it. B. FITC height versus side scatter area graph showing the gated plots and these plots indicated the fluorescence signal the concentration of 1nM fluorescein conjugated control siRNA treated MCF-7/Dox cell line.	32
Figure 3.5 A. Side scatter area versus forward scatter graph for the concentration of 3nM fluorescein conjugated control siRNA treated MCF-7/Dox cells and gated area was shown on it. B. FITC height versus side scatter area graph showing the gated plots and these plots indicated the fluorescence signal the concentration of 3nM fluorescein conjugated control siRNA treated MCF-7/Dox cell line.	32
Figure 3.6 A. Side scatter area versus forward scatter graph for the concentration of 5nM fluorescein conjugated control siRNA treated MCF-7/Dox cells and gated area was shown on it. B.	

FITC height versus side scatter area graph showing the gated plots and these plots indicated the fluorescence signal the concentration of 5nM fluorescein conjugated control siRNA treated MCF-7/Dox cell line.33

Figure 3.7 A. Side scatter area versus forward scatter graph for the concentration of 8nM fluorescein conjugated control siRNA treated MCF-7/Dox cells and gated area was shown on it. B. FITC height versus side scatter area graph showing the gated plots and these plots indicated the fluorescence signal of 8nM fluorescein conjugated control siRNA treated MCF-7/Dox cell line. .33

Figure 3.8 A. Side scatter area versus forward scatter graph for the concentration of 10nM fluorescein conjugated control siRNA treated MCF-7/Dox cells and gated area was shown on it. B. FITC height versus side scatter area graph showing the gated plots and these plots indicated the fluorescence signal of 10nM fluorescein conjugated control siRNA treated MCF-7/Dox cell line.34

Figure 3.9 Fluorescence intensity bar graph of fluorescein conjugated control siRNA oligo per pixel for different concentrations. *** $p < 0.0001$ compared to control untreated MCF-7/Dox cells.34

Figure 3.10 A. qPCR Amplification Plots for *VIM* gene. B. qPCR Melting-curve Analysis for *VIM* gene. C. Quantification information for *VIM* gene according to the standart curve.36

Figure 3.11 A. qPCR Amplification Plots for β -actin gene. B. qPCR Melting-curve Analysis for β -actin gene. C. Quantification information for β -actin gene according to the standart curve.37

Figure 3.12 *VIM* gene expression levels in untreated MCF-7/Dox and MCF-7/S cell lines. *** $p < 0.05$ compared to control untreated MCF-7/Dox cells.38

Figure 3.13 A. qPCR Amplification Plots for *VIM* gene after transfection with *VIM* siRNA and mock siRNA in MCF-7/Dox cell line. B. qPCR Melting-curve Analysis for *VIM* gene after transfection with *VIM* siRNA and mock siRNA in MCF-7/Dox cell line. C. Quantification information for *VIM* gene after transfection with *VIM* siRNA and mock siRNA in MCF-7/Dox cell line,according to the standart curve.39

Figure 3.14 A. qPCR Amplification Plots for β -actin gene after transfection with *VIM* siRNA and mock siRNA in MCF-7/Dox cell line. B. qPCR Melting-curve Analysis for β -actin gene after transfection with *VIM* siRNA and mock siRNA in MCF-7/Dox cell line. C. Quantification information for β -actin gene after transfection with *VIM* siRNA and mock siRNA in MCF-7/Dox cell line,according to the standart curve.40

Figure 3.15 *VIM* gene expression after treatment with *VIM* siRNA and mock siRNA oligos for 48 and 72 hours in MCF-7/Dox cell line. ** $p < 0.05$ compared to 48 and 72 hours mock siRNA treatment controls.41

Figure 3.16 A. MCF-7/S cells which does not contain vimentin protein. B. MCF-7/Dox cells which contains vimentin protein. The indication was done to show the vimentin content of these cells.42

Figure 3.17 Western Blot analyses for Vimentin Protein (57 kDa) expression. Lane A. Protein levels of vimentin in *VIM* siRNA transfected MCF-7/Dox cell line Lane B. Protein levels of vimentin in mock siRNA transfected MCF-7/Dox cell line (control line).43

Figure 3.18 Boyden Chamber Assay for untreated MCF-7/S cell line. In A., B., C., D and E. MCF-7/S cells were subjected to boyden chamber assay for 6, 12, 24,48 and 72 hours respectively. For detecting the migrated cells, giemsa stain was used.45

Figure 3.19 Boyden Chamber Assay for untreated MCF-7/Dox cell line. In A., B., C., D and E. MCF-7/Dox cells were subjected to boyden chamber assay for 6, 12, 24,48 and 72 hours respectively. For detection of the migrated cells, giemsa stain was used.....46

Figure 3.20 Boyden Chamber and Matrigel Assays for untreated MCF-7/Dox and untreated MCF-7/S cell lines. A. MCF-7/Dox cells were subjected to boyden chamber assay for 24 hours and migrated cells are shown. B. MCF-7/S cells were subjected to boyden chamber assay for 24 hours and migrated cells are shown. C. MCF-7/Dox cells were subjected to matrigel assay for 24 hours and invaded cells are shown. D. MCF-7/S cells were subjected to matrigel assay for 24 hours and invaded cells are shown. For detection of the migrated and invaded cells, giemsa stain was used. 47

Figure 3.21 A. Migrated cell number comparison between MCF-7/S and MCF-7/Dox cell lines after Boyden Chamber Assay. B. Invaded cell number comparison between MCF-7/S and MCF-7/Dox cell lines after Matrigel Assay. $**p < 0.05$ compared to migrated MCF-7/S cell number and $***p < 0.05$ compared to invaded MCF-7/S cell number.48

Figure 3.22 Vimentin has an important role in *Slug* and *Ras* induced migration and upregulation of *Axl* (Vuoriluoto et al, 2011).49

Figure 3.24 Boyden Chamber and Matrigel Assays for *VIM* and mock siRNA transfected MCF-7/Dox cell lines. A. mock siRNA transfected MCF-7/Dox cells were subjected to boyden chamber assay for 24 hours and migrated cells are shown. B. *VIM* siRNA transfected MCF-7/Dox were subjected to boyden chamber assay for 24 hours and migrated cells are shown. C. mock siRNA transected MCF-7/Dox cells were subjected to matrigel assay for 24 hours and invaded cells are shown. D. *VIM* siRNA transfected MCF-7/Dox cells were subjected to matrigel assay for 24 hours and invaded cells are shown. For detection of the migrated and invaded cells, giemsa stain was used.51

Figure 3.25 A. Migrated cell number of *VIM* siRNA transfected MCF-7/Dox cell line comparing to mock siRNA MCF-7/Dox cell line (control line) after Boyden Chamber Assay. B. Invaded cell number of *VIM* siRNA transfected MCF-7/Dox cell line comparing to mock siRNA MCF-7/Dox cell line (control line) after Matrigel Assay. $**p < 0.05$ compared to migrated MCF-7/S cell number and $***p < 0.05$ compared to invaded MCF-7/S cell number.....52

Figure E. 1 Flow cytometry analysis according to the gated area showing untransfected cell control results.73

Figure E. 2 Flow cytometry analysis according to the gated area showing 1 nM fluorescein conjugated control siRNA transfected cell control results.73

Figure E. 3 Flow cytometry analysis according to the gated area showing 3 nM fluorescein conjugated control siRNA transfected cell control results.74

Figure E. 4 Flow cytometry analysis according to the gated area showing 5 nM fluorescein conjugated control siRNA transfected cell control results.74

Figure E. 5 Flow cytometry analysis according to the gated area showing 8 nM fluorescein conjugated control siRNA transfected cell control results.75

Figure E. 6 Flow cytometry analysis according to the gated area showing 10 nM fluorescein conjugated control siRNA transfected cell control results.75

Figure E. 7 Flow cytometry analysis according to the gated area showing the FITC-H versus Cell Count histogram graph for untransfected cell control.76

Figure E. 8 Flow cytometry analysis according to the gated area showing the FITC-H versus Cell Count histogram graph for 1 nM fluorescein conjugated control siRNA transfected cell results. ..76

Figure E. 9 Flow cytometry analysis according to the gated area showing the FITC-H versus Cell Count histogram graph for 3 nM fluorescein conjugated control siRNA transfected cell results. ..77

Figure E. 10 Flow cytometry analysis according to the gated area showing the FITC-H versus Cell Count histogram graph for 5 nM fluorescein conjugated control siRNA transfected cell results. ..77

Figure E. 11 Flow cytometry analysis according to the gated area showing the FITC-H versus Cell Count histogram graph for 8 nM fluorescein conjugated control siRNA transfected cell results. ..78

Figure E. 12 Flow cytometry analysis according to the gated area showing the FITC-H versus Cell Count histogram graph for 10 nM fluorescein conjugated control siRNA transfected cell results..78

LIST OF ABBREVIATIONS

MDR	Multidrug Resistance
R	Resistant
S	Sensitive
VIM	Vimentin
bp	Base pair
DEPC	Diethylpyrocarbonate
dH ₂ O	Distilled water
DMSO	Dimethyl Sulfoxide
dNTP	Deoxy Nucleotide Triphosphate
DOX	Doxorubicin
dsRNA	Double Strand RNA
EtBr	Ethidium Bromide
MCF-7/S	Sensitive MCF-7
MCF-7/Dox	Doxorubicin resistant MCF-7
PBS	Phosphate buffered saline
qPCR	Quantitative Real-Time Polymerase Chain Reaction
RISC	RNA-inducing silencing complex
RNAi	RNA Interference
siRNA	Small Interfering RNA
rpm	Revolution per minute
RT	Reverse Transcription
SEM	Standart Error of the Means
TAE	Tris-acetate-EDTA
GSH	Glutathione
EDTA	Ethylenediaminetetraacetate
AEC	3-amino-9-ethylcarbazol
V	Volt
A	Amper
w/v	Weight per volume
C _T	Treshold cycle value

CHAPTER 1

INTRODUCTION

1.1. Cancer Biology

It has been calculated that around 7.5 million people die because of cancer on a yearly basis of statistics. Moreover, the new cases is expected to reach to around 15 million by 2020 based on a report has been done by World Health Organization (WHO).

Cancer is a class of diseases defined as uncontrolled cell growth instead of dying. Around 100 different cancer types have been reported so far and each has been classified by the type of the cell that is impaired. Cancer cells can also spread to other tissues (malignant tumor) or stay at the tissue that they initially develop (benign tumor).

Cancer cells formation happen because of several DNA damages. Once this kind of damages occur, a normal cell can either repairs them by several mechanisms or dies. Whereas, in cancer cells, the impaired DNA can not be repaired, and the cell does not die like it should. Instead, the cancer cell goes on making new cancer cells. Moreover, these new cancer cells have the same abnormal DNA as the first cancer cell does. Although, these abnormalities on DNA can be inherited, most of these are caused by acquired mutations that happen while the normal cell is reproducing or by something in the environment such as cigarette smoking, unhealthy eating and sun exposure (Rieger, 2004).

The basic purpose of cancer research is exposing the molecular pathways and trying to understand the mechanisms underlying the cancer development processes.

More than the last forty years of our knowledge about the cancer has been enriched substantially by the discovery of the mutations that produce oncogenes with dominant gain of function and tumor suppressor genes with recessive loss of function as well as epigenetic variations.

1.2. Breast Cancer

There are several cancer types and the one of these which most known is breast cancer. According to the recent statistics, approximately 230,000 invasive breast cancer were diagnosed in women and together with this statistics, It has been identified that more than 55,000 new cases of non-invasive breast cancer in 2011 (in USA). Moreover, around 39,000 women were die in 2011 because of breast cancer in the USA. Although women in the USA, breast cancer death rates are higher than those for any other cancer, besides lung cancer, the recent reports said that men are at risk either and also in our country, breast cancer was the most common cancer type among the women in Turkey, in 2005 (WHO Report, 2006).

Usually breast cancer either begins in the cells of the lobules, which are the milk-producing glands, or the ducts, the passages that drain milk from the lobules to the nipple. Less commonly, breast cancer can begin in the stromal tissues, which include the fatty and fibrous connective tissues of the breast. Over time, cancer cells can invade nearby healthy breast tissue and make their way into the underarm lymph nodes, small organs that filter out foreign substances in the body. If cancer cells get into the lymph nodes, they then have a pathway into other parts of the body. The breast cancer's stage refers to how far the cancer cells have spread beyond the original breast cancer is always caused by a genetic abnormality. However, only 5-10% of cancers are due to an abnormality inherited.

1.3. Treatment of Breast Cancer

There are several treatments for cancer such as surgery, hormonal therapy, targeted therapy, radiation therapy and chemotheraphy (<http://www.breastcancer.org>).

1.3.1. Surgery

It is the first come treatment to defeat for breast cancer. There are three main types of surgery, lumpectomy, mastectomy. In lumpectomy, the tumor is removed with only a small amount of surrounding breast tissue, while in mastectomy, all of the breast tissue is removed. As a study reported that women who were treated with lumpectomy only or with lumpectomy plus breast irradiation therapy was compared with women who were treated with total mastectomy. This study was resulted that there were no significant differences between in survival of the women who treated with lumpectomy and the women who treated with mastectomy (Fisher et al, 2002). Lymph node removal also can take place in lumpectomy and mastectomy if the biopsy shows that breast cancer has spread outside the milk duct (<http://www.breastcancer.org/treatment/surgery/>).

1.3.2. Hormonal Therapy

In general, drugs using in hormonal therapy treat hormone-receptor-positive breast cancers in either by lowering the amount of the hormone estrogen or by blocking the action of estrogen on breast cancer cells in the body(<http://www.breastcancer.org/treatment/hormonaltherapy/>).

Tamoxifen (a non-steroidal estrogen antagonist) is the most well-known used drug for hormonal therapy and It was shown to increase survival of breast cancer patients (Gradishar et al, 2000). Some studies have shown that 5 years of tamoxifen treatment are much better than 1–2 years of such treatment. However, there are no convincing data that verify the use of tamoxifen for longer than 5 years outside the setting of a clinical trial. Although tamoxifen has been associated with the risk of endometrial cancer slightly, the benefits of tamoxifen treatment are far better than its risks in the majority of women. Tamoxifen may be combined with combination chemotherapy, particularly in premenopausal women; such combinations may further reduce the risk of reappearance (National Institutes of Health Consensus Development Panel, (2001)).

1.3.3. Targeted Therapy

Targeted therapy treatments target at specific development of cancer cell growth and division, using drugs or other agents. In these treatment, generally Avastin, Herceptin, Iressa, and Tykerb are used as a drug. These drugs have specific effects on cancer cells.

A study showed that the HER-2/neu (Figure 1.1), which is a member of the epidermal growth factor receptor and an oncogene, encodes a transmembrane called tyrosine kinase receptor, which is linked to prognosis and response to therapy with the anti-HER-2 monoclonal antibody, trastuzumab (trade name Herceptin) in patients with advanced metastatic breast cancer. It was shown that with targeted therapies consist of trastuzumab combined with chemotherapy, hormonal therapy and radiation therapy have been succeeded in treatment of HER2/neu positive breast cancer for women. (Ross et al, 2004).

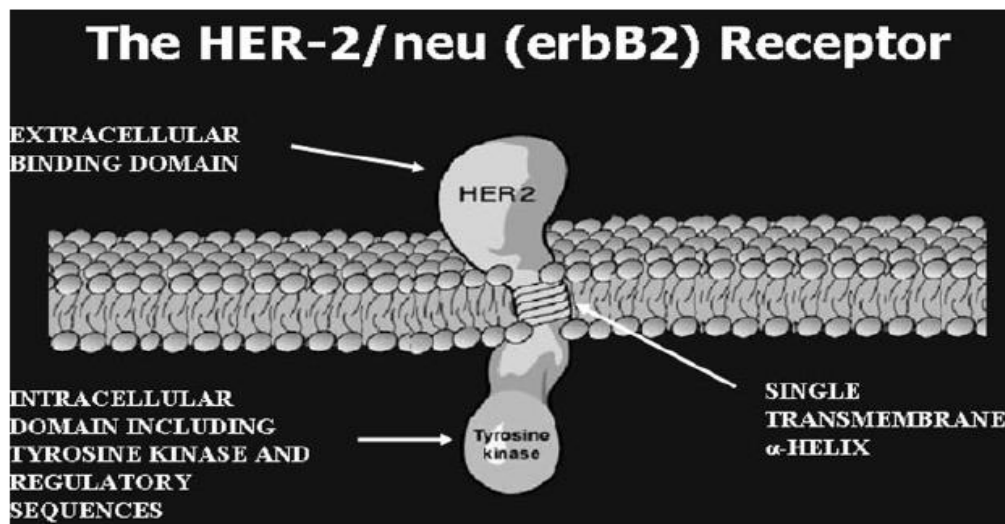


Figure 1.1 The HER2/neu Tyrosine Kinase Receptor (Ross et al, 2004).

1.3.4. Radiation Therapy

The main aim of this therapy (also called radiotherapy) is the use of high-energy x-rays or gamma rays to penetrate and kill cancer cells to be able to shrink tumors.

This therapy is mostly applied after lumpectomy and after mastectomy in some cases. Therefore, the risk of the remaining cancer cells effect can be eliminated. (<http://www.breastcancer.org/treatment/radiation>).

The effect of radiotherapy commonly influence on DNA or molecules which have an effect on DNA. These sort of changes affect negatively the cell division, regulation (Baba & Catoi, 2007).

1.3.5. Chemothreapy

In chemotherapy, several powerful drugs are used to target and eliminate the fast- proliferating breast cancer cells. Although chemotherapy for breast cancer is frequently used with other treatments such as surgery, It also may be used as the primary treatment, when surgery is not an option. There are diverse chemotherapy drugs which are available to treat breast cancer. These drugs may be used either individually or in combination to increase the effectiveness of the treatment.

Chemoterapy can be classified briefly in three main clinical groups;

1. Chemoterapy only,
2. Adjuvant chemotherapy consist of other treatment such as surgery, radiation therapy
3. Neoadjuvant chemotherapy is for patients whom directly surgery is inconvenient and the patient desires an attempt at breast conservation (DeVita & Chu, 2008).

During adjuvant chemotherapy, also called combination chemotherapy, usually more than one drug is given and they are used to destroy the cancer cells and this chemoterapy can include chemotherapy, hormonal therapy, the targeted drug trastuzumab (Herceptin®) and radiation therapy. A recent study has indicated that adjuvant chemotherapy for early-stage breast cancer helps to prevent the cancer from returning (Early Breast Cancer Trialists' Collaborative Group, (2005)).

Neoadjuvant chemotherapy is a treatment given before primary therapy. The main aim of this chemotherapy is to shrink a tumor that is inoperable. Therefore, after this treatment, tumor can be surgically ejected from the body (Mauri et al, 2005).

Neoadjuvant chemotherapy is generally applied under the similar circumstances as adjuvant chemotherapy. If a tumor does not respond to become shrink or keep growing during neoadjuvant chemotherapy, another type of chemotherapy or surgery can be performed, depending on the phase of the cancer.

A great deal of drugs are used in the breast cancer chemotherapy and they are shown in a list below.

- Tamoxifen
- Paclitaxel
- Docetaxel
- Doxorubicin (Adriamycin®)
- Cyclophosphamide
- Methotrexate
- 5-Fluorouracil
- Vinca Alkaloids- Vincristine & Vinblastine
- Gemcitabine
- Epirubicin

Tamoxifen is commonly used to treat patients with early-stage breast cancer and also those with metastatic breast cancer. It also helps to prevent the original breast cancer from reapperance and also helps to prevent the development of new cancers in the other breast. Tamoxifen slows or stops the development of breast cancer cells, as a treatment for metastatic breast cancer. This drug also works against the estrogen effect, and so treatment with tamoxifen is very efficient in estrogen receptor (+) breast cancers, which need estrogen to develop.

Paclitaxel and Docetaxel have an inhibitory effect on mitosis. These drugs target fastly growing cancer cells, in a way that sticks to them while they are dividing, and so by the help of the effect of these drugs, breast cancer cells can not complete their division process.

Doxorubicin (Adriamycin ®) is applied to treat early-stage breast cancer, HER2-positive breast cancer, and metastatic breast cancer. This drug sometimes used with cyclophosphamide, 5-fluorouracil and methotrexate and through this drug combination, remarkable results have been acquired on breast cancer treatment (Shen et al, 2004).

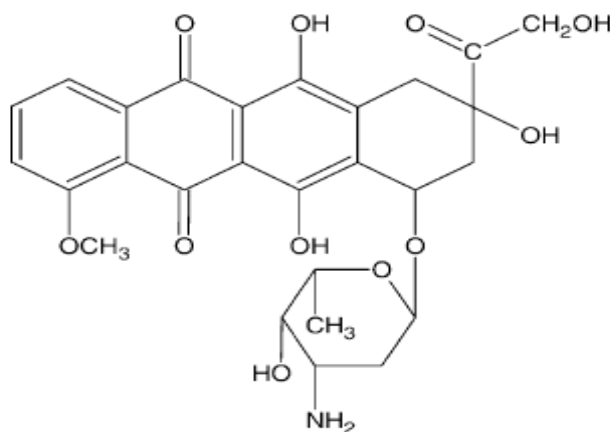
Vincristine and vinblastine are vinca alkaloids and both have inhibitory effect on mitosis and in that way they are used in cancer chemotherapy. These vinca alkaloids effects cause corruption of spindle fibers. Therefore, chromosomes fail to move apart from each other during metaphase stage in mitosis.

Gemcitabine is a member of a group of chemotherapy drugs for breast cancer known as antimetabolites. Its effect is to avoid cells to making new DNA and RNA molecules, and so resulting the cells to die.

Epirubicin is a chemotherapeutic drug that is used for the treatment of breast cancer that has spread to the lymph nodes following breast cancer therapy. This drug prohibit cells from replicating themselves. Therefore, both cancer and healthy cells can not proliferate and eventually die.

1.3.5.1. Doxorubicin (Adriamycin®)

Doxorubicin (Figure 1.2) is a widely used chemotherapy drug which is classified as an “anthracycline antibiotic” and exhibits a broad spectrum against leukemias, lymphomas and solid tumors (Swift et al, 2006).



Doxorubicin

Figure 1.2 Doxorubicin is an anthracycline antibiotic (Pajeva et al, 2004).

The interaction of doxorubicin with DNA and DNA associated enzymes is well recognized. Doxorubicin binds to DNA and reduces the nucleic acid synthesis, via blockage of DNA

polymerase effect (Shen et al, 2008). Moreover, doxorubicin is known as a topoisomerase II poison. It balances the cleavable complex between topoisomerase II enzyme subunits and DNA and this resulting in breaking of DNA double-strand by intercalation into DNA, which induces an apoptotic response and interfere with DNA synthesis (Swift et al, 2006). Doxorubicin has also a capability to create a diverse of free radicals in cells. These free radicals, produced by doxorubicin, have an effect on DNA directly. Therefore, they can be responsible for unfavorable conditions for cell division (Costa & Nepomuceno, 2006; Keizer et al, 1990). It has been reported that doxorubicin has not only an effect on DNA directly, but also has a cytotoxic affect on through interaction with the negatively charged phospholipids of cell membrane (Nicolay et al, 1988; Pajeva et al, 2004; Triton & Yee, 1982). When doxorubicin binds and insert into the cell membrane, it effects the intrinsic transport characterization of the cell membrane (Pajeva et al, 2004; Speelmans et al, 1994). As a summary, some related pathways is shown in Figure 1.3.

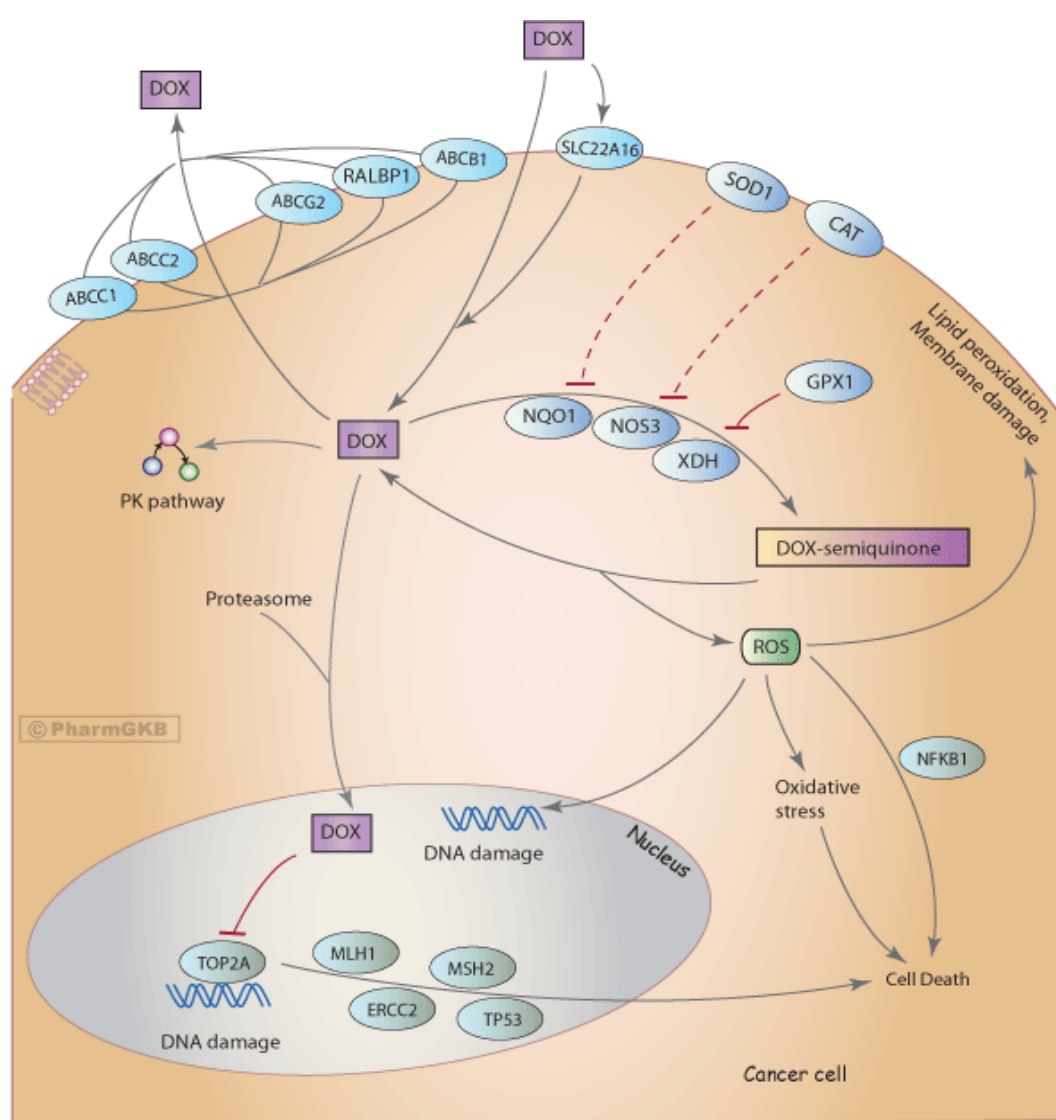


Figure 1.3 Doxorubicin pathways in cancer cell lines, showing the cell death mechanism. (Thorn et al, 2011).

Doxorubicin has also effects on cardiotoxicity as a side effect in cancer patients (Wang et al, 2004). The exact mechanism of cardiotoxicity of doxorubicin is still controversial and there has been two main theories, so far;

- iron-related free radicals and formation of doxorubicinol (DOXol) metabolite (interferes with iron calcium regulations) and,
- mitochondrial disruption (Minotti et al, 2004; Wallace, 2007).

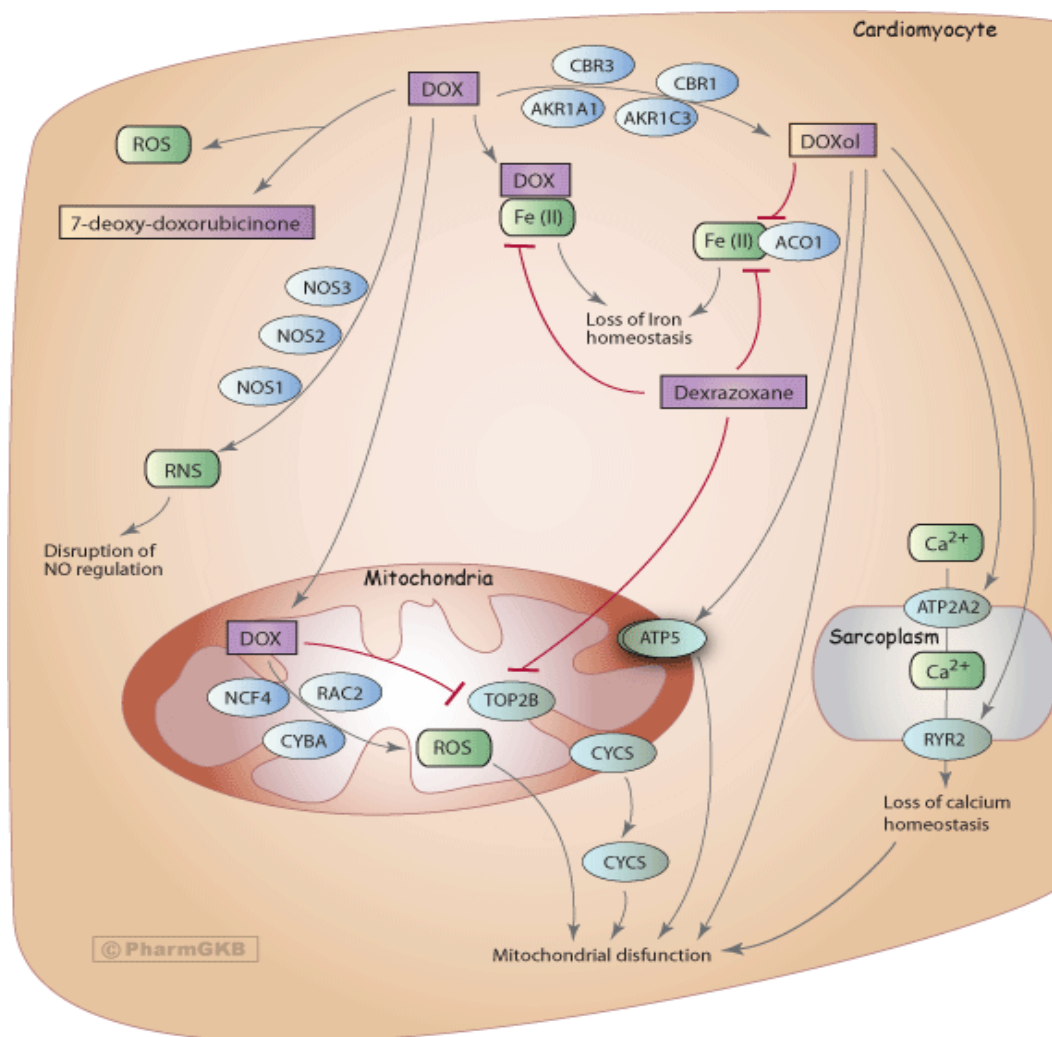


Figure 1.4 Doxorubicin pathways in cancer cell lines, showing the cardiotoxicity mechanism. (Thorn et al, 2011).

One of the strongest supporting evidence for the iron hypothesis is “that the iron chelator, dexrazoxane is protective against doxorubicin-induced toxicity (Swain et al, 1997)” and “the best evidence supporting the mitochondrial hypothesis is in the association of the genetic variants in several component genes of the mitochondrial NAD(P)H oxidase complex with doxorubicin cardiotoxicity (Wojnowski et al, 2005)”. Metabolism of doxorubicin within the mitochondria can disrupt respiration and leads to the release of cytochrome-C initiating apoptosis (Clementi et al, 2003) (Figure 1.4).

In addition to problems with cardiotoxicity, resistance is also a problem limiting its use. . The mechanism of resistance involves ABCB1 (MDR1, Pgp) (Germann, 1996) and ABCC1 (MRP1) (Cole et al, 1992) and other transporters (ABCC2, ABCC3, ABCG2, and RALBP1) (Singhal et al, 2003). Another mechanism of doxorubicin resistance is the amplification of TOP2A. The amplification of TOP2A has a complicated relationship to neighboring gene HER-2 (ERBB2), used as a marker for breast cancer treatments in particular the HER-2-targeted trastuzumab. The amplification of ERBB2 gene also affects the doxorubicin response (Oakman et al, 2009).

1.4. Multidrug Resistance (MDR)

There are several treatment strategies for cancer patients, such as local surgical treatment or radiation (about 50% of total cancer cases), and for even patients with metastasis, chemotherapy, immunotherapy and biological- response modifiers. However, it is a big question to be answered that why can some patients be cured by these approaches and others respond transiently or incompletely? Host and tumour genetic alterations, epigenetic changes and tumour environment all seem to contribute to the complex mechanisms of drug resistance for cancer cells which limits the effectiveness of chemotherapeutic drugs (Gorre et al, 2001).

There is still a big question to be answered that whether tumors may be originally resistant to chemotherapeutic drugs, before the treatment, or multidrug resistance can be occurred by chemotherapeutic drugs during treatment, so it means tumors are sensitive and then become resistant because of the chemotherapy (Longley & Johnston, 2005).

There are two main groups of resistance to anticancer drugs:

- Impairment of delivery of anticancer drugs to tumour cells,
- Drug-dependent changes due to genetic and epigenetic variations which effect drug sensitivity in the cancer cells.

Disruption of drug delivery to tumors can be resulted from poor absorption of orally administered drugs, increased drug metabolism or increased excretion, resulting in lower levels of drug in the blood and reduced diffusion of drugs from the blood into the tumour mass (Jain, 2001; Pluen et al, 2001). In a study, it was reported that some cancer cells that are sensitive to chemotherapy as monolayer in culture become resistant when transplanted into animal models. This indicates that environmental factors, such as the extracellular matrix or physical shape of tumour, might be involved in drug resistance (Durand & Olive, 2001).

The underlying mechanisms of drug resistance have been intensely studied, in the experimental models that can be produced by in vitro drug dose selection with cytotoxic agents. Cancer cells in culture can either become resistant to a single drug or a group of drugs with a similar mechanism of action. After selection for resistance to a single drug, cells might also show cross-resistance to other structurally and mechanistically unrelated drugs, a phenomenon that is known as multidrug resistance. As can be seen in Figure 1.5, different types of cellular multidrug resistance mechanisms have been described, so far. Becoming resistant to anti-cancer drugs generally induces from expression of ATP-dependent efflux pumps, which belong to a family of ATP-binding cassette (ABC) transporters. By over-expression of these pumps in cancer cells, resistance occurs due to the increasement of drug effluxion and this lowers intracellular drug concentrations. Drugs that are effected by classical multidrug resistance can be grouped as the vinca alkaloids (vinblastine and vincristine), the anthracyclines (doxorubicin and daunorubicin), actinomycin-D (an antitumor antibiotic) and paclitaxel (the microtubule-stabilizing drug) (Ambudkar et al, 1999). Resistance can also be appeared by reduced drug uptake. Some water-soluble drugs that are uptaken by endocytosis or through the tranporters and carriers on the cell membrane might fail to accumulate in the cytosol, by the effect of increased efflux. These drugs are the antifolate

methotrexate, nucleotide analogues, such as 5-fluorouracil and 8-azaguanine, and cisplatin (Shen et al, 2000).

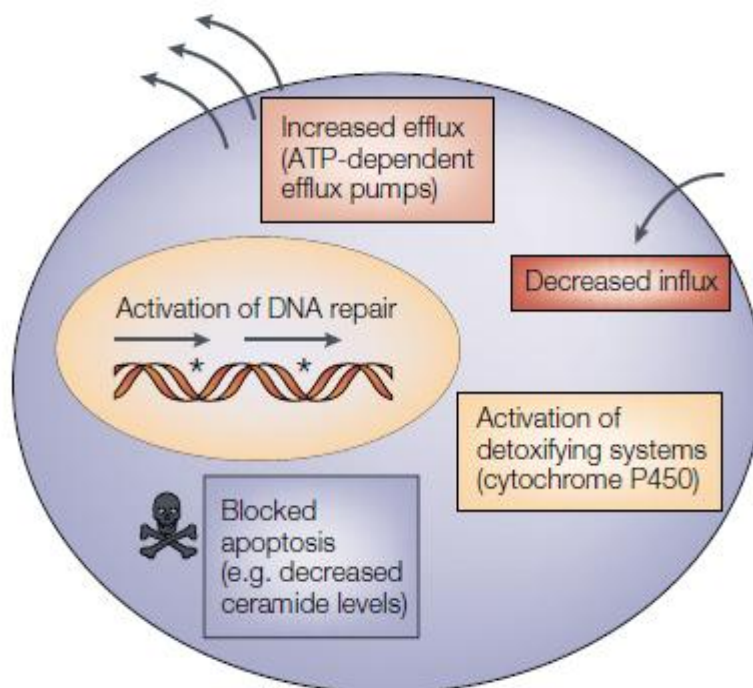


Figure 1.5 Cellular factors that induce drug resistance (Gottesman et al, 2002).

The coordination between P-glycoprotein (PgP; a multidrug transporter) and cytochrome P450 3A has been investigated (Durand & Olive, 2001; Schuetz et al, 1996) .

It is so important about cancer cells having multidrug resistance are genetically different. As a different type of multidrug resistant, doxorubicin resistance generally related to over-expression of MDR1/MRP, altered levels of topoisomerase II expression and mutated forms of it, deficiency of DNA mismatch repair system, resistance to apoptosis and lastly structural changes in the cell membrane lipid composition (Pajeva et al, 2004; Paul & Cowan, 1999).

1.5. Metastasis and Invasiveness

Invasion and metastasis are the most dangerous and fatal aspects for patients who suffer from cancer (Kohn & Liotta, 1995). When a tumor gains invasive characteristics, it can spread easily in the body. In some cancer type, such as breast cancer, there are several benefits from developed screening methods and by the help of methods diagnosis can be done earlier.. Continuing with the breast cancer example, the relapse rate in stage I, with less than 1 cm disease, remains 20 to 25%, indicating that the unveiling of metastatic potential is an earlier event than had been thought. Thus, less than one-third of newly diagnosed cancer patients potentially can be cured by local therapeutic modalities alone. The size and age variation in metastases and their heterogeneous composition

over time block complete surgical destruction of disease and can limit the effectiveness of many systemic anticancer drugs.

A study was performed for breast cancer patients showed that the cells either synthesize osteopontin or bind and sequester it from the microenvironment. This behavior was correlated with tumor invasiveness and poor prognosis. There are several theoretic aspects for tropism of organs. One of these, tumor cells can invade equally in all organs, but grow only in several specific organs. Data to support this can be found in the different patterns of growth and dissemination using subcutaneously implanted xenografts, compared with orthotopic implantation (Fidler & Hart, 1982). Preferential growth and homing may be induced by the local microenvironment. Secondly, circulation of tumor cells may adhere specifically to the endothelial luminal surface only in the targeted organ.

To induce successful metastasis to a site distant from the primary tumor, neoplastic cells migrate from the primary tumor mass and successfully traverse tissue barriers. This may involve simple cell locomotion from the primary into the interstitial stroma or may require penetration and proteolysis of tissue obstacles. Further, tumor cells have to survive the stage of vascular transport and arrest in the capillary beds of distant organs to engage in a second round of invasion—extravasation—whereby neoplastic cells exit from the vessel lumen into the local angiogenesis in this new environment to grow from micrometastases into the progressively enlarging tumors that will threaten the survival of the host.

The mammalian organism is divided into a series of tissue compartments separated by the extracellular matrix. The basement membrane and its underlying interstitial stroma constitute the extracellular matrix and are the major connective tissue units separating organ compartments. Tumor cells penetrate the epithelial basement membrane and enter the underlying interstitial stroma during the transition from in situ to invasive carcinoma (Kohn & Liotta, 1995; Liotta, 2004). The basement membrane is a dense meshwork of type IV collagen, glycoproteins, such as laminin and fibronectin, proteoglycans, and embedded growth factors. Once the tumor cells invade the underlying stroma, they gain access to the lymphatics and blood vessels for distant dissemination. General and widespread changes occur in the organization, distribution, and quantity of the epithelial basement membrane during the transition from benign to invasive carcinoma.

1.6. Vimentin

Vimentin, a 57 kDa protein, is one of the most widely expressed and a type III intermediate filament (IF) as a member of the intermediate filament protein family. Vimentin is expressed in a wide range of cell types, including pancreatic precursor cells, sertoli cells, neuronal precursor cells, trophoblastic giant cells, fibroblasts, endothelial cells lining blood vessels, renal tubular cells, macrophages, neutrophils, mesangial cells, leukocytes and renal stromal cells (Cochard & Paulin, 1984; Evans, 1998). Vimentin is so important due to being a most well-known marker of epithelial-mesenchymal transition (EMT) (Thiery, 2002). This EMT is characterized by the expression of vimentin in epithelial cells. In another study, it was shown that the vimentin knock-out mice exhibit impairment in wound healing in both embryonic and adult periods, resulted in decline of migration capacity (Eckes et al, 2000).

Though vimentin is considered to maintain the structural processes of the cell and mediate many other fascinating functions, in knockout mice models which are lack of vimentin showed totally normal phenotypes and did not show any apoptotic effects (Colucci-Guyon et al, 1994). However, a more detailed study showed that the vimentin (–/–) mice exhibit impaired wound healing in both embryonic and adult stages due to the weak and severely disabled fibroblasts that were not in a

capacity to migrate (Eckes et al, 2000) and died due to end-stage renal failure in a pathological situation involving the reduction of renal mass when compared to their wild-type littermates, showed decreased flow-induced dilation during arterial remodeling, suggesting that vimentin modulates arterial structural responses to altered blood flow and finally, vimentin deficient lymphocytes showed a decreased homing capacity to lymph nodes and spleen.

There are several studies suggesting that vimentin has not an essential role for efficient tumor growth and differentiation in vivo (Langa et al, 2000), whereas some other studies reported that a tumor promoter role of vimentin in cancer in vitro (Ivaska et al, 2007; Ivaska et al, 2005).

This disagreement might be related to the fact that vimentin is differentially expressed in different cell types and it might play a tissue-specific function or there might be a redundancy in the function among IF proteins.

1.6.1. Vimentin in Breast Cancer

Over-expression of vimentin is frequently related to increased migration/invasion capacity of the cancer cells. Vimentin is mainly used as a marker for EMT in association with other known markers (Figure 1.6). Majority of the cancers over express vimentin and it is used as an indicator of poor prognosis.

Vimentin expression was shown in several aggressive breast cancer cell lines (Gilles et al, 2003) and its over expression was correlated with increased migration and invasion characteristics of breast cancer cells (Korsching et al, 2005). Furthermore, it was determined that non-invasive MCF-7 cells showed distinct motility and invasive characteristics via over expression of vimentin (Korsching et al, 2005). Also in this study, these characteristics decreased by down-regulation of vimentin with antisense oligos in MDA-MB-231 cells, which originally express vimentin (Korsching et al, 2005). Interestingly, in MCF-10A cells, which has over-expressed vimentin, it was determined that the cell migration potential of this line was dependent on EGF expression level (Gilles et al, 1999).

Histological examination of human breast carcinoma samples showed that vimentin expression is predominantly found in highgrade ductal carcinomas with low estrogen receptor levels (Domagala et al, 1990). Recent studies have reported “ that vimentin plays a major role in the EMT process of breast cancers and its knock-down resulted in a decrease in genes linked with breast cancer invasion and the basal-like phenotype including Axl, ITGB4 and PLAUG with a subsequent increase in the genes abundant in normal mammary epithelium including RAB25 and EHF. Furthermore, vimentin was shown to play a key role in the regulation of Axl and also Slug- and Ras-induced migration in breast cancer cells (Vuoriluoto et al, 2011)”.

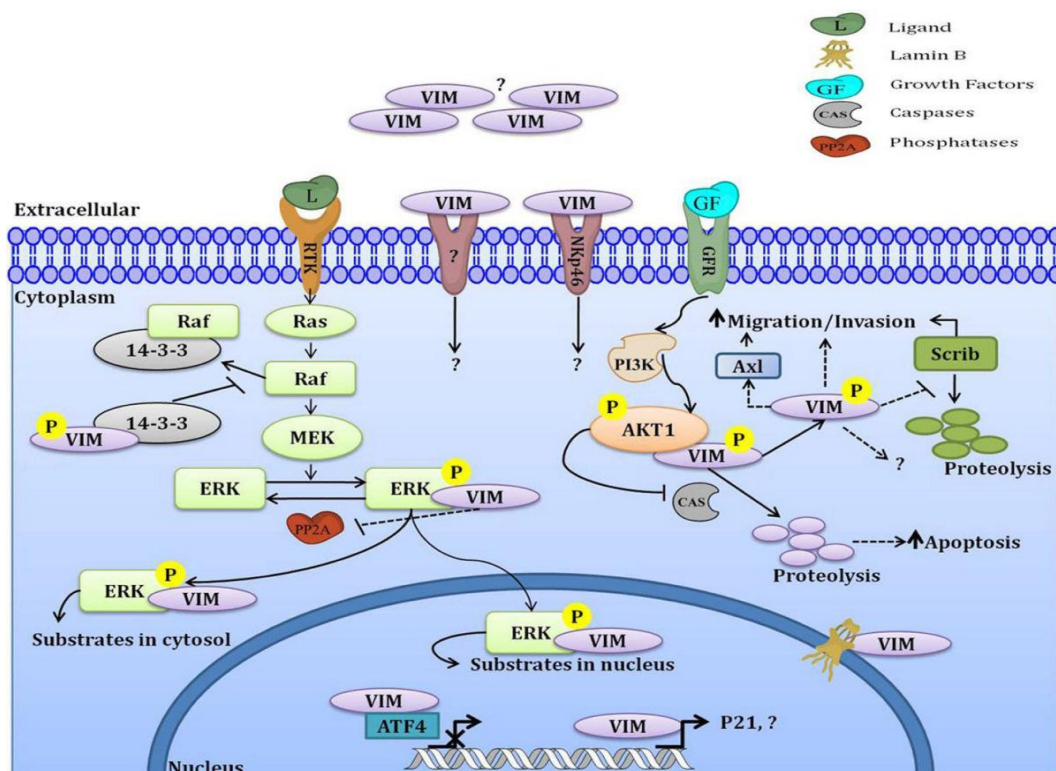


Figure 1.6 Vimentin's role in cancer and some related pathways (Satelli & Li, 2011).

In conclusion, to be able to see the effect of vimentin gene on metastatic and invasive properties of interested cell lines, silencing of this gene is needed to be performed. The strategy of RNA interference targeting of vimentin are potentially effective in modulating cell migration and carcinoma cell invasion (McInroy & Maatta, 2007).

1.6.1.1. RNA Interference Strategy

One of the most affecting events of the almost past 10 years in the field of molecular biology has been the discovery of RNA interference (RNAi). Although RNAi is an evolutionarily conserved phenomenon for sequence-specific gene silencing in mammalian cells, exogenous small interfering RNA (siRNA) and vector-based short hairpin RNA (shRNA) can also invoke RNAi responses. Both are now not only experimental tools for analyzing gene function but also are expected to be excellent techniques for drug target discovery and the emerging class of gene medicine for targeting cureless diseases such as cancer (Takeshita & Ochiya, 2006).

RNAi was first described in animal cells by Fire and colleagues in the nematode *Caenorhabditis elegans* as a naturally occurring cellular mechanism that induces post-transcriptional gene silencing, in which double-stranded RNA (dsRNA) suppresses the expression of a target gene by triggering specific degradation of the complementary mRNA sequence (Fire et al, 1998). It is thought that the natural role of RNAi is a cellular defense against viral infection or potentially harmful destabilizing genomic invader such as transposons. RNAi can also be induced in mammalian cells by the introduction of synthetic small interfering RNA (siRNA) 21–23 base pairs in length (Elbashir et al, 2001) or by plasmid (Paul et al, 2002) and viral vector systems (Brummelkamp et al, 2002) that express short hairpin RNAs (shRNA) that are subsequently processed to siRNA by the cellular machinery.

Once the dsRNA enters the cell, it is cleaved by an enzyme, naming Rnase III which is Dicer, into 21- to 23- nucleotide small interfering RNAs (siRNAs), which have symmetric 2-3 nucleotide 3' overhangs and 5' phosphate and 3' hydroxyl groups (Figure 1.7) (Dillin, 2003).

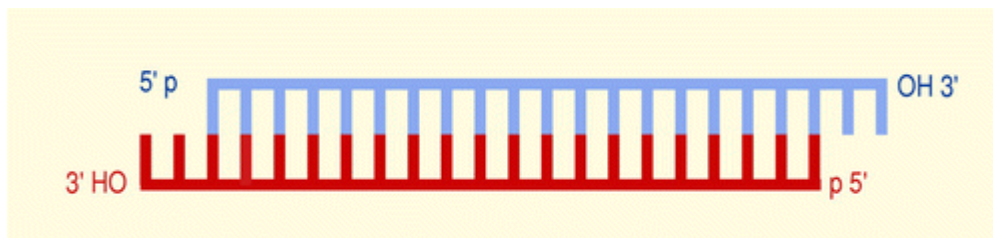


Figure 1.7 Schematic overview of short interfering RNA (siRNA) molecule (Lage, 2005).

These RNA duplexes complexed with a large multiprotein RNA-inducing silencing complex (RISC), guiding RISC to a complementary target mRNA and triggering its endonucleolytic cleavage by Slicer (Argonaute-2), an enzyme residing within the RISC complex (Pai et al, 2006). The target mRNA cleavage happens at a single site which is 10 nucleotides away from 5' phosphate of the antisense strand of siRNA molecule. Owing to the loss of either 5' 7-methylguanine cap or 3' poly(A) tail structures, the cleaved target mRNA is not protected by these sites and so degraded by exonucleases (Figure 1.8).

Addition of dsRNA into mammalian cells does not cause in efficient Dicer-mediated form of siRNA. However, this problem can be solved by introducing synthetic 21-nt siRNA duplexes (Nieth et al, 2003). Although it is easier to manage than shRNAs, the biggest disadvantage of silencing by siRNAs is their transient and time limited inhibition effect on gene expression. Especially in more fastly dividing cells, the RNAi efficiency happens in a short time, peaking at about 3 days and lasting for around 1 week. The underlying reasons may include the increasing dilution of the siRNA with repeated cell division, as well as ongoing cellular enzymatic degradation (Pai et al, 2006).

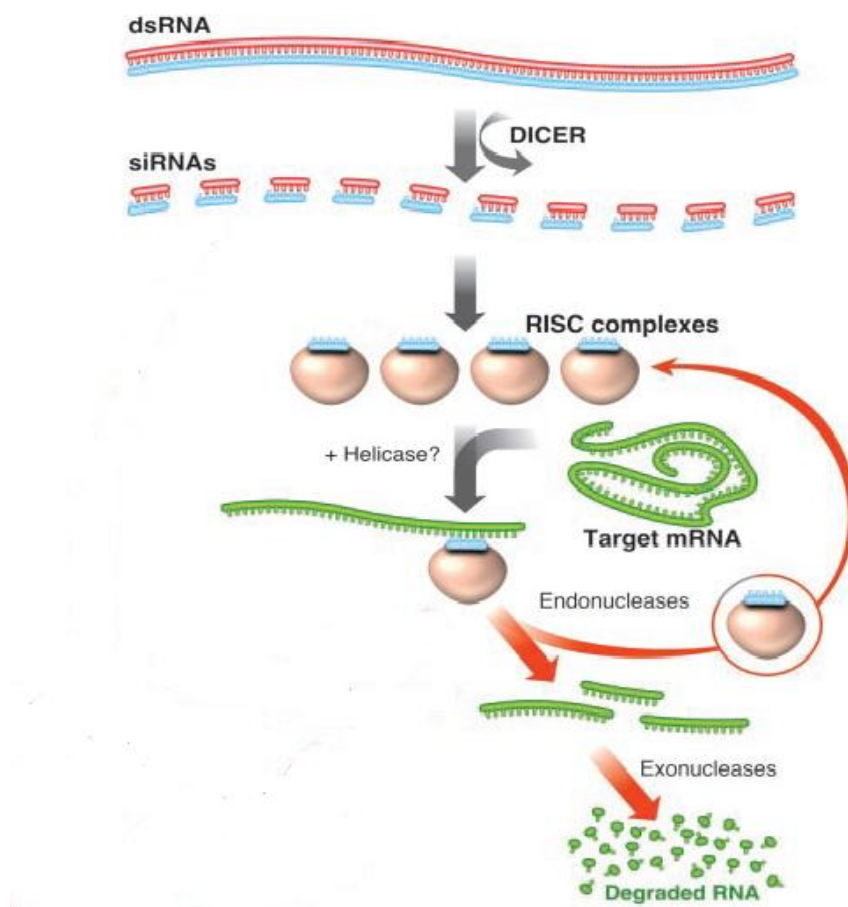


Figure 1.8 Mechanism of RNA interference (Dillin, 2003).

In order to make siRNAs more resistant to activity of RNases, some chemical modifications can be performed. siRNAs can be coupled with fusogenic peptides, linked to antibodies to cell surface receptor ligands for cell-specific delivery, or encased in lipid complexes, cationic liposomes or other types of particles (Pai et al, 2006; Shankar et al, 2005), which would increase their effectiveness in potential therapeutic applications.

It was shown that the specificity of siRNAs as well as shRNAs is sequence as well as concentration dependent. At around concentration of 100 nM, siRNAs and shRNAs can induce several genes, many of which are known to be involved in apoptosis and cell stress response (Persengiev et al, 2004; Semizarov et al, 2003). The non specific effect of high concentration can be avoided by reduction of siRNA concentration. However, the levels of gene silencing can not be adjusted with shRNAs due to their stable suppression effects. Moreover, technical and ethical problems owing to the use of expression vectors, especially potential retrovirus-based shRNA delivery systems are needed to be addressed (Nieth et al, 2003). Lastly, it can be said that the synthetic siRNAs are more suitable for combination therapies.

1.7. Aim of the Study

The main purpose in this study is determination of the changes in metastatic and invasive characteristics in MCF-7/Dox cell lines, after silencing of vimentin gene by specific siRNA. Selective down-regulation of *VIM* expression can be resulted in decline of metastasis and invasiveness of this cell line. The objectives of this study might be listed as:

- Determination of *VIM* expression level in MCF-7/Dox cell line comparing with *VIM* expression level in MCF-7/S cell line.
- Determination of the most efficient siRNA concentration and downregulation of *VIM* expression in Doxorubicin resistant MCF-7 cell line.
- Investigation of changes for vimentin levels after silencing of *VIM*.
- Investigation of metastatic behavior of MCF-7/Dox cells after silencing of *VIM* in order to assess the relationship of vimentin expression and cell motility.
- Determination of invasive characteristics of MCF-7/Dox cells after silencing of *VIM* in order to assess the relationship of vimentin expression and invasiveness.

CHAPTER 2

MATERIALS AND METHODS

2.1 Materials

2.1.1 Cell Lines

MCF-7 is a type of breast cancer cell line, which was characterized by Şap Institute, Ankara, Turkey. MCF-7/Dox, Doxorubicin resistant cell line was developed from the parental MCF-7 cell line (MCF-7/S) previously in our laboratory by stending drug application in dose incresement (final dose: 1µM) and indicate to express high levels of vimentin (Kars et al, 2006).

2.1.2 Chemicals and Reagents

Doxorubicin (DOX) were provided by Prof. Dr. Fikret Arpacı (Gülhane Military Medical Academy, School of Medicine, Department of Oncology). The stock solution was prepared as 3.4mM with sterile distilled water.

RPMI 1640 medium and fetal bovine serum (FBS) were purchased from Thermo Scientific HyClone, Germany. Gentamycin, trypsin-EDTA, trypan blue were obtained from Biological Industries, Isreal. Phospahte buffered saline (PBS) and dimethyl sulfoxide (DMSO) were obtained from Sigma-Aldrich, USA. Triton X-100 and paraformaldehyde were purchased from Sigma (Taufkirchen, Germany). Glacial acetic acid and ethanol were obtained from Merck, Germany. HiPerFect siRNA transfection reagent were purchased from Qiagen, Germany. DEPC, β-mercaptoetanol and agarose gel were obtained from Applichem, Germany. NucleoSpin® RNA II RNA isolation kit was purchased from Macherey-Nagel, Germany. Light-Cycler-FastStart DNA Master SYBR Green I kit was obtained from Roche Diagnostic, Switzerland. Moloney-Murine Leukemia Virus Reverse Transcriptase, dNTP set, MgCl₂, *Taq* DNA polymerase, 6X loading buffer, High Range ladder, 50 bp DNA ladder were purchased from Fermantas, Lithuania. ThinCert™ cell culture inserts were obtained from Greiner Bio-one, Netherlands and for invasion assay, matrigel was purchased from BD Biosciences, USA. Giemsa solution was obtained from Merck, Germany. M-PER protein isolation kit (Pierce, Rockford, IL, USA) containing protease inhibitors (Roche, Mannheim, Germany) was purchased for protein isolation. Coomassie Plus protein assay reagent and chemiluminescence kit ECL Plus was obtained from Pierce (Rockford, IL, USA). Prestained pageruler protein ladder was purchased from Fermantas, Lithuania. VIM antibody was obtained from Santa Cruz (CA, USA). Tris/EDTA buffer, pH 9, AEC Substrate chromogen, streptavidin, biotinylated goat antiserum and ultramount moutning medium was obtained from Dako, Denmark. Monoclonal Mouse Anti-Vimentin Clone V9 antibody was also

purchased from Dako, Denmark. Ultra V block was purchased from Thermo Fisher Scientific, USA.

2.1.3 siRNA

FlexiTube Gene Solution oligo, *VIM* siRNA was obtained from Qiagen, Germany and control siRNA was purchased from Santa Cruz, USA. In order to determine the most efficient siRNA concentration, Fluorescein (FITC) conjugated SignalSilence[®] Control siRNA (Cell Signalling Technology[®], USA) was used.

2.1.4 Primers

VIM and *β-actin* primers were purchased from Alpha DNA, Canada. Primer sequences and their amplicon sizes are shown in Table 2.1.

Table 2.1 Primers used in quantitative real-time polymerase chain reaction (qPCR) and the amplicon sizes.

Primer	Sequence	Size of Amplicon
<i>VIM Sense</i>	5'ATCTGGATTCACTCCCTCTGGTTG3	161 bp
<i>VIM Antisense</i>	5'TGCTGGTAATATATTGCTGCACTG3	
<i>β-actin Sense</i>	5'CCAACCGCGAGAAGATGA 3'	97 bp
<i>β-actin Antisense</i>	5'CCAGAGGCGTACAGGGATAG3'	

2.2 Methods

2.2.1 Cell Culture

2.2.1.1 Cell Line and Culture Conditions

Parental MCF-7 cells (MCF-7/S) and doxorubicin resistant cells (MCF-7/Dox) were preserved in 12 mL of RPMI 1640 medium (Appendix A) with 10% (v/v) fetal bovine serum (FBS) and 1% (v/v) gentamycin in T-75 tissue culture flasks with filter cap (Thermo Fisher Scientific, USA). These flasks were incubated at 37 °C in a 5% (v/v) CO₂ in a Heraeus incubator (Hanau, Germany).

2.2.1.2 Passaging of Cells

Cell passaging means detachment of the cells from the surface treated area of culture flask with their substrate and transferring them to new culture flask. When cells covered the surface area of culture flask largely, cells were needed to passage by trypsinization inside of the laminar flow cabinet. In trypsinization process, medium was discarded and cells were washed with 4-5 mL of PBS to eliminate the inactivation effect of the serum for trypsin. Trypsin-EDTA (1 mL) was added on the cells and incubated at 37 °C for 5-7 minutes until the cells detached. These cells were resuspended in medium which contains serum and required number of cells were transferred to a new culture flask. Lastly, Doxorubicin (1µM) was added to the doxorubicin resistant MCF-7 (MCF-7/Dox) cells after every passage for the maintainance of the resistance.

2.2.1.3 Cell Freezing

In cell freezing process, detached cells were resuspended in 4 mL of medium which contains serum and added on a 15 mL Falcon tube (Greiner Bio-one, Netherlands). After that, cells were centrifuged 1,000 rpm for 6 min. After discarding supernatant, the cell pellet bottom of the falcon tube was homogenized in 4 mL of PBS and centrifuged at 1,000 rpm for 6 min again. The supernatant was removed and cells were resuspended in the freezing medium (10% (v/v) DMSO + 90% (v/v) FBS) to have a final concentration of approximately 2 million cells per mL. Lastly, the cell suspension was added into a cryovial (Greiner Bio-one, Netherlands) and the cells were respectively incubated at 4 °C for 30 minutes and at -20 °C for 3-4 hours and finally at -80 °C for overnight. If long term storage is needed, cryovials can be transferred to a liquid nitrogen tank.

2.2.1.4 Thawing Frozen Cells

Because of the toxic effect DMSO which above 4 °C to the cells, thawing the frozen cells quickly is very important at 37 °C. After this quick thawing process, cells were transferred to a 15 mL Falcon tube (Greiner Bio-one, Netherlands) and then centrifuged at 1,000 rpm for 6 min. Finally, cells were seeded into a culture flask in culture medium which contains serum.

2.2.1.5 Viable Cell Counting by Trypan Blue Exclusion Method

The activity of Trypan Blue stain is based on the chromophore is negatively charged and does not interact with the cell unless the membrane is damaged (Freshney, 1987). Therefore the dead cells are stained into blue and so viable cell exclusion can be done.

The suspension of cell was mixed with trypan blue solution (0.5%) with a ratio of 9:1 and counted in a Neubauer hemacytometer (Bright-line, Hausser Scientific, USA) under phase contrast microscopy (Olympus, USA).

The hemacytometer includes 16 large squares and each square is divided into 16 small squares. One small square represents a volume of 0.00025mm^3 . The number of cell in 1 mL could be determined by the help of the formula below (Equation 2.1):

$$\text{Cell number/mL} = \text{Average count per square} \times \text{Dilution factor} \times 4 \times 10^6 \quad (2.1)$$

2.2.2 siRNA and Transfection

2.2.2.1 FlexiTube *VIM* siRNA and *Mock* siRNA

VIM siRNA *mock* siRNA were both custom designed and consist of 21 nucleotides. The most efficient *VIM* siRNA was purchased from Qiagen. The *VIM* siRNA sequence targeted directly *VIM* mRNA at sequence 5'AAGATCCTGCTGGCCGAGCTC 3'. The *mock* siRNA consists of a scrambled sequence that does not lead to the specific degradation of any cellular message in human genome. The table 2.2 shows the sequences of *VIM* siRNA.

Table 2.2. The sequences of *VIM* siRNA.

siRNA	Sequence
<i>VIM</i> Sense	5' GAUCCUCUGGCCGAGCUCTT 3'
<i>VIM</i> Antisense	5' GAGCUCGGCCAGCAGGAUCTT 3'

2.2.2.2 Transfection

Transfection was performed using HiPerFect transfection reagent and serum free medium according to the manufacturer's instructions. The most efficient concentration of siRNA was determined by the results of flow cytometry analysis. The final concentration of siRNA was 5 nM (approximately 150 ng) and diluted in 100 μL of serum free medium and 12 μL of transfection reagent was added to the diluted siRNA and mixed by vortexing. The mixture was incubated for 5-10 minutes at room temperature to allow to the formation of transfection complexes. This mixture was added drop-wise on seeded cells on a 6-well plate. 2×10^5 cells were seeded on per well of a 6-well plate in 2300 μL of culture medium containing serum and antibiotics. After adding the

transfection complex onto the cells, 6-well plate was swirled gently to ensure uniform distribution of the transfection complex. Lastly, cells were incubated with the transfection complexes under their normal growth conditions and observed gene silencing after 48 or 72 hours transfection.

2.2.3 Reverse Transcription-Quantitative Polymerase Chain Reaction (RT-qPCR)

2.2.3.1 Isolation of Total RNA

In order to Rnase inactivation, all the materials were treated with diethyl carbonate (DEPC) treated distilled water (Appendix B).

NucleoSpin® RNA II RNA isolation kit was used for total RNA isolation according to the manufacturer's protocol.

Untreated MCF-7/S and MCF-7/Dox cells and transfected with *VIM* and *mock* siRNA MCF-7/Dox cells were used for total RNA isolation. Transfected cells were harvested after 48 and 72 hours from 6-well plates. In order to have a cell pellet, cells were discarded, trypsinized and centrifuged at 1,000 rpm for 6 minutes. Supernatant was poured off and cell pellet was homogenized in 350 µL of Buffer

RA1 and 3,5 µL of β-mercaptoethanol. After that, this mixture was vortexing vigorously to ensure proper digestion of cell membrane. Then, the mixture was added on a NucleoSpin® Filter and centrifuged for 1 minutes at 11,000 X g. The NucleoSpin® Filter was discarded and 350 µL ethanol (70%) was added to the homogenized lysate and mixed by pipeting up and down for 5-6 times. For RNA binding, NucleoSpin® RNA II Columns were used for each preparation. The lysate was pipetted up and down for 2-3 times and loaded to the NucleoSpin® RNA II Columns. 350 µL MDB (Membrane Desalting Buffer) was added and centrifuged at 11,000 g for 1 minutes. At that time, Dnase reaction mixture containing 90 µL Reaction Buffer and 10 µL reconstituted rDNase was prepared and 95 µL Dnase reaction mixture was applied directly onto the center of silica membrane of the column and then incubated at room temperature for 15 minutes. In order to inactivation of rDNase reaction mixture, 200 µL Buffer RA2 was added and centrifuged at 11,000 g for 30 seconds. As second washing step, 600 µL Buffer RA3 was applied and centrifuged for 30 seconds at 11,000 g. For final washing step, 250 µL Buffer RA3 was added and centrifuged for 2 minutes at 11,000g. Finally, for eluting the total RNA, 40 µL Rnase-free water was applied and centrifuged at 11,000 g for 1 minute.

2.2.3.2 Quantifying RNA by Spectral Absorption

The optical density was measured at 260 and 280nm for determination of the concentration and purity of isolated total RNA samples. RNA can be quantified using absorption of light at 260 and 280nm (A₂₆₀/A₂₈₀). Ideally, this ratio should be close to 2 for higher quality of samples. For quantification of total RNA purity, where absorbance ratio of 260nm to 280 nm is considered (Equation 2.2).

[RNA] = A260 X DF X 40.0 ;
A260 = Absorbance at 260 nm,
DF = Dilution Factor,
40.0 = Average Extinction Coefficient of RNA (2.2)

2.2.3.3 Agarose Gel Electrophoresis for Monitoring RNA Samples

It is important to observe the thoroughness of RNA samples and the DNA contamination for further experiments' quality. Agarose gel electrophoresis was performed in order to get this information.

1% agarose gel was prepared for having the best results. 0,5 g agarose was weighted and dissolved in 50 μ L of 1X TAE buffer (Appendix B). The agarose gel solution was boiled until it melted. After the agarose gel mixture was cooled, 4 μ L ethidium bromide solution (Appendix B) was added and agarose gel solution was poured into electrophoresis apparatus and the comb was placed. After solidification, 4 μ L of RNA sample and 4 μ L of 2X RNA loading dye (Appendix B) were mixed and loaded. After loading, the samples were run at 80V for 40 minutes and then monitored by UV gel acquisition system.

2.2.3.4 cDNA Synthesis

The quantification of interested mRNA, cDNA synthesis was performed. 1 μ g total RNA and 20 pmol random hexamer primer was used for both *VIM* and *β -actin* mRNAs.

During the whole cDNA synthesis process, DEPC treated materials were used. Autoclaved 0.5 mL eppendorf tube was used. 1 μ L total RNA, 20 pmol of the random hexamer primer and Rnase-free water were put into the 0.5 mL eppendorf tube with a total volume of 11 μ L. This mixture was incubated at 70 $^{\circ}$ C for 5 minutes. Afterwards, 2 μ L of Rnase-free water, 4 μ L of 5X reverse transcriptase buffer and 2 μ L of 10 mM dNTP mix were added and incubated at 37 $^{\circ}$ C for 5 minutes. At last, 1 μ L Moloney-Murine Leukemia Virus Reverse Transcriptase added into the eppendorf tube and incubated at 42 $^{\circ}$ C for 1 hour and the final incubation was performed at 70 $^{\circ}$ C for 10 minutes. After the final incubation, cDNA was stored at -20 $^{\circ}$ C.

2.2.3.5 Quantitative Real-Time Polymerase Chain Reaction (RT-qPCR)

This method was performed in Rotor-Gene (Corbett Research, Australia). Light-cycler-Faststart DNA Master SYBR Green I Kit (Roche Diagnostics) was used for detection of amplification products, according to the manufacturer's protocol.

The mixture was prepared in the autoclaved 0.2 mL eppendorf tubes. This mixture included 10 μ L SYBR Green PCR master mix (2X), 0.3 μ L antisense and sense primers, 2.8 μ L cDNA and to make the final volume 20 μ L, 6.9 μ L Dnase-free water. Untreated MCF-7/S and MCF-7/Dox samples and *VIM* and *mock* siRNA transfected MCF-7/Dox samples was run with non template control and three diluted standarts. Non template control consisted of DNase-free water, instead of cDNA and standarts were prepared from MCF-7/S cDNAs and diluted respectively 1:10, 1:50 and 1:100. Each samples were prepared as triplicates and put into the machine and amplification

conditions (Table 2.3) for *VIM* and *β-actin* genes were programmed. QPCR amplification plots were monitored by plotting fluorescence versus threshold cycle number.

In order to be sure that only expected products were generated, melting curve analysis had been done. All PCR products should have the same melting temperature, by this means It can be clearly understood that there is not any mispriming, DNA contamination or primer dimer.

Table 2.3 Amplification Conditions for *VIM* and *β-actin* Genes.

	<i>VIM</i>	<i>β-actin</i>
Pre-incubation	95 °C, 10 min	95 °C, 10 min
Denaturation	94 °C, 30 sec	94 °C, 30 sec
Annealing	54 °C, 30 sec	54 °C, 30 sec
Extension	72 °C, 30 sec	72 °C, 30 sec
Melting	50-99 °C	50-99 °C
Cycle number	45	40

2.2.3.6 Quantitation of RT-qPCR Products

For quantification of all PCR products, delta delta Ct ($2^{-\Delta\Delta Ct}$) method was performed. This method serves the quantitation of fold changes in gene expressions and normalized them to an internal control. Furthermore, by the help of this quantitation method, It is possible to make some relative groups, like treated and untreated control or a sample at time zero in a time-course study (Livak & Schmittgen, 2001). The equation below (Equation 2.3) was used for quantitation of the *VIM* and *β-actin* gene expression levels and *VIM* gene was normalized to the *β-actin* (internal gene). The threshold cycle values for *VIM* and *β-actin* genes are shown in Appendix C.

$$\text{Fold Change} = 2^{-\Delta\Delta Ct}$$

$$\Delta\Delta Ct = (C_{T \text{ Target}} - C_{T \text{ Internal Control}})_{\text{Treatment}} - (C_{T \text{ Target}} - C_{T \text{ Internal Control}})_{\text{No Treatment}} \quad (2.3).$$

2.2.3.7 Statistical Analysis

All data were prepared as three different runs and each run was performed in triplicates and expressed as mean \pm standard error of the means (SEM). Statistical analysis was evaluated by the use of SPSS 13.0 Software (SPSS Inc., USA). In order to compare mean differences in *VIM* gene expression level both in MCF-7/S and MCF-7/Dox cell lines two paired student t-test was used. In order to detect the differences in variance in transfection efficiency in time, one way ANOVA was used together with Bonferroni Multiple Comparison Test as a post-hoc test. The *p* values less than or equal to 0.05 was considered as statistically significant ($p < 0.05$). The significance was denoted as * $p < 0.05$, ** $p < 0.01$, *** $p < 0.001$.

2.2.4 Determination of siRNA Efficiency

2.2.4.1 Flow Cytometry Analysis

Flow cytometry analysis was carried out at Gülhane Military Medical Academy, Department of Immunology and this service was kindly provided by Prof. Dr. Fikret Arpacı and the senior biologist Aysel Pekel.

Fluorescein (FITC) conjugated SignalSilence® Control siRNA (Cell Signaling Technology®, USA) was used to assess transfection efficiency by BD FACSCanto™ flow cytometer.

Fluorescein (FITC) conjugates can be used with any flow cytometer equipped with an argon laser that emits at 488 nm. The peak emission of FITC is at 525 nm, which is measured in the FL-1 channel. FITC conjugates can also be performed for fluorescence microscopy.

All the samples are prepared in a dark laminar flow cabinet to avoid inactivation effect of the light on fluorescein dye. Five different transfection solution containing five different siRNA concentration (Table 2.4), but same volume of transfection reagent were prepared and MCF-7/Dox cells were transfected in 6-well plate, according to the manufacturer's instructions. 2×10^5 cells were seeded per well of a 6-well plate. After 14 hours of transfection, cells were washed with PBS for three times and then trypsinized, centrifugated for 6 min at 1,000 rpm. The supernatant was discarded and cell pellet was homogenized. Five different sample which have five different siRNA concentration and a cell control including only MCF-7/Dox cells were run into the machine and results were saved and analysed.

Table 2.4 Transfection Solutions

Solutions	siRNA Concentration
1	1nM siRNA
2	3nM siRNA
3	5nM siRNA
4	8nM siRNA
5	10nM siRNA

2.2.4.2 Fluorescence Microscopy after Control siRNA Treatment

In the cause of detection and monitoring of fluorescein (FITC) conjugated into the cells, fluorescence microscopy technique was performed by the kindly help of Prof. Dr. Fikret Arpacı and senior biologist Aysel Pekel at Gülhane Military Medical Academy.

Eclipse 80i Fluorescence Microscope (Nikon, Japan) was used for monitoring of fluorescein (FITC) conjugated siRNA transfected cells. In this microscope, B-2E/C (FITC) channel was chosen for the best quality of visualization.

Five different transfection solution containing five different siRNA concentration as given in Table 2.4, but same volume of transfection reagent were prepared and MCF-7/Dox cells were transfected in 6-well plate, according to the manufacturer's instructions. 2×10^5 cells were seeded per well of a 6-well plate. After 14 hours of transfection, cells were washed with PBS for three times and then trypsinized, centrifugated for 6 min at 1,000 rpm. The supernatant was discarded and cell pellet was homogenized. The highest amount of Fluorescein (FITC) conjugated control siRNA (10 nM) was chosen for the ideal visualization of transfected cells. The images of cells were photographed with 20 X objective by DS-5M digital camera (Nikon, Japan) which inbuilt on the fluorescence microscope and saved.

2.2.4.3 Statistical Analysis

The percentage of MCF-7/Dox cells which uptake fluorescein (FITC) conjugated control siRNA were determined using BD FACSDiva™ Software and the results were expressed as mean \pm SEM (Standard Error of Mean). The differences in variance of the mean fluorescence intensity were determined by one way ANOVA test together with Dunnett's Multiple Comparison Test as a post-hoc test. The p values less than or equal to 0.05 was considered as statistically significant ($p < 0.05$). The significance was denoted as $*p < 0.05$, $**p < 0.01$, $***p < 0.001$.

2.2.5 VIM Expression Analyses by Immunocytochemistry

In order to determine the VIM expression level in MCF-7/S and MCF-7/Dox cell lines, cell suspensions of 500 cells/mm³ (μ l) were prepared separately for these cell lines with PBS and added 0.1 ml of cell suspension to microscope slides coated with Poly-L-Lysine. Slides were positioned in slide holders with filter cards and attached to cytocentrifuge rotor. Samples were centrifuged at 1000 rpm for 10 minutes. Slides were removed and immediately dipped in 95% ethanol and 5% glacial acetic acid (Merck, Germany) fixative for 2 minutes, respectively. Slides were rinsed three times for 5 minutes with PBS to remove fixative. Slides were incubated with 0.25-0.5% Triton X-100 (Sigma, Taufkirchen, Germany). in PBS for 10 minutes to permeabilize the membranes of cells. Slides were again rinsed three times for 5 minutes in order to remove detergents. Slides were washed with ethanol three times for 15 minutes and then washed with distilled water for 5 minutes. Slides were microwaved in Tris/EDTA buffer, pH 9 (Dako, Denmark) three times for 5 minutes for retrieval of antigen. After microwaving, slides waited for 20 minutes in order to cool to room temperature. After this step, slides were washed with distilled water and then washed with PBS for 10 minutes. After this step, in order to block the endogenous peroxidase slides were incubated in 3% peroxide (H₂O₂) in PBS for 10 minutes. Ultra V Block (Thermo Fisher Scientific) was applied to the slides as protein block prior to the first primary

antibody and incubated for 5 minutes and after this step slides were incubated with vimentin primary antibody for 30 minutes. After incubation with vimentin primary antibody, slides were washed with PBS for 10 minutes and then incubated with biotinylated goat antiserum (Dako, Denmark) for 20 minutes. After this step, slides were washed with PBS for 10 minutes and then incubated with streptavidin (Dako, Denmark) for 20 minutes. After this step, slides were incubated with AEC Substrate chromogen (Dako, Denmark) until they get coloured (pink) (approximately 5-10 minutes). Coloured slides were washed with distilled water and washed with hematoxylin for 5 minutes. After washing with distilled water, three or four drops of ultramount mounting medium (Dako, Denmark) was applied to the slides with a thin layer. Slides were photographed under a Leica light microscope.

2.2.6 VIM Protein Expression Analyses

2.2.6.2 Protein isolation and quantification

Proteins of *VIM* siRNA and mock siRNA transfected MCF-7/Dox cells were isolated by using M-PER protein isolation kit (Pierce, Rockford, IL, USA) containing protease inhibitors (Roche, Mannheim, Germany) according to the manufacturer's guidelines. The protein content was measured using the modified Bradford Assay using a Coomassie Plus protein assay reagent with 1:10 dilutions in molecular biology grade water.

2.2.6.3 Vimentin Western blot analyses

Whole-cell extracts (60µg) and prestained PageRuler protein ladder (Fermentas) were separated in a 10% polyacrylamide gel and transferred onto a PVDF membrane at 4°C for 1,5 hours. The membrane was blocked in 10% skim milk and probed with vimentin antibody (1:500 dilution) followed by a horseradish peroxidase-conjugated rabbit anti-goat (1:2000 dilution) secondary antibody. After final washing steps with PBS-T, the excess buffer on the membrane was removed and the bands were visualized by using an enhanced chemiluminescence kit (Pierce) according to the manufacturer's instructions. Briefly, 1.5 ml of solution A was mixed with 1.5 ml of solution B of the chemiluminescence kit and applied onto the surface of membrane, left for 1 minute after which the membrane was dried and wrapped with stretch film. The image was taken by a Kodak X-ray processor.

Equal protein loading was confirmed by probing the same membrane for β-actin. The membrane was stripped after vimentin western blot analysis by using a mild stripping buffer at RT for 15 minutes with shaking, and then it was blocked in 10% skim milk and probed with a HRP conjugated β-actin monoclonal antibody (1:2000 dilution). After final washing steps with PBS-T the bands were visualized by enhanced chemiluminescence kit as described above.

2.2.6.4 Statistical Analyses

Data analysis and graphing was performed using the GraphPad Prism 5 software package. Statistical analysis between experimental results was based on Mann Whitney U-test. The *p* values less than or equal to 0.05 was considered as statistically significant ($p < 0.05$). The significance was denoted as * $p < 0.05$, ** $p < 0.01$, *** $p < 0.001$. Densitometric analyses of Western blots were carried out with image processing programme Image J.

2.2.7 Detecting Cell Motility and Cell Invasion and Image Analysis

2.2.7.1 Cell Migration Assay

In order to determine metastatic ability, boyden chamber cell migration assay was performed. First of all, the differences on cell migration between Doxorubicin sensitive MCF-7 and Doxorubicin resistant MCF-7 cells were illustrated and then *VIM* siRNA transfected MCF-7/Dox cells were used to show *VIM* gene effect on cell migration.

Transwell cell migration assays were performed in a 24 well-plate. 300 μ L medium containing serum was added onto the lower compartments of 24 well-plate and 8 μ m Transwell filters (upper compartment) were put onto the these lower compartments. Therefore the migrated cells passed through the pores of the membrane and migrated onto the lower surface of the filter.

Untreated MCF-7/S and MCF-7/Dox cells and transfected MCF-7/Dox cells were used for understanding of their migration abilities.

Transfection was performed by following the manufacturer's instructions, as mentioned previously. 2×10^5 MCF-7/Dox cells were seeded on 6-well plate before the short time of transfection and transfection solution including 6 μ L *VIM* siRNA, 12 μ L HiPerFect transfection reagent (Qiagen) and 82 μ L serum free medium to make final volume of 100 μ L was prepared and added on the seeded cells drop-wise. The same instruction was followed for *mock* siRNA transfection. After 48 hours of transfection with both *VIM* and *mock* siRNA, cells were harvested by trypsin-EDTA and centrifuged at 1,000 rpm for 6 minutes. After discarding of supernatant cells were washed with serum free medium for three times for removing of serum. After that, 100 μ L of cell suspension containing 5×10^4 cells was put onto membrane of the 8 μ m Transwell filters (upper compartment) (Figure 2.1). After 24 hours incubation at 37 $^{\circ}$ C with 5% CO₂, Transwell was waited on 100% methanol for 10 minutes and stained with Giemsa solution for 2 minutes at room temperature. In order to removing of unmigrated cells, membrane of Transwells were swabbed of by sterile cotton swabs twice and washed with distilled water for 3 times. After the drying out process, the membranes of Transwell filters were cut off and fixed onto the surface of a microscop slide by the help of a drop of oil. All the migratory cells were counted at 20 X magnification under a Leica light microscope. The experiment was performed with 4 replicates for each sample.

2.2.7.2 Cell Invasion Assay

Understanding of invasion capability is a very important issue for metastatic phenotype, thus boyden chamber cell invasion assay with matrigel gives the best results. Because the matrigel is a gelatinous protein mixture which secreted by Engelbreth-Holm-Swarm (EHS) mouse sarcoma cells. Its main components are structural proteins such as collagen, entactin, and laminin which allow the cells invade a barrier of ECM (extracellular matrix) like environment.

Firstly, differences in invasiveness between MCF-7/S and MCF-7/Dox cell lines were detected by the help of this method. After that, MCF-7/Dox cells were transfected by both *VIM* and *mock* siRNA according to the manufacturer's protocol which mentioned before. 2×10^5 cells were seeded on 6-well plate before the short time of transfection. Transfection solution which contents of 6 μ L *VIM* siRNA, 12 μ L HiPerFect transfection reagent (Qiagen) and 82 μ L serum free medium to make final volume of 100 μ L was prepared. The transfection solution was added on cells inside of 6 well-plate, drop-wise. After 48 hours of this transfection period, cells were trypsinized, centrifuged at 1,000 rpm for 6 minutes. Supernatant was poured out and the cell pellet was homogenized. After 3 steps of washing the cells with serum free medium, 100 μ L of cell

suspension including 1×10^5 cells was prepared. Before the preparation of this cell suspension, the matrigel was waited on ice at 4°C overnight, since matrigel solidifies very quickly, and also all the materials needed to be used in this process was left at -20°C overnight, either. After this step, 100 μL of matrigel was put onto the membranes of Transwell (upper compartment) to make them matrigel coated. In this process, 24 well-plate was used as in migration assay. The 24 well-plate was incubated at 37°C with 5% CO_2 for 5-6 hours. After this incubation period, 100 μL cell suspension was added on matrigel coated Transwell membrane (upper compartment). 300 μL of medium including serum also was added onto the lower compartment's into the 24 well-plate. Upper compartment was put onto the lower chamber and incubated at 37°C with 5% CO_2 for 24 hours. After this final incubation period, Transwells were left on 100% methanol for 10 minutes and then, waited on Giemsa solution for 2 minutes at room temperature. Cleaning of uninvaded cells, sterile cotton swabs were used for 3 or 4 times. After that, Transwells were washed for three times with distilled water to ensure removal of the uninvaded cells. After the drying out process, the membranes of Transwell filters were cut off and fixed onto the surface of a microscope slide by the help of a drop of oil. All the migratory cells were counted at 20 X magnification under a Leica light microscope. The experiment was performed with 4 replicates for each sample.

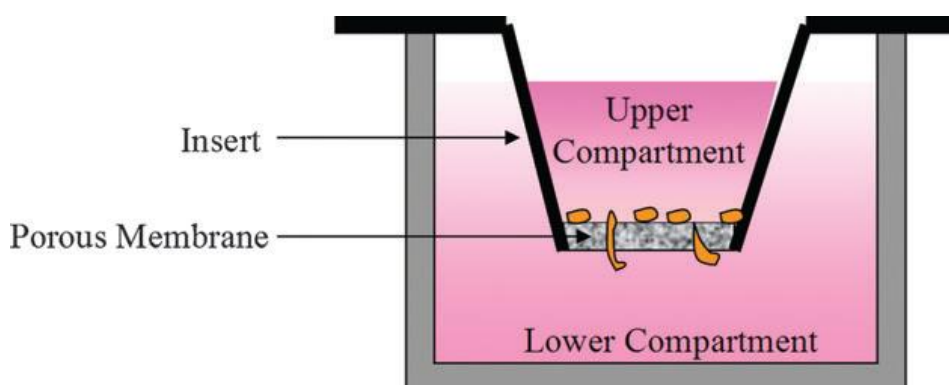


Figure 2.1 The Boyden Chamber assay is shown as two compartments separated with a porous membrane in which cells can pass through. The lower compartment has the medium containing serum or several chemoattractant solutions like fibronectin. Therefore, cells can be forced to pass through to lower compartment. These migratory cells get stuck in porous membrane of Transwell and then is counted to determination of migration ability (Toetsch et al, 2009).

2.2.7.3 Statistical Analysis

All data were prepared as three different runs and each run was performed in triplicates and expressed as mean \pm standard error of the means (SEM). Statistical analysis was evaluated by the use of SPSS 13.0 Software (SPSS Inc., USA). Membranes of Transwells were counted and photographed at 20 X magnification under a Leica light microscope. Counting results were taken from 4 replicates for each sample and analysed by using of two paired student t-test analysis method for comparison of numbers of migrated and invaded untransfected MCF-7/S, MCF-7/Dox and *VIM* and *mock* siRNA transfected MCF-7/Dox cells. The p values less than or equal to 0.05 was considered as statistically significant ($p < 0.05$). The significance was denoted as $*p < 0.05$, $**p < 0.01$, $***p < 0.001$.

CHAPTER 3

RESULTS AND DISCUSSION

3.1 Total RNA Isolation

In order to amplify the target gene in PCR, cDNA preparation is needed from the total RNA. Quality, purity and concentration of the RNAs are very important parameters, so they should be tested before cDNA synthesis. Intactness of the RNA samples were tested by agarose gel electrophoresis where as for RNA quantification spectrophotometric analyses was performed.

cDNAs are only synthesis from mRNA samples, but visualization of mRNAs is not possible because of their less amount (not more than 3%). Whereas total RNAs are rich in rRNAs (approximately 85%), so only rRNA bands can be monitored in a UV transilluminator.

Three bands were detected on gel which were corresponded to 28S, 18S and 5S rRNA . It is shown in Figure 3.1 that there were no DNA contamination and the isolated RNAs were intact.

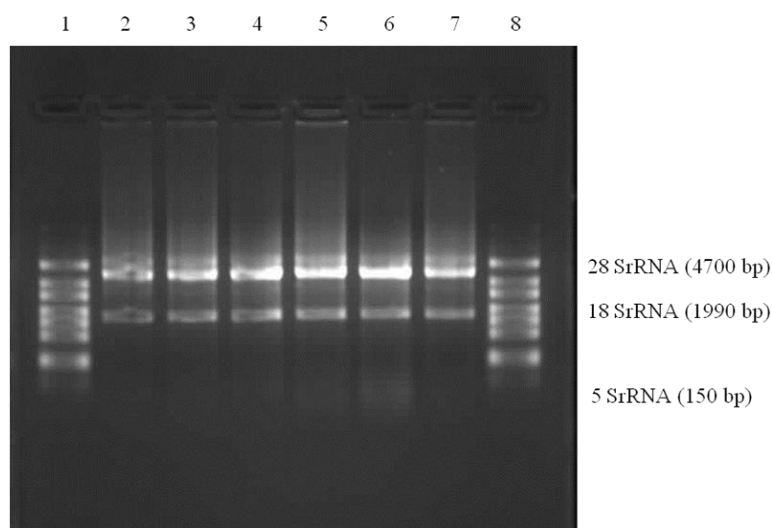


Figure 3.1 Lane 1 and Lane 8. RNA ladder/Lanes 2 to 6. Total RNAs isolated from untreated MCF-7/Dox, mock siRNA treated MCF-7/Dox, *VIM* siRNA treated MCF-7/Dox and untreated MCF-7/S cell lines respectively on 1.2 % agarose gel.

3.2 Determination of Transfection Efficiency

Doxorubicin resistant MCF-7 cells were transfected by fluorescein conjugated SignalSline[®] control siRNA, which has the same charge, configuration and length (21nt), to detection of the most efficient siRNA concentration. The uptake levels of this control siRNA molecules was measured by the usage of BD Biosciences FACS Canto flow cytometer after 14 hours of transfection.

Firstly, MCF-7/Dox cells which were transfected with 5nM siRNA oligo were monitored as a fluorescence image by the usage of fluorescence microscope (Figure 3.2). By the usage of FITC channel, cells can be seen clearly due to green fluorescein dye. It means that the fluorescein conjugated SignalSline[®] control siRNA was successfully uptaken by the MCF-7/Dox cells.

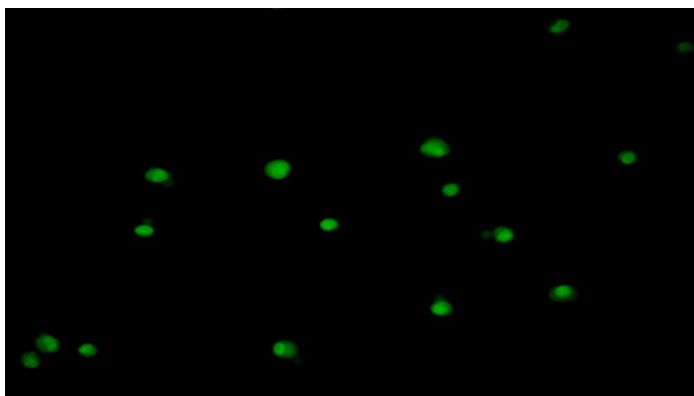


Figure 3.2 MCF-7/Dox cells transfected with fluorescein conjugated SignalSline[®] control siRNA oligo (5nM). The image was taken by Nikon Eclipse 80i fluorescence microscope and with FITC channel (10X).

Although it is expected that the target specific siRNA molecules should effect on only their target mRNA molecules, according to the literature there is a widespread non-specific effect that siRNA could potentially display (Jackson et al, 2003).

Recent studies have shown that transcripts having less than 100% complementarity with an siRNA can be targeted for knock-down by the RNAi pathway (Jackson et al, 2003). This phenomenon, referred to as “off-targeting” is concentration dependent, responsible for up to threefold suppression of dozens of genes, and mediated by either the sense or antisense strand of the siRNA (Fedorov et al, 2006). Moreover, according to another study, it has been shown that around 75% of 359 published siRNA sequences have a risk of non-specific effects by using popular BLAST searching tool, which is inappropriate for such short oligos as siRNAs (Snove & Holen, 2004; Snove et al, 2004).

Even though these negative effects can prevent to have the efficient experimental results and may limit the usage of siRNA, this problem can be overcome by following the stringent design rules, and the determination of the proper concentration level of target specific siRNA, which were also obeyed during selection of *VIM* siRNA in this study (Cui et al, 2004; Elbashir et al, 2001).

It was also reported that at higher siRNA levels may take part in apoptosis and also response for against stress may be influenced nonspecifically (Semizarov et al, 2003).

According to another study, siRNAs and shRNAs can activate one of the cell's antiviral defense mechanisms, called dsRNA-dependent protein kinase (PKR) (Lage, 2005; Sledz et al, 2003). When this defense mechanism is activated, PKR phosphorylate the translation initiation factor (eIF2) and after this phosphorylation, downregulation of translation and sequence independent mRNA degradation occurs (Lage, 2005).

In the light of these informations, determination of siRNA concentration is so important in this study, in order to find out the most efficient siRNA concentration, flow cytometry analyses were first performed for untreated MCF-7/Dox cells (as a cell control) by using 5 different fluorescein conjugated control siRNA concentrations (1nM, 3nM, 5nM, 8nM and 10nM). Although the control cells were not treated with fluorescein conjugated control siRNA, these cells have an auto absorbance and 0,3% of these cells were seen as if they were treated Figure 3.3). Figures 3.4-5-6-7-8 show cells treated with 1nM, 3nM, 5nM, 8nM and 10nM respectively. In each figure, side scatter area versus forward area scatter height gives the gated area for each sample. Then plots from this area were analysed with graphs containing FITC height versus sidescatter area which gives the amount of uptaken fluorescein conjugated control siRNA.

Forward scatter (FSC) tool was used for identifying cell size and side scatter (SSC) was performed for identification of granularity. As a result, how many cells which are in same size uptake the fluorescein conjugated control siRNA could be detected.

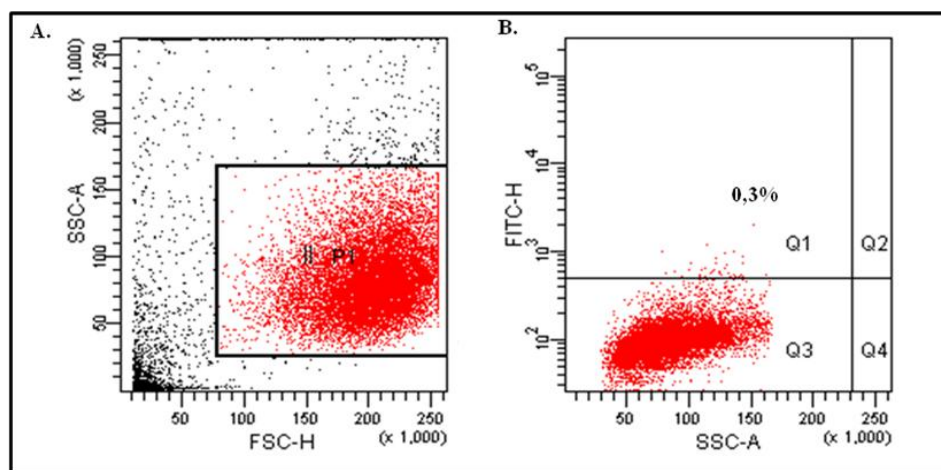


Figure 3.3 A. Side scatter area versus forward scatter graph for cell control (untreated MCF-7/Dox cell line) and gated area was shown on it. B. FITC height versus side scatter area graph showing the gated plots and these plots indicated the fluorescence signal of untreated Doxorubicin resistant MCF-7 cell line.

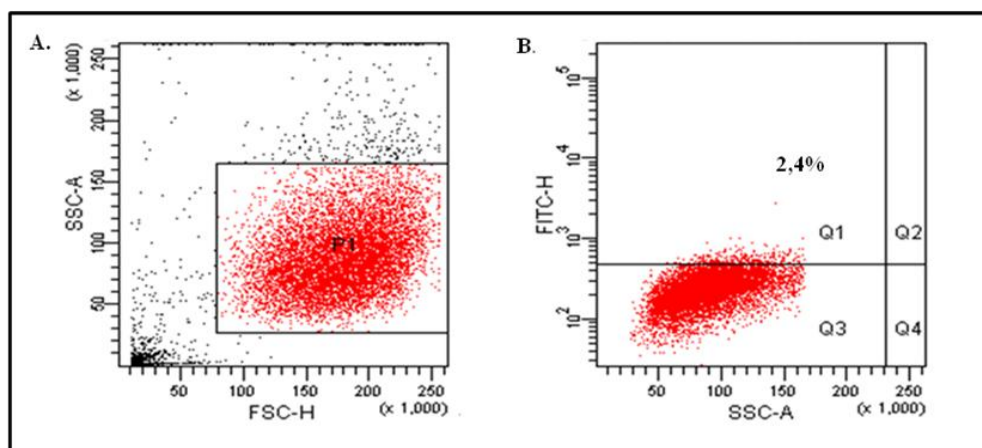


Figure 3.4 A. Side scatter area versus forward scatter graph for the concentration of 1nM fluorescein conjugated control siRNA treated MCF-7/Dox cells and gated area was shown on it. B. FITC height versus side scatter area graph showing the gated plots and these plots indicated the fluorescence signal the concentration of 1nM fluorescein conjugated control siRNA treated MCF-7/Dox cell line.

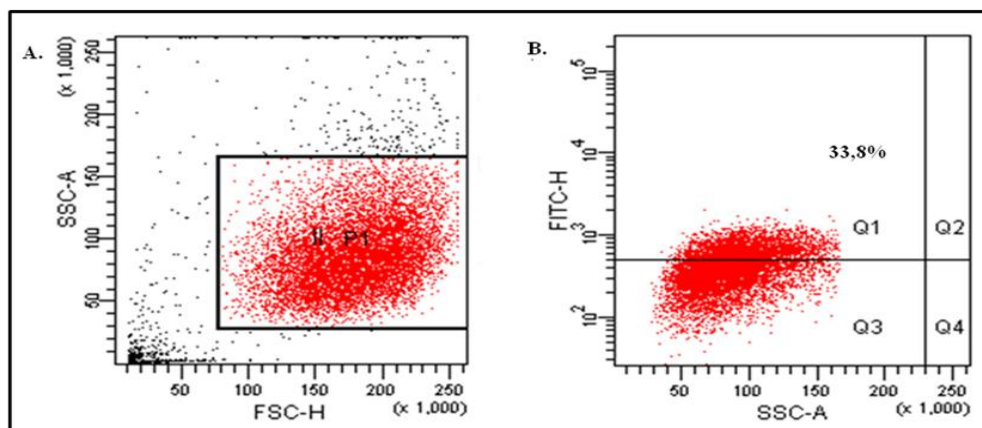


Figure 3.5 A. Side scatter area versus forward scatter graph for the concentration of 3nM fluorescein conjugated control siRNA treated MCF-7/Dox cells and gated area was shown on it. B. FITC height versus side scatter area graph showing the gated plots and these plots indicated the fluorescence signal the concentration of 3nM fluorescein conjugated control siRNA treated MCF-7/Dox cell line.

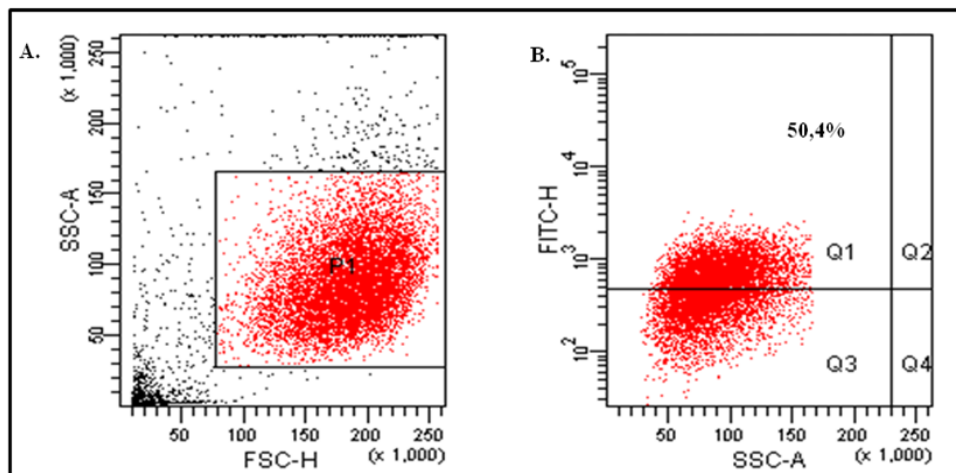


Figure 3.6 A. Side scatter area versus forward scatter graph for the concentration of 5nM fluorescein conjugated control siRNA treated MCF-7/Dox cells and gated area was shown on it. B. FITC height versus side scatter area graph showing the gated plots and these plots indicated the fluorescence signal the concentration of 5nM fluorescein conjugated control siRNA treated MCF-7/Dox cell line.

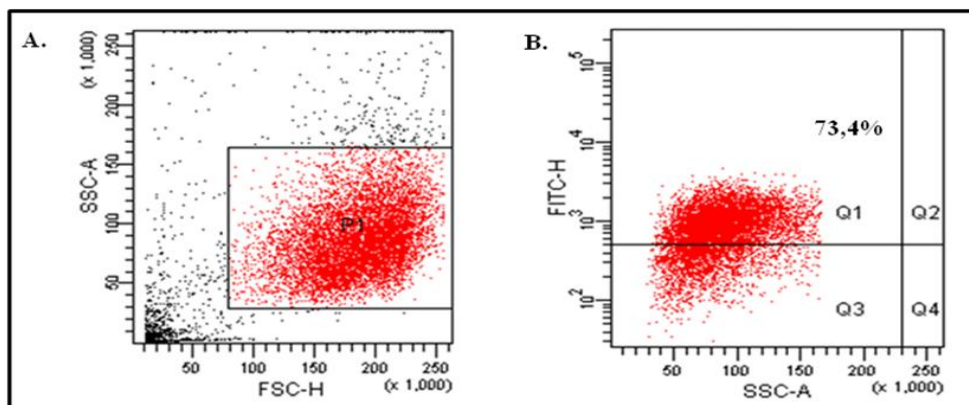


Figure 3.7 A. Side scatter area versus forward scatter graph for the concentration of 8nM fluorescein conjugated control siRNA treated MCF-7/Dox cells and gated area was shown on it. B. FITC height versus side scatter area graph showing the gated plots and these plots indicated the fluorescence signal of 8nM fluorescein conjugated control siRNA treated MCF-7/Dox cell line.

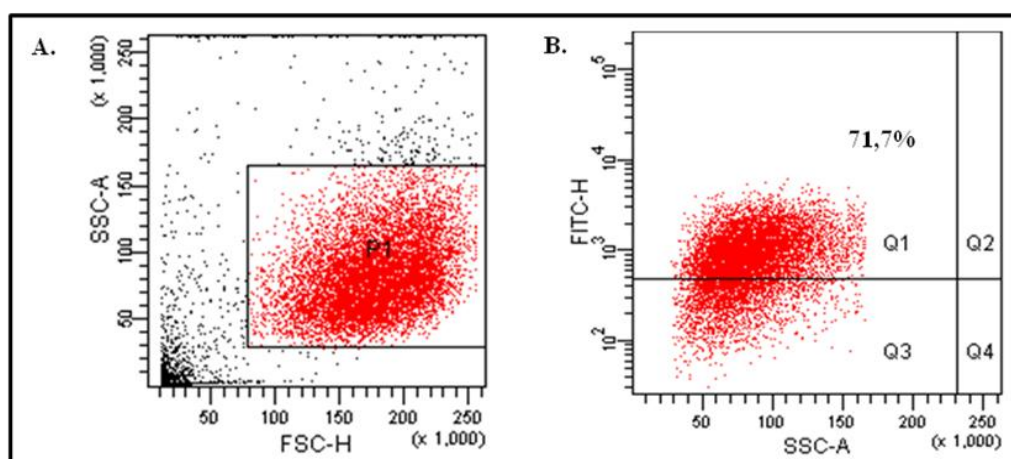


Figure 3.8 A. Side scatter area versus forward scatter graph for the concentration of 10nM fluorescein conjugated control siRNA treated MCF-7/Dox cells and gated area was shown on it. B. FITC height versus side scatter area graph showing the gated plots and these plots indicated the fluorescence signal of 10nM fluorescein conjugated control siRNA treated MCF-7/Dox cell line.

The fluorescence signal was quantified and shown as a bar graph (Figure 3.9). The bar graph showed a continuous increase in the signal by increasing siRNA oligo concentration. According to the transfection reagent protocol, 1nM siRNA would have been the most proper siRNA concentration for MCF-7 cell line. However, the flow cytometry analysis was shown that the level of uptake for this concentration was too low. Although, the fluorescence intensities with 8nM and 10nM siRNA oligo concentrations were significantly higher than the fluorescence intensity at 5nM siRNA oligo concentration, for having safer results in terms of the non-specific interactions 5nM siRNA oligo was selected for further experiments. In conclusion, it was clearly seen that 5nM siRNA oligo amount was efficiently uptaken by the MCF-7/Dox cells and despite the higher fluorescence intensity of 8nM and 10nM siRNA oligos were determined as not required, because of possible non-specific responses in the cells.

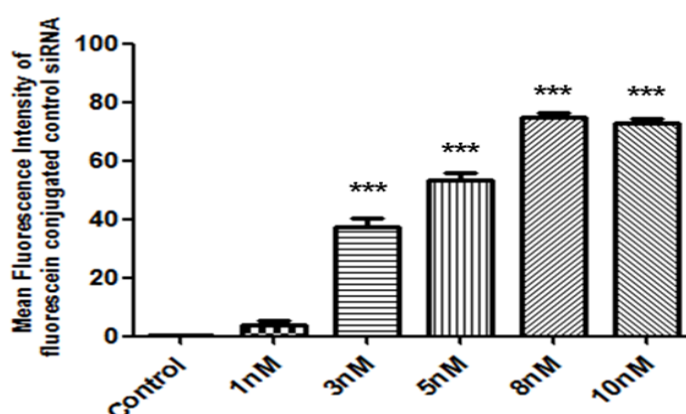


Figure 3.9 Fluorescence intensity bar graph of fluorescein conjugated control siRNA oligo per pixel for different concentrations. *** $p < 0.0001$ in comparison to control untreated MCF-7/Dox cells.

3.3 Quantitative Real-Time Polymerase Chain Reaction (qPCR): Expression analysis of *VIM* and β -actin genes

According to the results of a previous study, it was shown that the vimentin gene expression level was almost 100-fold higher in doxorubicin resistant MCF-7 cell line with respect to its drug sensitive control (MCF-7/S), according to the microarray analysis and immunocytochemical analysis (Iseri et al, 2010). In another study, immunofluorescence microscopy results showed “that vimentin expression was significantly high in MCF-7/Dox cell line. However, MCF-7/S cell line was lack of vimentin expression (Sommers et al, 1992)”.

These studies constituted the main idea of this study to silencing of vimentin gene in MCF-7/Dox cell line and indicated the changes of metastatic and invasive characteristics of this cell line and at first, in order to display *VIM* expression level difference in MCF-7/S and MCF-7/Dox cell lines, qPCR was performed and seen that *VIM* expression level was notably higher in MCF-7/Dox cell line than in MCF-7/S cell line. Amplification plots were displayed by plotting fluorescence versus threshold cycle number as a cycling run. After this cycling run, a melt step was added for both *VIM* and β -actin genes to visualize the dissociation kinetics of the amplified products (Figures 3.10-11).

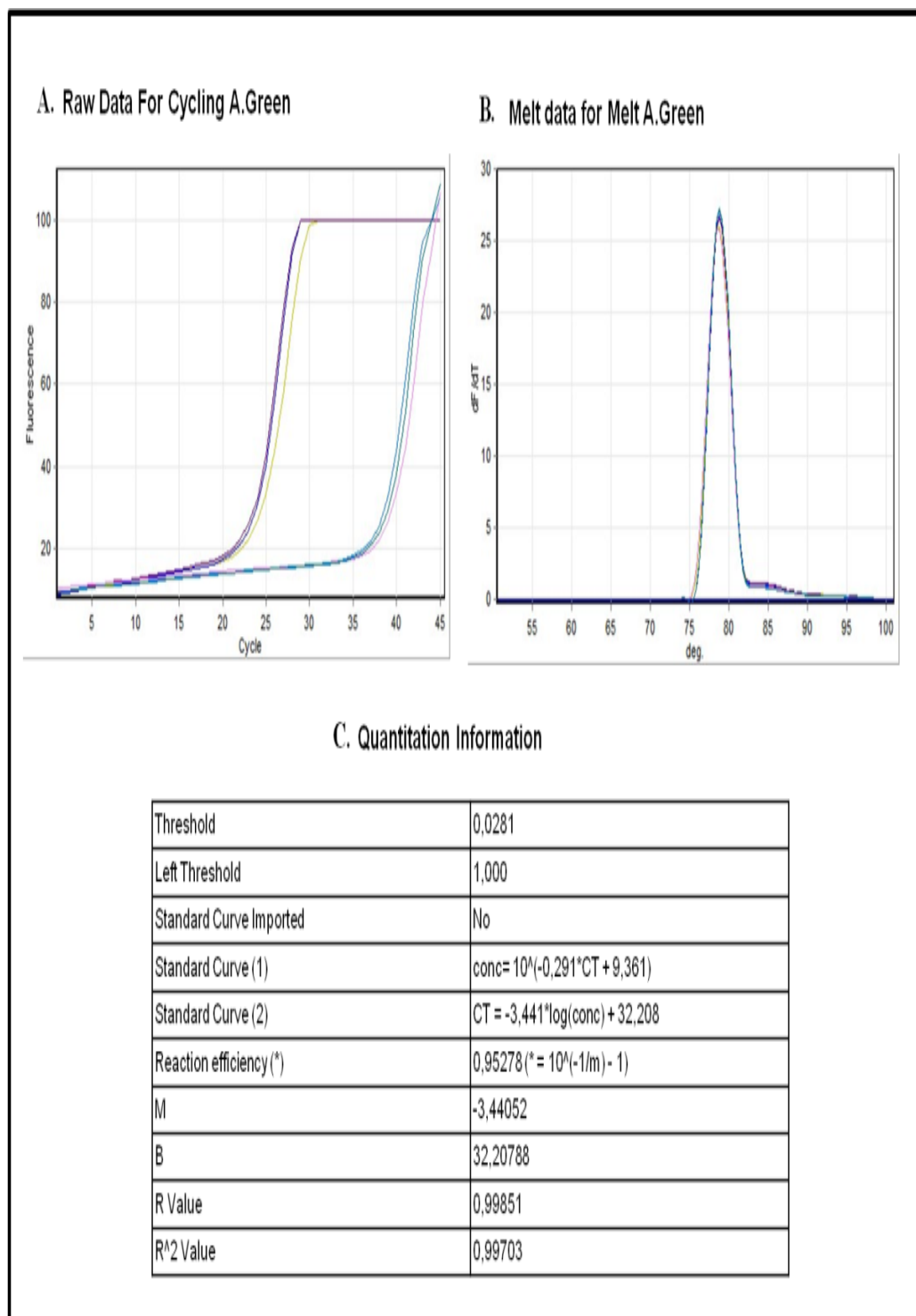


Figure 3.10 A. qPCR Amplification Plots for *VIM* gene. B. qPCR Melting-curve Analysis for *VIM* gene. C. Quantification information for *VIM* gene according to the standart curve.

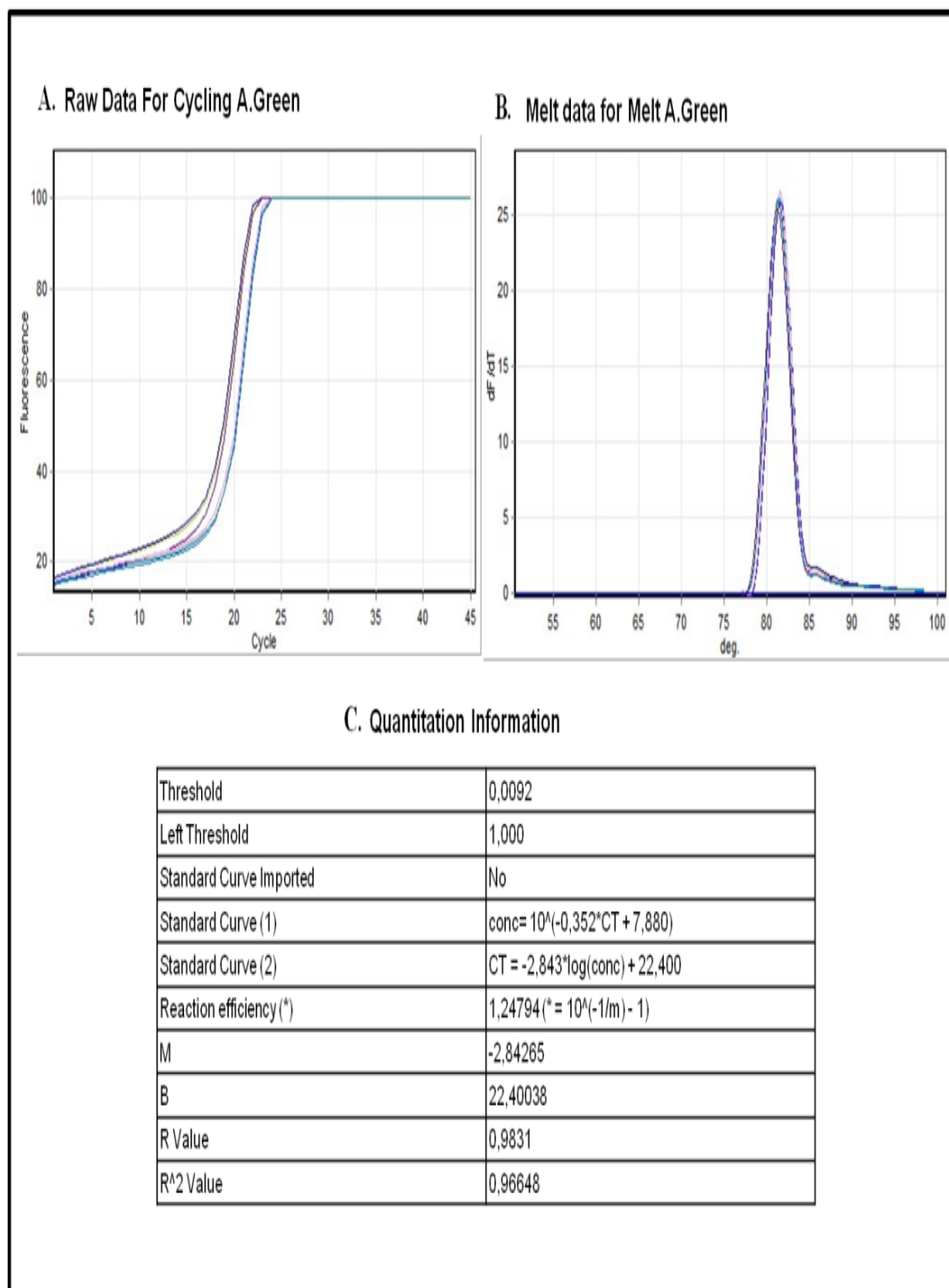


Figure 3.11 A. qPCR Amplification Plots for *β-actin* gene. B. qPCR Melting-curve Analysis for *β-actin* gene. C. Quantification information for *β-actin* gene according to the standart curve.

$2^{-\Delta\Delta CT}$ quantitation method (Livak & Schmittgen, 2001) was used for the normalization of *VIM* by using β -actin gene for both MCF-7/Dox and MCF-7/S cell lines. The results show that *VIM* gene expression was 422 fold higher in Doxorubicin resistant MCF-7 subline with respect to Doxorubicin sensitive MCF-7 cells (Figure 3.12). This result is parallel to the literature.

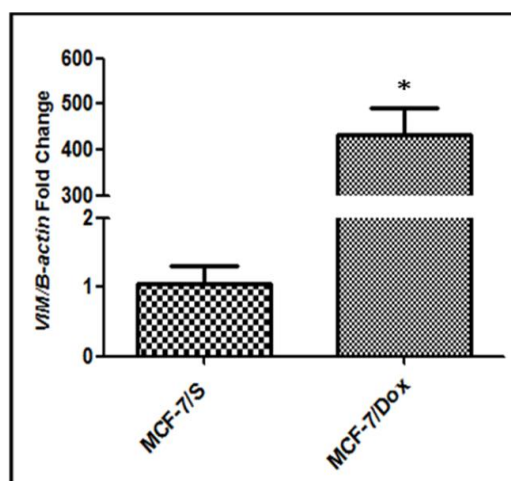


Figure 3.12 *VIM* gene expression levels in untreated MCF-7/Dox and MCF-7/S cell lines. * $p < 0.05$ compared to control untreated MCF-7/Dox cells.

There are several studies showing the relation between *VIM* expression and metastasis. Vimentin is highly expressed in mesenchymal cells and can be related to metastasis (Nijkamp et al, 2011). In another study, it was demonstrated that the overexpression of *VIM* was significantly associated with metastatic behavior of hepatocellular carcinoma ($p < 0.01$). This result was strongly suggested that the overexpression of *VIM* may play an important role in the metastasis of hepatocellular carcinoma (Hu et al, 2004). In other study has shown that silencing of *VIM* resulted in decrease in metastasis and invasion of 1E8-H prostate cancer cell line (Wei et al, 2008). *VIM* silencing also resulted in impairment of metastasis and invasiveness in both metastatic cell lines, SW480 colon cancer and MDA-MB-231 breast cancer cells (McInroy & Maatta, 2007). Similar to these reports, in this study, it was shown that vimentin expression levels were significantly high in several cell lines whereas not in MCF-7/S cell line.

In the light of these studies and reports, MCF-7/Dox cells, which express higher levels of vimentin, were transfected with the concentration of 5nM *VIM* siRNA and the concentration of 5nM mock siRNA, after determination of fluorescence intensity levels of these cells via using flow cytometry results. Transfection was performed with both *VIM* and mock siRNAs for 48 and 72 hours and qPCR was applied for both *VIM* and β -actin genes. Amplification plots were displayed by plotting fluorescence versus threshold cycle number. After having this cycling run, a melt step was added for both *VIM* and β -actin genes to visualize the dissociation kinetics of the amplified products (Figures 3.13-14).

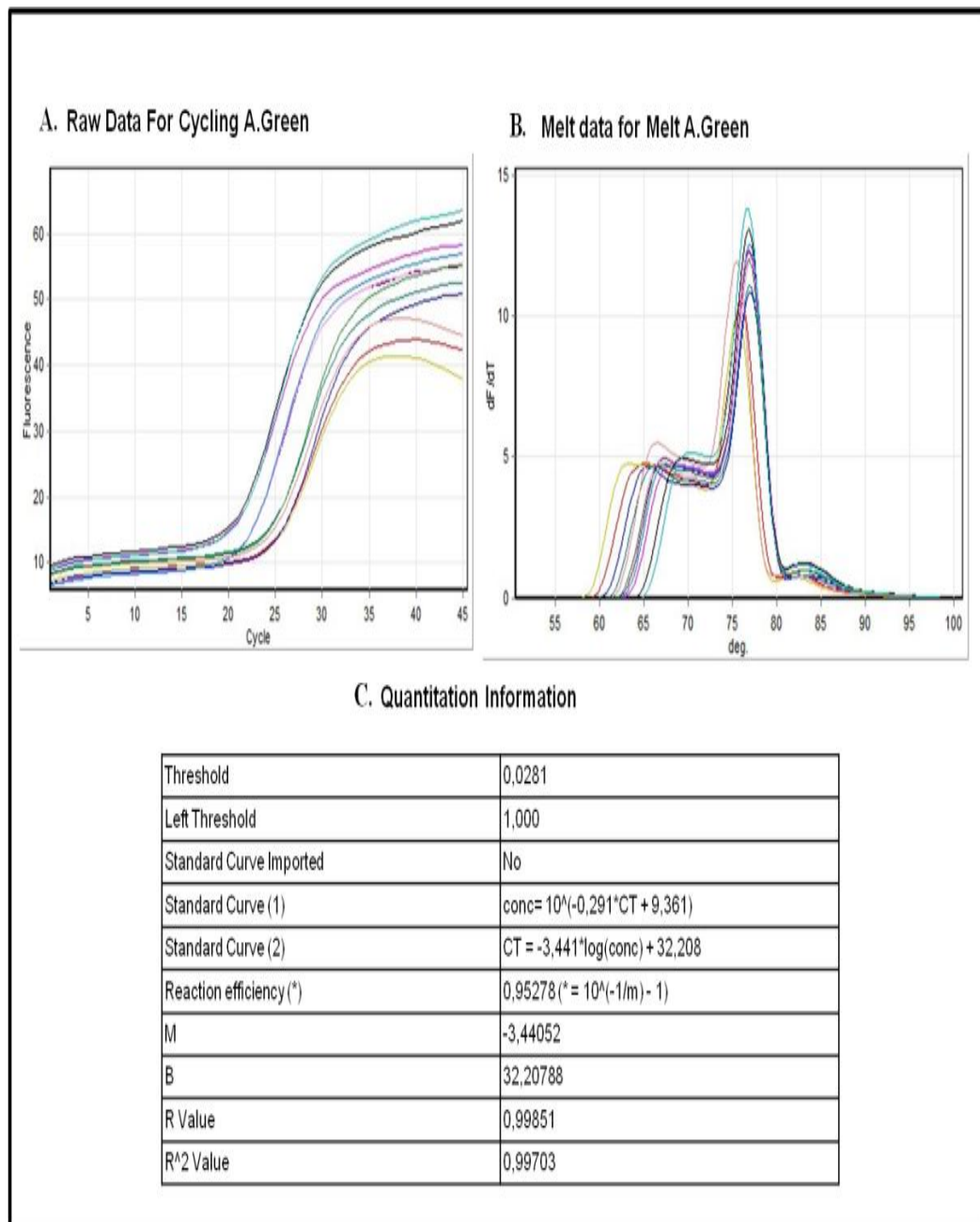


Figure 3.13 A. qPCR Amplification Plots for VIM gene after transfection with VIM siRNA and mock siRNA in MCF-7/Dox cell line. B. qPCR Melting-curve Analysis for VIM gene after transfection with VIM siRNA and mock siRNA in MCF-7/Dox cell line. C. Quantification information for VIM gene after transfection with VIM siRNA and mock siRNA in MCF-7/Dox cell line, according to the standard curve.

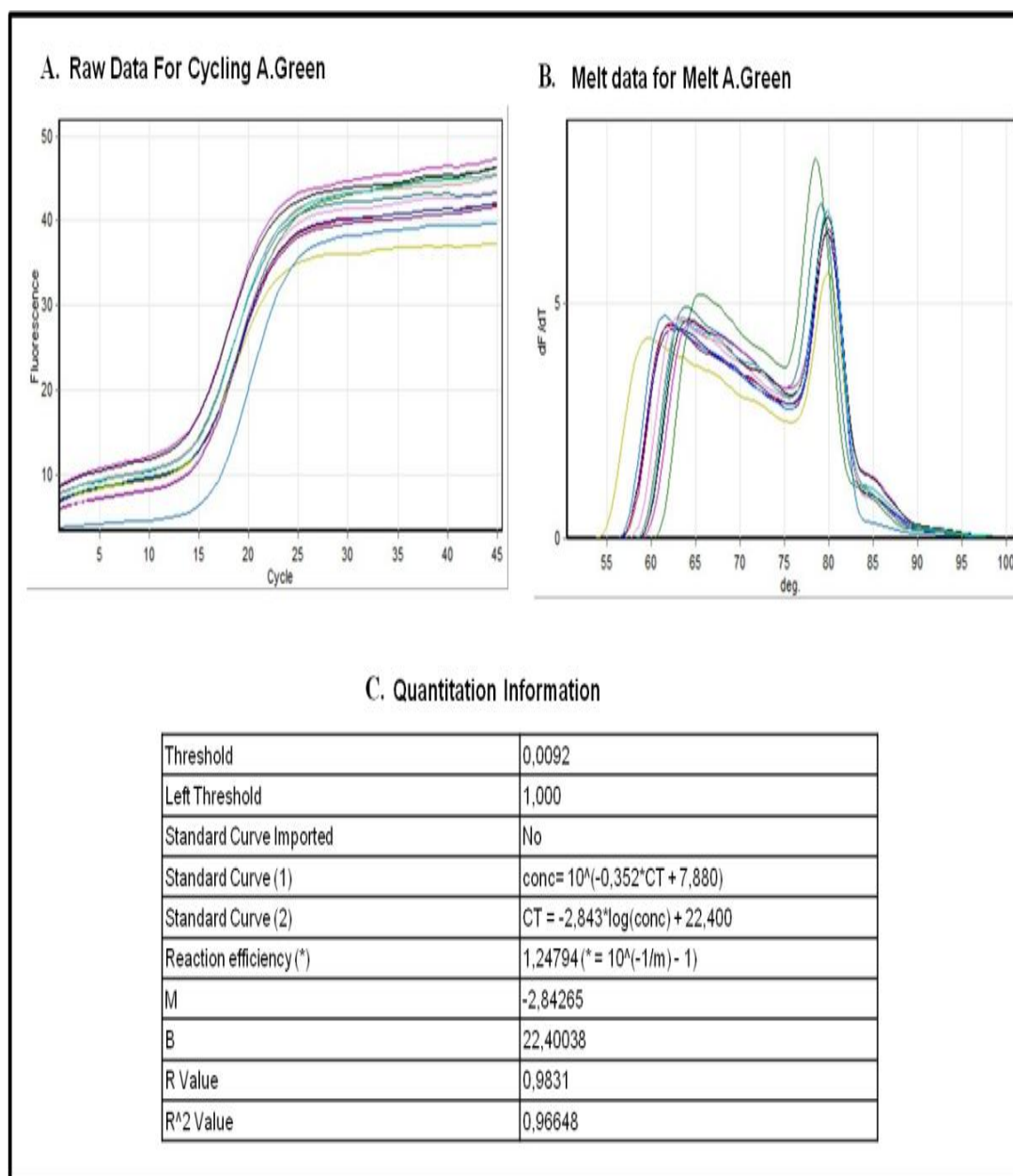


Figure 3.14 A. qPCR Amplification Plots for β -actin gene after transfection with *VIM* siRNA and mock siRNA in MCF-7/Dox cell line. B. qPCR Melting-curve Analysis for β -actin gene after transfection with *VIM* siRNA and mock siRNA in Doxorubicin resistant MCF-7 cell line. C. Quantification information for β -actin gene after transfection with *VIM* siRNA and mock siRNA in Doxorubicin resistant MCF-7 cell line, according to the standard curve.

The amplification data of *VIM* gene was normalized to β -actin gene and subjected to $2^{-\Delta\Delta\text{CT}}$ quantitation method (Livak & Schmittgen, 2001). The results are demonstrated as a bar graph in Figure 3.15.

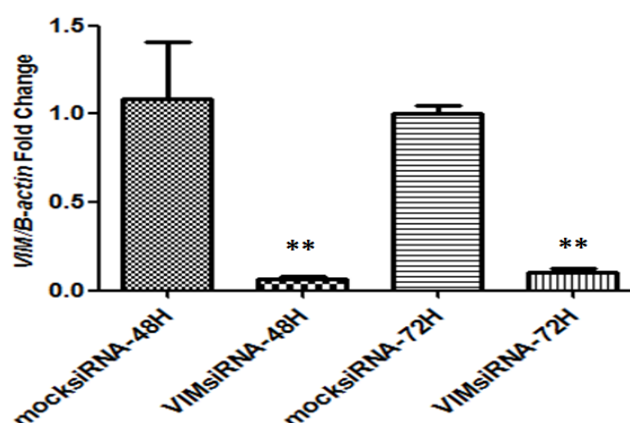


Figure 3.15 *VIM* gene expression after treatment with *VIM* siRNA and mock siRNA oligos for 48 and 72 hours in MCF-7/Dox cell line. ** $p < 0.05$ compared to 48 and 72 hours mock siRNA treatment controls.

In Figure 3.15, downregulation of *VIM* gene expression was evaluated with qPCR after 48 and 72 hours after transfection with *VIM* siRNA. *VIM* mRNA level decreased to 94% after 48 hours treatment with *VIM* siRNA compared to mock siRNA treated control and after 72 hours transfection, *VIM* mRNA level decreased to 90% of the initial level of mock siRNA treated mRNA level. In conclusion, it can be said that the decline of *VIM* was more efficient after 48 hours transfection than after 72 hours transfection. As a transient transfection time, 48 and 72 hours could be considered as non-effective. However, MCF-7/Dox cell line has a long doubling time (51.5 hours), so under this circumstance, siRNA duplexes can inhibit *VIM* effectively for a longer time, when compared to the cells which have faster division characteristics.

One of the most impressive cases of the last several years is the discovery of RNA interference mechanisms (RNAi). This method introducing synthetic small RNA (siRNA) or hairpin RNAs (shRNA) that expressed by plasmid and viral vector systems (Takeshita & Ochiya, 2006).

McInroy and Määttä reported 72% knock-down of vimentin gene expression after 48 hours of transfection with vimentin gene specific siRNA, resulted in decline of metastasis and invasiveness in SW480 (Human colon adenocarcinoma cell line) and MDA-MB-231 (a metastatic human breast cancer cell line) cell lines (McInroy & Maatta, 2007). Also up to 95% inhibition of vimentin gene expression was determined in HN12 (metastatic head and neck cancer cell) cell line by shRNA silencing (Paccione et al, 2008). In another study, PC-3M (a highly metastatic cell line of prostate cancer) cells were transfected with vimentin gene specific siRNA for 48 hours and the expression of vimentin gene was reduced by 35% in comparison to the controls (Nijkamp et al, 2011; Pan et al, 2012a; Pan et al, 2012b).

In comparison to the literature, in this study 90% and 94% gene silencing with specific *VIM* siRNA in MCF-7/Dox cells has a high efficiency for *VIM* inhibition, although the siRNA concentration was kept as low as 5nM.

3.3 Immunocytochemistry Analyses: Determination of VIM expression level in MCF-7/S and MCF-7/Dox cell lines

As a non-invasive breast cancer cell line, MCF-7 cells are vimentin-negative cell line (Hendrix et al, 1997; Ivaska et al, 2005; McInroy & Maatta, 2007; Vuoriluoto et al, 2011). Whereas, doxorubicin resistant MCF-7 cell becomes vimentin-positive, which was previously shown in this study as in mRNA level by qPCR (Iseri et al, 2010; Sommers et al, 1992). It was important to make a comparison between MCF-7/S and MCF-7/Dox cell lines by means of VIM protein expression level on this study. As mentioned and discussed on previous sections of this study, protein level results supported to qPCR analysis results and also to literature. Immunocytochemistry analysis was performed to visualised the VIM protein levels both in MCF-7/S and MCF-7/Dox cell lines and results can be seen in Figure 3.16.

In a study performed by Iseri in our laboratory previously, it was shown that the mesenchymal vimentin was overexpressed in paclitaxel, docetaxel and doxorubicin resistant MCF-7 cells, by immunocytochemistry method. (Iseri *et al.*, 2010). It was previously reported that expression of vimentin causes cytoskeletal reorganization and associated with a poor prognosis and/or a tendency to develop metastasis in breast cancer (Sarrío et al, 2008).

Snail family proteins (Snail, Slug and Twist) are transcription factors and their expression levels are the key regulatory elements of EMT along with the control of expression of many genes, including cell-cell-adhesion, cell survival and apoptosis. Vimentin is one of these genes, as a marker of EMT. The overexpression of Slug (SNAIL2) in Doxorubicin resistant MCF-7 cells and this can increase the expression level of vimentin (Iseri et al, 2011).

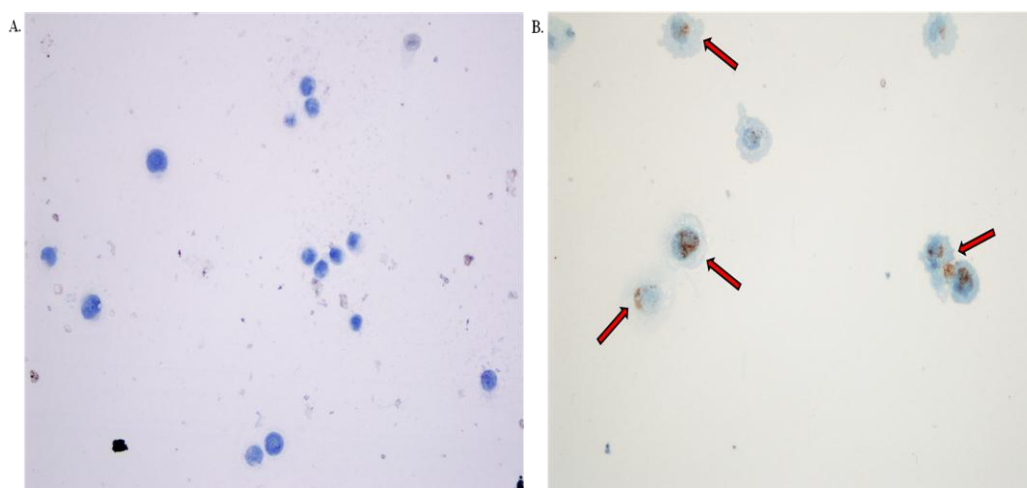


Figure 3.16 A. MCF-7/S cells which does not contain vimentin protein. B. MCF-7/Dox cells which contains vimentin protein. The indication was done to show the vimentin content of these cells.

3.4 Western Blot Analyses: Detection of decline of vimentin after transient transfection with *VIM* siRNA

After determination of the most efficient siRNA concentration by the help of flow cytometry analyses and finding of the most efficient time for transient transfection through qPCR results, as a next step, decline of the amount of vimentin protein concentration was detected by western-blot analyses.

After transfection of MCF-7/Dox cells with *VIM* siRNA total protein isolation was done and western-blot analysis was performed using a mouse monoclonal antibody for vimentin protein as mentioned in material and methods chapter. β -actin was used as a control for normalization.

Vimentin and β -actin protein bands from transfected MCF-7/Dox cell lines were seen in Figure 3.17. Protein levels of vimentin was reduced by 22% in *VIM* siRNA transfected MCF-7/Dox cell line when compared to mock siRNA transfected MCF-7/Dox cell line.

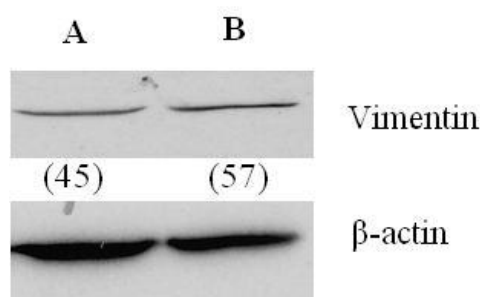


Figure 3.17 Western Blot analyses for Vimentin Protein (57 kDa) expression. Lane A. Protein levels of vimentin in *VIM* siRNA transfected MCF-7/Dox cell line Lane B. Protein levels of vimentin in mock siRNA transfected MCF-7/Dox cell line (control line).

There are several studies showing that many metastatic and invasive breast cancer cell lines express vimentin (Neve et al, 2006), and also it was shown that over-expression of vimentin in MCF-7 cell lines increases trafficking of integrin cell motility and also cell invasiveness (Hendrix et al, 1997; Ivaska et al, 2005).

Knocking down of vimentin gene in MDA-MB-231 (a metastatic human breast cancer cell line) was performed in a study and resulted in reduction of metastatic behaviour. By silencing of vimentin gene, the decline of metastatic and invasive characteristics was related to specific changes in invasiveness-related gene expression including upregulation of *RAB25* (small GTPase Rab25) and downregulation of *AXL* (receptor tyrosine kinase Axl), *PLAU* (plasminogen activator, urokinase) and *ITGB4* (integrin b4-subunit) (Vuoriluoto et al, 2011).

McInroy and Määttä reported that 72% knock-down of vimentin gene expression after 48 hours of transfection with vimentin gene specific siRNA compared to control siRNA transfected line, resulted in decline of metastasis and invasiveness in both SW480 (Human colon adenocarcinoma cell line) and MDA-MB-231 (a metastatic human breast cancer cell line) cell lines (McInroy & Maatta, 2007).

In order to have information for *VIM* silencing, Elbashir and his co-workers tried four different *VIM* siRNA duplex sequences and only one of them worked efficiently in western blot analyses (Elbashir et al, 2002).

Transfection with siRNA duplexes, as a transient transfection method, for 48 hours could not be more efficient for the huge amount of vimentin amplicons in Doxorubicin resistant MCF-7 cell line. Furthermore, the qPCR results have been showed that the mRNA levels of vimentin was highly down regulated (90%-94%). Using siRNA oligos for transfection can cause problems to be able to display the decline of protein levels in as short as 48 hours, because of the degradation of siRNA oligos during tranfection in cell (Chiu & Rana, 2003; Snove & Holen, 2004). Furthermore, it will be possible to see that this reduction amounts for vimentin protein can be considered as functional to see the changes in metastatic and invasive characteristics in next section.

3.5 Boyden Chamber and Matrigel Assays: Visualization of changes in metastatic and invasive characteristics

Boyden chamber and matrigel assay methods were performed in order to visualize the differences in metastatic and invasive characteristics between untreated MCF-7/S and untransfected MCF-7/Dox cell lines. Determination of the most efficient application time for this methods, untransfected MCF-7/S and untransfected MCF-7/Dox cells were subjected to boyden chamber assay for 6, 12, 24, 48 and 72 hours. In Figures 3.18 and 3.19, it can be clearly seen that after 48 and 72 hours treatment, migrated untransfected MCF-7/Dox cells were uncountable, on the other hand 6 and 12 hours treatments were too short for untransfected MCF-7/S cells, being a poorly metastatic and invasive cell line. Furthermore, because of the risk of siRNA degradation during cell migration through the porous compartment of chambers, 48 and 72 hours were too long period of time. In conclusion, 24 hours were determined as the best application time for both boyden chamber and matrigel assays (Figure 3.20). Comparison of metastatic and invasiveness behaviors of these cell was shown as a bar graph in Figure 3.21.

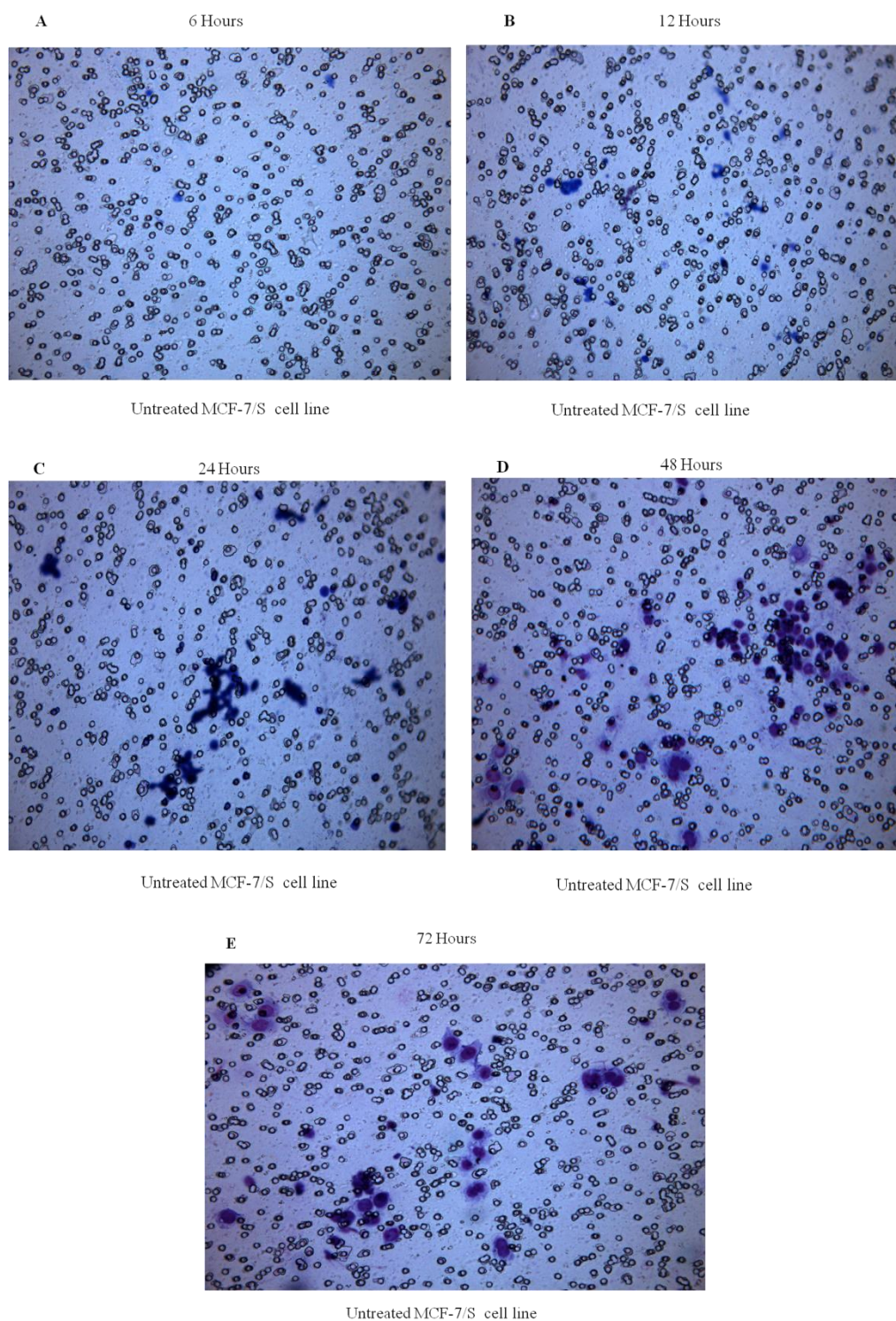


Figure 3.18 Boyden Chamber Assay for untreated MCF-7/S cell line. In A., B., C., D and E. MCF-7/S cells were subjected to boyden chamber assay for 6, 12, 24,48 and 72 hours respectively. For detecting the migrated cells, giemsa stain was used.

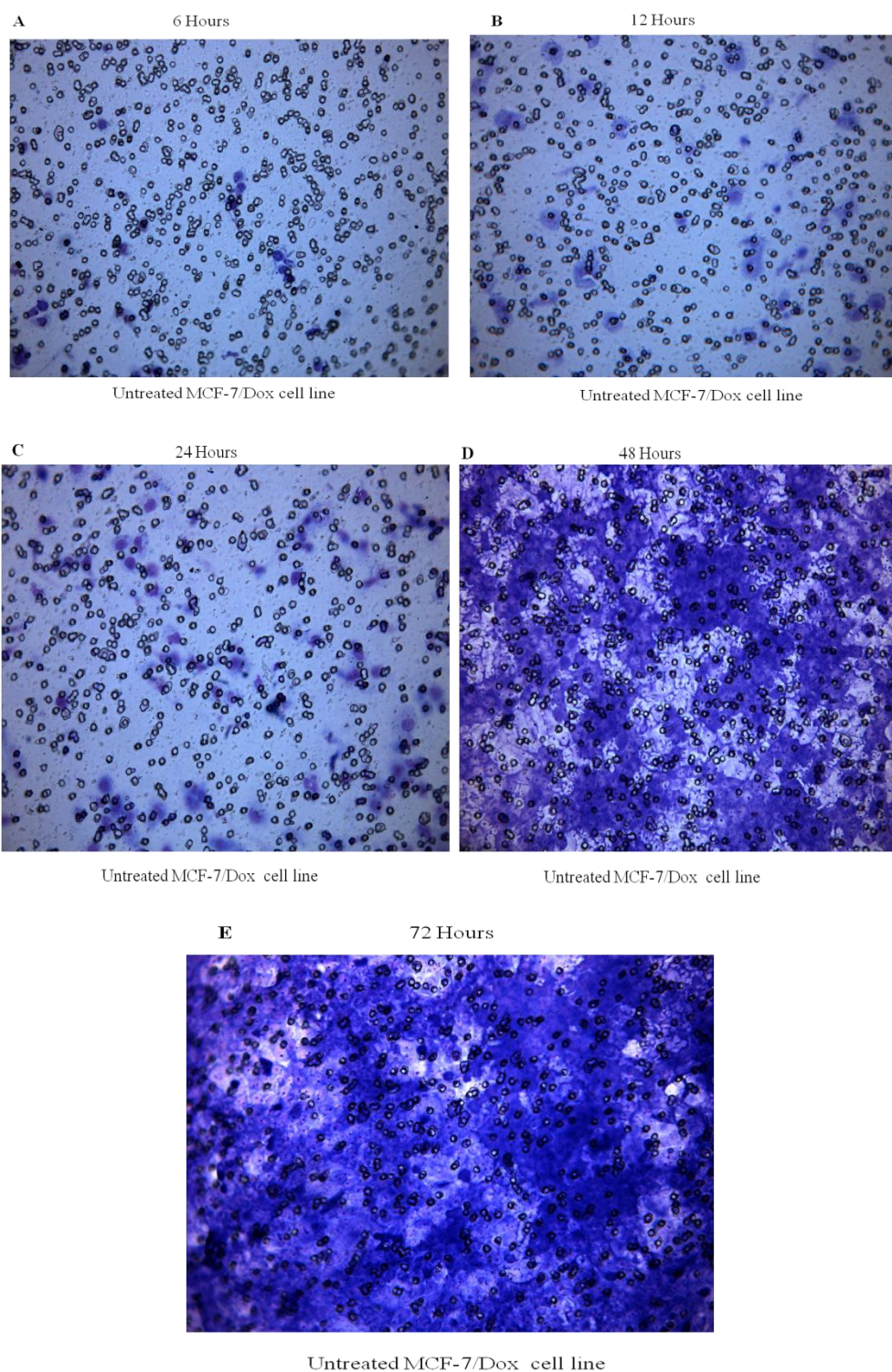


Figure 3.19 Boyden Chamber Assay for untreated MCF-7/Dox cell line. In A., B., C., D and E. MCF-7/Dox cells were subjected to boyden chamber assay for 6-12-24-48-72 hours respectively. For detection of the migrated cells, giemsa stain was used.

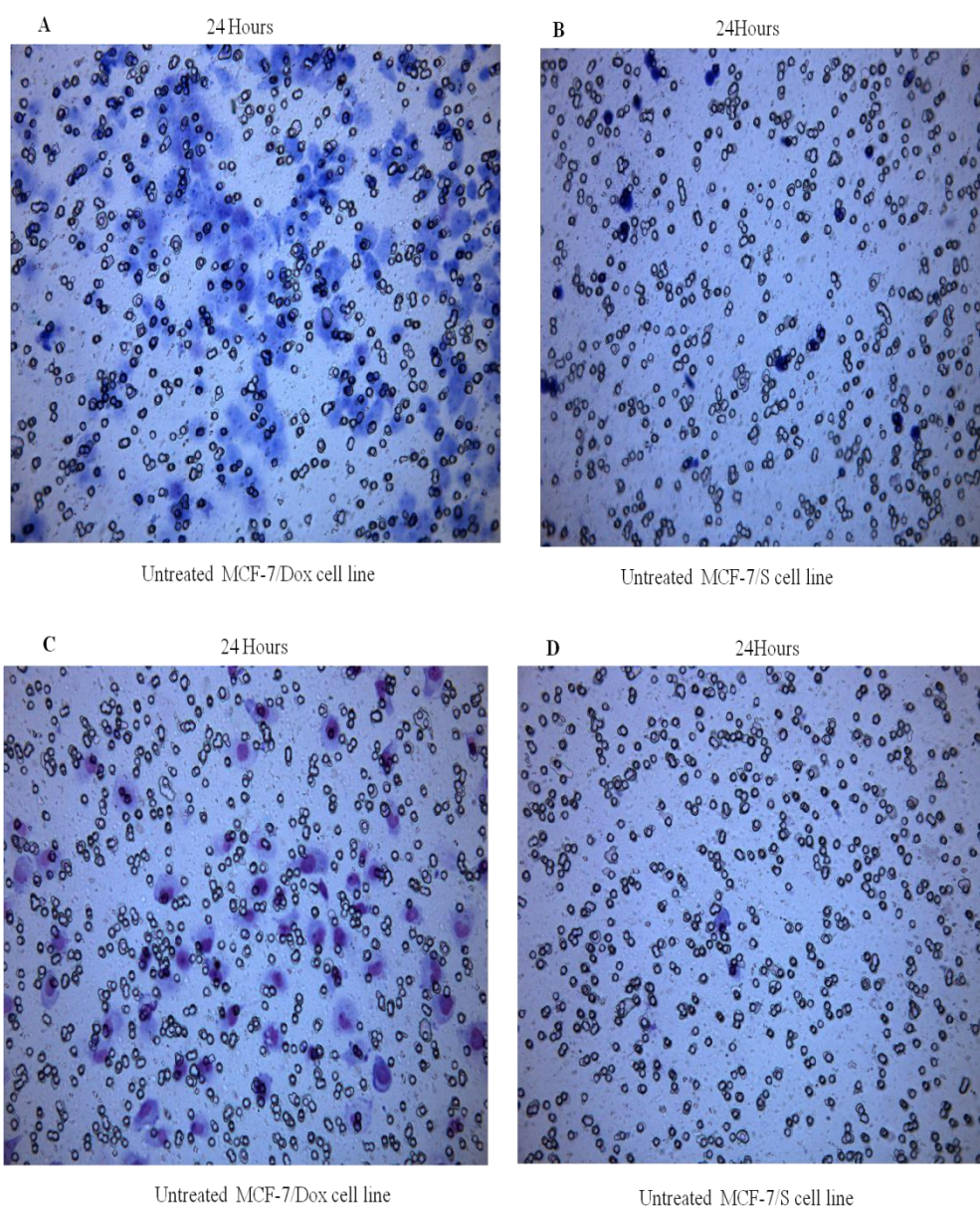


Figure 3.20 Boyden Chamber and Matrigel Assays for untreated MCF-7/Dox and untreated MCF-7/S cell lines. A. MCF-7/Dox cells were subjected to boyden chamber assay for 24 hours and migrated cells are shown. B. MCF-7/S cells were subjected to boyden chamber assay for 24 hours and migrated cells are shown. C. MCF-7/Dox cells were subjected to matrigel assay for 24 hours and invaded cells are shown. D. MCF-7/S cells were subjected to matrigel assay for 24 hours and invaded cells are shown. For detection of the migrated and invaded cells, giemsa stain was used.

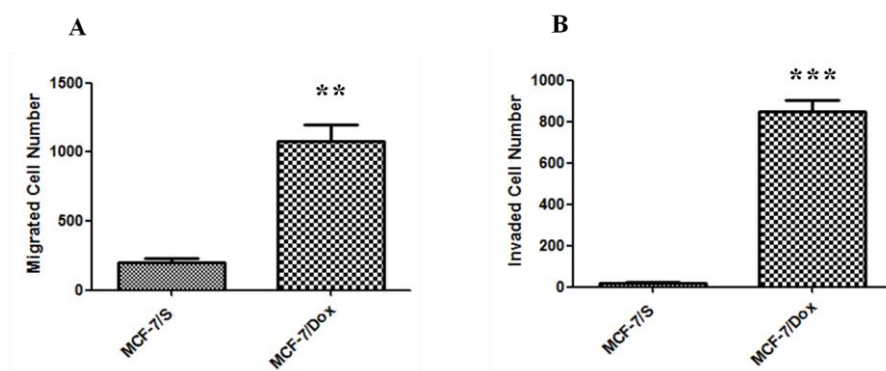


Figure 3.21 A. Migrated cell number comparison between MCF-7/S and MCF-7/Dox cell lines after Boyden Chamber Assay. B. Invaded cell number comparison between MCF-7/S and MCF-7/Dox cell lines after Matrigel Assay. ** $p < 0.05$ compared to migrated MCF-7/S cell number and *** $p < 0.05$ compared to invaded MCF-7/S cell number.

These images and graphs clearly indicate that MCF-7/Dox cells are a highly metastatic cell line. Whereas, MCF-7/S cells have not been shown as aggressive ability. Recent studies showed that this situation was related to differences in vimentin expression levels between drug resistant and drug sensitive MCF-7 cell lines (Valque et al, 2012; Vuoriluoto et al, 2011). In this study and in other several studies, it was demonstrated that MCF-7/S cells exhibit negligible vimentin (Iseri et al, 2010; Mendez et al, 2010; Thompson et al, 2005). Whereas, MCF-7/Dox cells have a high amount of vimentin (Iseri et al, 2010).

In recent years, several evidences have been suggested that metastasis might be improved against to resist apoptosis and highly metastatic cancer cells show greater ability of survival and resistance to apoptosis than poorly metastatic cell lines (Shtivelman, 1997). Thus, it can be thought that cancer cells may obtain invasive and metastatic characteristics, during resistance gaining, although these mechanisms remain poorly understood.

There are some recent studies that have been mentioned to these unknown mechanisms. Kang and his colleagues showed that MCF-7/Dox cells were highly metastatic and invasive, comparing to MCF-7/S cells. They thought that this increment could be related to overexpressed *Cox-2* gene. They demonstrated that invasiveness of MCF-7/Dox cells resulted from overexpression of *Cox-2*, which was induced by either the *EGFR*-activated *PI3K/Akt* or *MAPK* pathway. Inhibition of either *Cox-2* or the *PI3K/Akt* pathway efficiently inhibited the metastasis and invasiveness of MCF-7/Dox cells (Kang et al, 2011). However, there are always other regulations, indeed. In another study, Yao and his co-workers showed the metastatic and invasive ability of MCF-7/Dox cell lines and they related *IL-18* overexpression to metastasis and invasiveness (Yao et al, 2011).

In this study, the relation between *VIM* expression and metastasis was investigated in MCF-7/Dox cell line, as drug resistant breast cancer cell line. There are several reports showing this relation in different cell lines. One of them reported that in highly metastatic cell lines, vimentin-positive SW480 (colon cancer cell line) and MDA-MB-231 (breast cancer cell line), vimentin was silenced with *VIM* siRNA and it was seen that metastatic and invasive characteristics of these lines impaired (McInroy & Maatta, 2007). In another study, it was indicated that an unknown and important relation between vimentin and the expression of *Axl* and suggested that *Axl* is an important proximal mediator of vimentin-induced effects on cell motility. Silencing of vimentin resulted in downregulation of *Axl* both on mRNA and protein levels and subsequent inhibition of cell motility in MDA-MB-231 cells. The same group also showed that *Slug* and *Ras*-induced EMT changes (cell migration, morphology and induction of *Axl*) were dependent on the upregulation of vimentin (Figure 3.22) (Vuoriluoto et al, 2011). And also Iseri et al. demonstrated the overexpression of vimentin and relevant pathways (Figure 3.23) (Iseri et al, 2011).

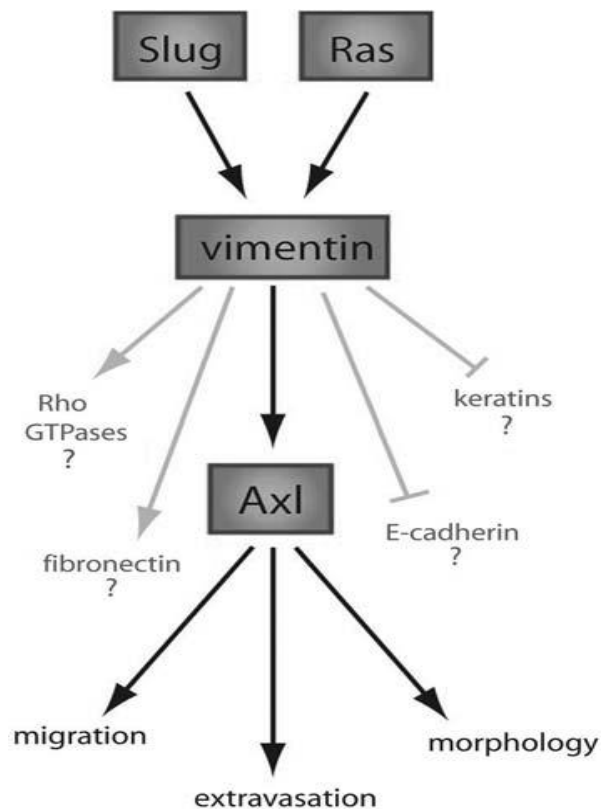


Figure 3.22 Vimentin has an important role in *Slug* and *Ras* induced migration and upregulation of *Axl* (Vuoriluoto et al, 2011).

Also another study demonstrate that the expression of vimentin in epithelial cells is sufficient to induce several important features of the EMT, including the increased cell motility and also acceptance of a mesenchymal shape (Mendez et al, 2010). In another study showed that *E-cadherin* and *Snail* upregulates the expression of the mesenchymal markers, vimentin and fibronectin, and proteins involved in cancer invasion such as metalloproteinases 2 and 9 (MMP2 and MMP9) (De Craene et al, 2005).

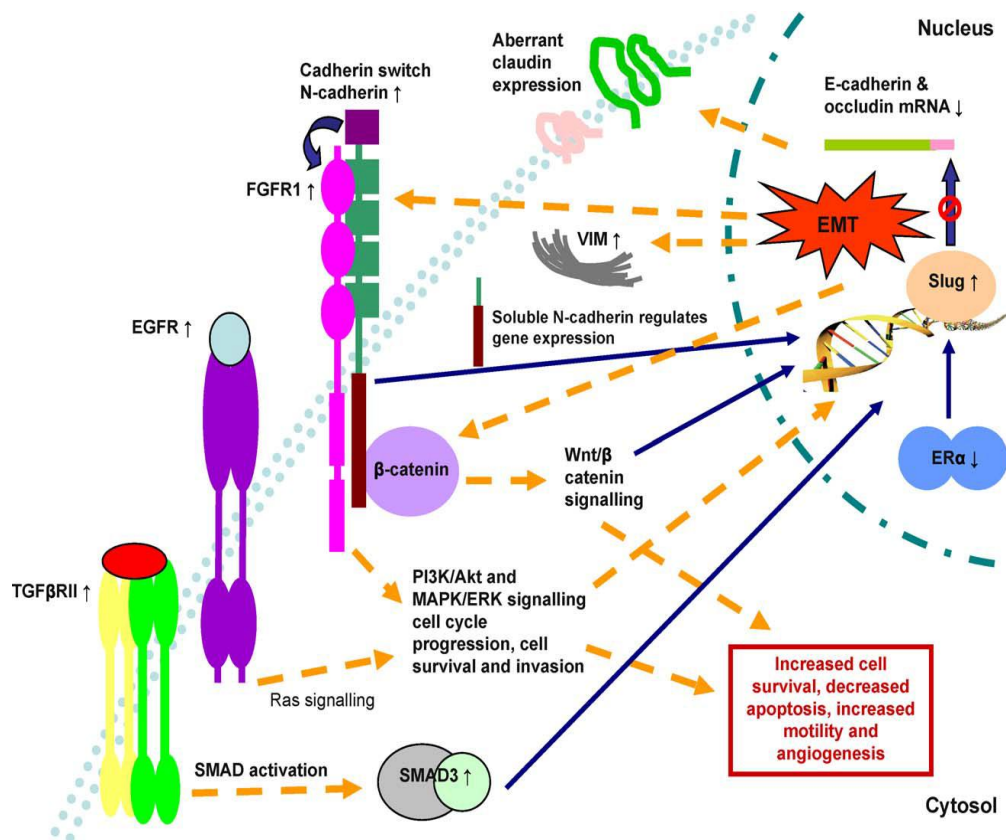


Figure 3.23 The relation between vimentin and other pathway in Doxorubicin resistant MCF-7 cell line (Iseri et al, 2011).

Hu and his co-workers reported that downregulation of vimentin expression resulted in decline of metastatic and invasive behaviors of a metastatic hepatocellular carcinoma cell line (H2-M) (Hu et al, 2004).

Another study showed that a phenotype resembling EMT in patients with head and neck squamous cell carcinoma (HNSCC) is related to loss of *E-cadherin* and gain of *vimentin*, with a significantly higher risk of metastasis formation (Nijkamp et al, 2011).

And lastly, a study reported that vimentin can promote tumor cell invasiveness by regulating the *E-cadherin/β-catenin* complex via *C-src* in some prostate cancer cells (Wei et al, 2008; Zhao et al, 2008).

In this study, in order to show the relation between the effect of vimentin expression and cell motility in MCF-7/Dox cells, the cells were transfected with both *VIM* and mock siRNA oligos for 48 hours with the concentration of 5nM, as mentioned in previous sections of this chapter. After this treatment, in order to determine the changes in the metastatic and invasive characteristics for transfected MCF-7/Dox cells were subjected to boyden chamber and matrigel assays and mock siRNA transfected MCF-7/Dox cells were used in same implementations as a control line. The migration and invasion characterisation of the transfected MCF-7/Dox cells were seen in Figure 3.24. The decline of metastatic and invasiveness behaviors of *VIM* siRNA transfected cell lines comparing to mock siRNA transfected cell line was shown as a bar graph in Figure 3.25.

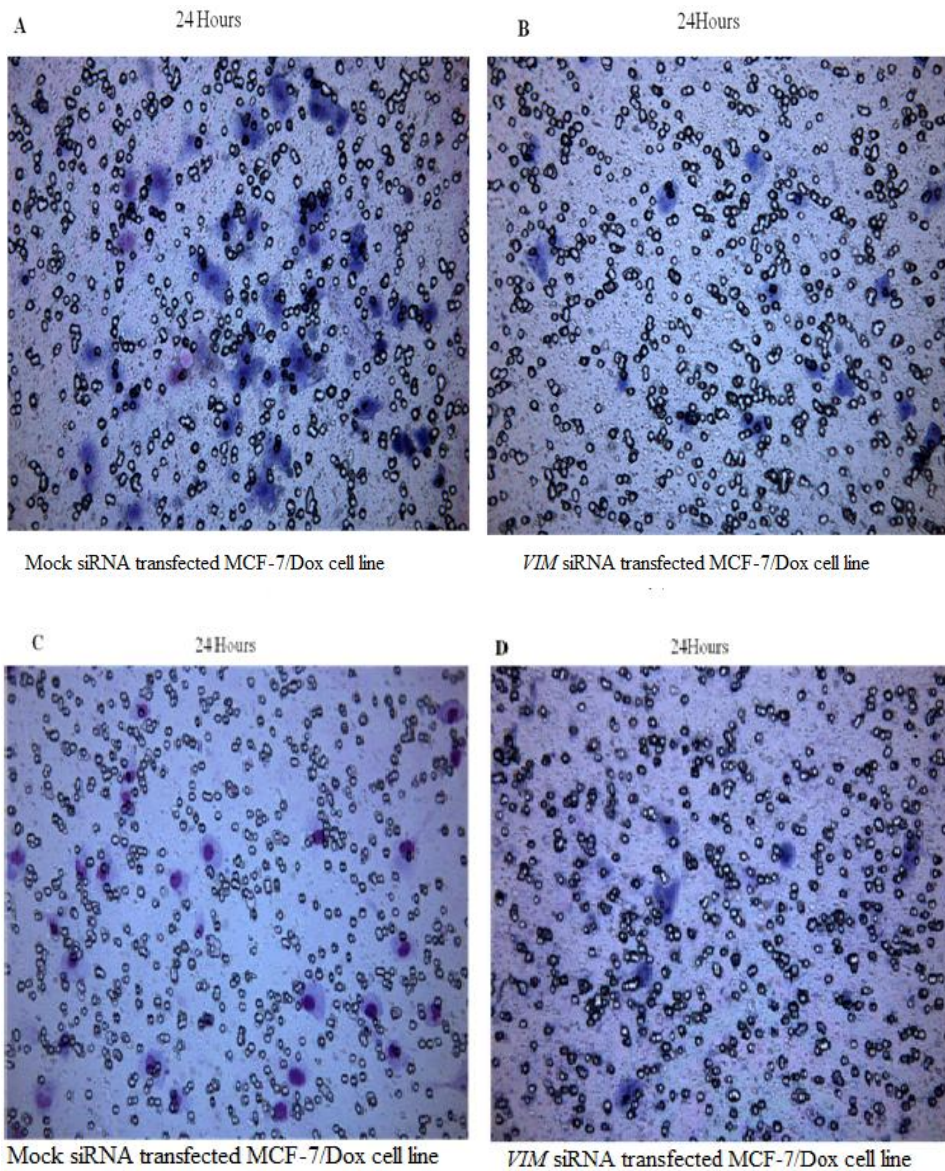


Figure 3.24 Boyden Chamber and Matrigel Assays for *VIM* and mock siRNA transfected MCF-7/Dox cell lines. A. mock siRNA transfected MCF-7/Dox cells were subjected to boyden chamber assay for 24 hours and migrated cells are shown. B. *VIM* siRNA transfected MCF-7/Dox were subjected to boyden chamber assay for 24 hours and migrated cells are shown. C. mock siRNA transected MCF-7/Dox cells were subjected to matrigel assay for 24 hours and invaded cells are shown. D. *VIM* siRNA transfected MCF-7/Dox cells were subjected to matrigel assay for 24 hours and invaded cells are shown. For detection of the migrated and invaded cells, giemsa stain was used.

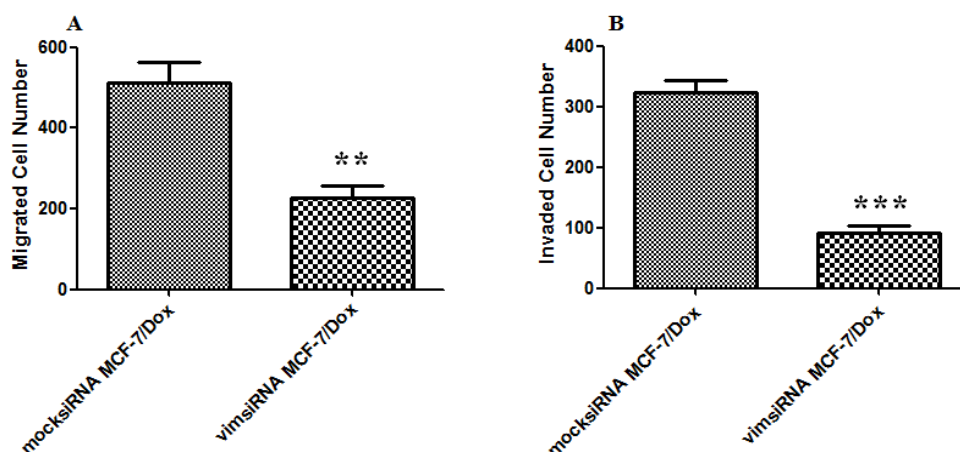


Figure 3.25 A. Migrated cell number of *VIM* siRNA transfected MCF-7/Dox cell line comparing to mock siRNA MCF-7/Dox cell line (control line) after Boyden Chamber Assay. B. Invaded cell number of *VIM* siRNA transfected MCF-7/Dox cell line comparing to mock siRNA MCF-7/Dox cell line (control line) after Matrigel Assay. ** $p < 0.05$ compared to migrated MCF-7/S cell number and *** $p < 0.05$ compared to invaded MCF-7/S cell number.

As a result, these findings shows that vimentin expression level has a role in cell motility and cell invasiveness of Doxorubicin resistant MCF-7 cell line. After transient silencing of this gene, the decline of metastasis and invasiveness has been indicated. It was clearly seen that the concentration of 5nM specific *VIM* siRNA treatment for 48 hours can be considered effective for determination of reduction of metastatic and invasive characteristics of MCF-7/Dox cell line.

CHAPTER 4

CONCLUSION

1. *VIM* expression in doxorubicin resistant MCF-7 cell line was higher with respect to the doxorubicin sensitive MCF-S cells and this result supported to the literature.
2. The amount of vimentin protein was also high in Doxorubicin resistant MCF-7 cell line and it was shown that as a vimentin-negative cell line MCF-7/S cells were lack of vimentin protein.
3. Successful uptake of Qiagen[®] oligo into the Doxorubicin resistant MCF-7 cell line demonstrated that 5 nM siRNA would be efficiently taken by the cells. Therefore, transfection with higher concentrations, which would possibly induce nonspecific in the cells, was not required for further experiments.
4. Around 90 – 94% reduction in *VIM* expression with the selected *VIM* siRNA duplex in MCF-7/Dox cell line shows its high efficiency for *VIM* inhibition even concentration of siRNA was low as 5 nM.
5. Down-regulation of *VIM* gene by transient siRNA transfection for 48 and 72 hours had an effect on reduction of vimentin protein. Although this reduction could be evaluated statistically not significant, it was enough to see the changes in metastatic and invasive characteristics of MCF-7/Dox cell line.
6. Silencing of vimentin encoding *VIM* gene led to decrease of metastatic behaviour of Doxorubicin resistant MCF-7 cell line up to a point.
7. Silencing of vimentin encoding *VIM* gene led to decrease of invasive behaviour of doxorubicin resistant MCF-7 cells up to a point.

Consequently, transient transfection with the selected siRNA duplex may be an efficient tool to decrease the metastatic and invasive phenotype of doxorubicin resistant MCF-7 cells and provide the decrease the rate of invasion of these cells to the other parts of the body and increase the success in chemotherapy by this way.

REFERENCES

- (2001) National Institutes of Health Consensus Development Conference statement: adjuvant therapy for breast cancer, November 1-3, 2000. *J Natl Cancer Inst Monogr* **5**: 5-15
- (2005) Effects of chemotherapy and hormonal therapy for early breast cancer on recurrence and 15-year survival: an overview of the randomised trials. *Lancet* **365**: 1687-1717
- Ambudkar SV, Dey S, Hrycyna CA, Ramachandra M, Pastan I, Gottesman MM (1999) Biochemical, cellular, and pharmacological aspects of the multidrug transporter. *Annu Rev Pharmacol Toxicol* **39**: 361-398
- Baba AI, Catoi C (2007) Principles of Anticancer Therapy. In *Comparative Oncology*, 2010/09/01 edn, 19. Romania: The Publishing House of the Romanian Academy
- Brummelkamp TR, Bernards R, Agami R (2002) Stable suppression of tumorigenicity by virus-mediated RNA interference. *Cancer Cell* **2**: 243-247
- Chiu YL, Rana TM (2003) siRNA function in RNAi: a chemical modification analysis. *RNA* **9**: 1034-1048
- Clementi ME, Giardina B, Di Stasio E, Mordente A, Misiti F (2003) Doxorubicin-derived metabolites induce release of cytochrome C and inhibition of respiration on cardiac isolated mitochondria. *Anticancer Res* **23**: 2445-2450
- Cochard P, Paulin D (1984) Initial expression of neurofilaments and vimentin in the central and peripheral nervous system of the mouse embryo in vivo. *J Neurosci* **4**: 2080-2094
- Cole SP, Bhardwaj G, Gerlach JH, Mackie JE, Grant CE, Almquist KC, Stewart AJ, Kurz EU, Duncan AM, Deeley RG (1992) Overexpression of a transporter gene in a multidrug-resistant human lung cancer cell line. *Science* **258**: 1650-1654
- Colucci-Guyon E, Portier MM, Dunia I, Paulin D, Pournin S, Babinet C (1994) Mice lacking vimentin develop and reproduce without an obvious phenotype. *Cell* **79**: 679-694
- Costa WF, Nepomuceno JC (2006) Protective effects of a mixture of antioxidant vitamins and minerals on the genotoxicity of doxorubicin in somatic cells of *Drosophila melanogaster*. *Environ Mol Mutagen* **47**: 18-24
- Cui W, Ning J, Naik UP, Duncan MK (2004) OptiRNAi, an RNAi design tool. *Comput Methods Programs Biomed* **75**: 67-73

De Craene B, van Roy F, Berx G (2005) Unraveling signalling cascades for the Snail family of transcription factors. *Cell Signal* **17**: 535-547

DeVita VT, Jr., Chu E (2008) A history of cancer chemotherapy. *Cancer Res* **68**: 8643-8653

Dillin A (2003) The specifics of small interfering RNA specificity. *Proc Natl Acad Sci U S A* **100**: 6289-6291

Domagala W, Lasota J, Bartkowiak J, Weber K, Osborn M (1990) Vimentin is preferentially expressed in human breast carcinomas with low estrogen receptor and high Ki-67 growth fraction. *Am J Pathol* **136**: 219-227

Durand RE, Olive PL (2001) Resistance of tumor cells to chemo- and radiotherapy modulated by the three-dimensional architecture of solid tumors and spheroids. *Methods Cell Biol* **64**: 211-233

Eckes B, Colucci-Guyon E, Smola H, Nodder S, Babinet C, Krieg T, Martin P (2000) Impaired wound healing in embryonic and adult mice lacking vimentin. *J Cell Sci* **113** (Pt 13): 2455-2462

Elbashir SM, Harborth J, Lendeckel W, Yalcin A, Weber K, Tuschl T (2001) Duplexes of 21-nucleotide RNAs mediate RNA interference in cultured mammalian cells. *Nature* **411**: 494-498

Elbashir SM, Harborth J, Weber K, Tuschl T (2002) Analysis of gene function in somatic mammalian cells using small interfering RNAs. *Methods* **26**: 199-213

Evans RM (1998) Vimentin: the conundrum of the intermediate filament gene family. *Bioessays* **20**: 79-86

Fedorov Y, Anderson EM, Birmingham A, Reynolds A, Karpilow J, Robinson K, Leake D, Marshall WS, Khvorova A (2006) Off-target effects by siRNA can induce toxic phenotype. *RNA* **12**: 1188-1196

Fidler IJ, Hart IR (1982) Recent observations on the pathogenesis of cancer metastasis. *Prog Clin Biol Res* **85 Pt B**: 601-619

Fire A, Xu S, Montgomery MK, Kostas SA, Driver SE, Mello CC (1998) Potent and specific genetic interference by double-stranded RNA in *Caenorhabditis elegans*. *Nature* **391**: 806-811

Fisher B, Anderson S, Bryant J, Margolese RG, Deutsch M, Fisher ER, Jeong JH, Wolmark N (2002) Twenty-year follow-up of a randomized trial comparing total mastectomy, lumpectomy, and lumpectomy plus irradiation for the treatment of invasive breast cancer. *N Engl J Med* **347**: 1233-1241

Freshney R (1987) *Culture of Animal Cells: A Manual of Basic Technique*, 1 edn. New York: Alan R. Liss, Inc.

Germann UA (1996) P-glycoprotein--a mediator of multidrug resistance in tumour cells. *Eur J Cancer* **32A**: 927-944

Gilles C, Polette M, Mestdagt M, Nawrocki-Raby B, Ruggeri P, Birembaut P, Foidart JM (2003) Transactivation of vimentin by beta-catenin in human breast cancer cells. *Cancer Res* **63**: 2658-2664

Gilles C, Polette M, Zahm JM, Tournier JM, Volders L, Foidart JM, Birembaut P (1999) Vimentin contributes to human mammary epithelial cell migration. *J Cell Sci* **112** (Pt **24**): 4615-4625

Gorre ME, Mohammed M, Ellwood K, Hsu N, Paquette R, Rao PN, Sawyers CL (2001) Clinical resistance to STI-571 cancer therapy caused by BCR-ABL gene mutation or amplification. *Science* **293**: 876-880

Gottesman MM, Fojo T, Bates SE (2002) Multidrug resistance in cancer: role of ATP-dependent transporters. *Nat Rev Cancer* **2**: 48-58

Gradishar W, Glusman J, Lu Y, Vogel C, Cohen FJ, Sledge GW, Jr. (2000) Effects of high dose raloxifene in selected patients with advanced breast carcinoma. *Cancer* **88**: 2047-2053

Hendrix MJ, Seftor EA, Seftor RE, Trevor KT (1997) Experimental co-expression of vimentin and keratin intermediate filaments in human breast cancer cells results in phenotypic interconversion and increased invasive behavior. *Am J Pathol* **150**: 483-495

<http://www.breastcancer.org>. (Last visited on 17.06.2012)

<http://www.breastcancer.org/treatment/hormonaltherapy/>. (Last visited on 17.06.2012)

<http://www.breastcancer.org/treatment/radiation>. (Last visited on 17.06.2012)

<http://www.breastcancer.org/treatment/surgery/>. (Last visited on 17.06.2012)

Hu L, Lau SH, Tzang CH, Wen JM, Wang W, Xie D, Huang M, Wang Y, Wu MC, Huang JF, Zeng WF, Sham JS, Yang M, Guan XY (2004) Association of Vimentin overexpression and hepatocellular carcinoma metastasis. *Oncogene* **23**: 298-302

Iseri OD, Kars MD, Arpacı F, Atalay C, Pak I, Gunduz U (2011) Drug resistant MCF-7 cells exhibit epithelial-mesenchymal transition gene expression pattern. *Biomed Pharmacother* **65**: 40-45

Iseri OD, Kars MD, Arpacı F, Gunduz U (2010) Gene expression analysis of drug-resistant MCF-7 cells: implications for relation to extracellular matrix proteins. *Cancer Chemother Pharmacol* **65**: 447-455

Ivaska J, Pallari HM, Nevo J, Eriksson JE (2007) Novel functions of vimentin in cell adhesion, migration, and signaling. *Exp Cell Res* **313**: 2050-2062

Ivaska J, Vuoriluoto K, Huovinen T, Izawa I, Inagaki M, Parker PJ (2005) PKCepsilon-mediated phosphorylation of vimentin controls integrin recycling and motility. *EMBO J* **24**: 3834-3845

Jackson AL, Bartz SR, Schelter J, Kobayashi SV, Burchard J, Mao M, Li B, Cavet G, Linsley PS (2003) Expression profiling reveals off-target gene regulation by RNAi. *Nat Biotechnol* **21**: 635-637

Jain RK (2001) Delivery of molecular and cellular medicine to solid tumors. *Adv Drug Deliv Rev* **46**: 149-168

Kang JH, Song KH, Jeong KC, Kim S, Choi C, Lee CH, Oh SH (2011) Involvement of Cox-2 in the metastatic potential of chemotherapy-resistant breast cancer cells. *BMC Cancer* **11**: 334

Kars MD, Iseri OD, Gunduz U, Ural AU, Arpaci F, Molnar J (2006) Development of rational in vitro models for drug resistance in breast cancer and modulation of MDR by selected compounds. *Anticancer Res* **26**: 4559-4568

Keizer HG, Pinedo HM, Schuurhuis GJ, Joenje H (1990) Doxorubicin (adriamycin): a critical review of free radical-dependent mechanisms of cytotoxicity. *Pharmacol Ther* **47**: 219-231

Kohn EC, Liotta LA (1995) Molecular insights into cancer invasion: strategies for prevention and intervention. *Cancer Res* **55**: 1856-1862

Korsching E, Packeisen J, Liedtke C, Hungermann D, Wulfing P, van Diest PJ, Brandt B, Boecker W, Buerger H (2005) The origin of vimentin expression in invasive breast cancer: epithelial-mesenchymal transition, myoepithelial histogenesis or histogenesis from progenitor cells with bilinear differentiation potential? *J Pathol* **206**: 451-457

Lage H (2005) Potential applications of RNA interference technology in the treatment of cancer. *Future Oncol* **1**: 103-113

Langa F, Kress C, Colucci-Guyon E, Khun H, Vandormael-Pournin S, Huerre M, Babinet C (2000) Teratocarcinomas induced by embryonic stem (ES) cells lacking vimentin: an approach to study the role of vimentin in tumorigenesis. *J Cell Sci* **113 Pt 19**: 3463-3472

Liotta LA (2004) Tumor invasion and metastasis: getting more basic to come closer to the patient. An interview with Lance A. Liotta. *Int J Dev Biol* **48**: 559-562

Livak KJ, Schmittgen TD (2001) Analysis of relative gene expression data using real-time quantitative PCR and the 2(-Delta Delta C(T)) Method. *Methods* **25**: 402-408

Longley DB, Johnston PG (2005) Molecular mechanisms of drug resistance. *J Pathol* **205**: 275-292

Mauri D, Pavlidis N, Ioannidis JP (2005) Neoadjuvant versus adjuvant systemic treatment in breast cancer: a meta-analysis. *J Natl Cancer Inst* **97**: 188-194

McInroy L, Maatta A (2007) Down-regulation of vimentin expression inhibits carcinoma cell migration and adhesion. *Biochem Biophys Res Commun* **360**: 109-114

Mendez MG, Kojima S, Goldman RD (2010) Vimentin induces changes in cell shape, motility, and adhesion during the epithelial to mesenchymal transition. *FASEB J* **24**: 1838-1851

Minotti G, Recalcati S, Menna P, Salvatorelli E, Corna G, Cairo G (2004) Doxorubicin cardiotoxicity and the control of iron metabolism: quinone-dependent and independent mechanisms. *Methods Enzymol* **378**: 340-361

Neve RM, Chin K, Fridlyand J, Yeh J, Baehner FL, Fevr T, Clark L, Bayani N, Coppe JP, Tong F, Speed T, Spellman PT, DeVries S, Lapuk A, Wang NJ, Kuo WL, Stilwell JL, Pinkel D, Albertson DG, Waldman FM, McCormick F, Dickson RB, Johnson MD, Lippman M, Ethier S, Gazdar A, Gray JW (2006) A collection of breast cancer cell lines for the study of functionally distinct cancer subtypes. *Cancer Cell* **10**: 515-527

Nicolay K, Sautereau AM, Tocanne JF, Brasseur R, Huart P, Ruysschaert JM, de Kruijff B (1988) A comparative model membrane study on structural effects of membrane-active positively charged anti-tumor drugs. *Biochim Biophys Acta* **940**: 197-208

Nieth C, Priebisch A, Stege A, Lage H (2003) Modulation of the classical multidrug resistance (MDR) phenotype by RNA interference (RNAi). *FEBS Lett* **545**: 144-150

Nijkamp MM, Span PN, Hoogsteen IJ, van der Kogel AJ, Kaanders JH, Bussink J (2011) Expression of E-cadherin and vimentin correlates with metastasis formation in head and neck squamous cell carcinoma patients. *Radiother Oncol* **99**: 344-348

Oakman C, Moretti E, Galardi F, Santarpia L, Di Leo A (2009) The role of topoisomerase IIalpha and HER-2 in predicting sensitivity to anthracyclines in breast cancer patients. *Cancer Treat Rev* **35**: 662-667

Paccione RJ, Miyazaki H, Patel V, Waseem A, Gutkind JS, Zehner ZE, Yeudall WA (2008) Keratin down-regulation in vimentin-positive cancer cells is reversible by vimentin RNA interference, which inhibits growth and motility. *Mol Cancer Ther* **7**: 2894-2903

Pai SI, Lin YY, Macaes B, Meneshian A, Hung CF, Wu TC (2006) Prospects of RNA interference therapy for cancer. *Gene Ther* **13**: 464-477

Pajeva I, Todorov DK, Seydel J (2004) Membrane effects of the antitumor drugs doxorubicin and thaliblastine: comparison to multidrug resistance modulators verapamil and trans-flupentixol. *Eur J Pharm Sci* **21**: 243-250

Pan TL, Wang PW, Huang CC, Yeh CT, Hu TH, Yu JS (2012a) Network analysis and proteomic identification of vimentin as a key regulator associated with invasion and metastasis in human hepatocellular carcinoma cells. *J Proteomics* **75**: 4676-4692

Pan Y, Zhong LJ, Zhou H, Wang X, Chen K, Yang HP, Xiaokaiti Y, Maimaiti A, Jiang L, Li XJ (2012b) Roles of vimentin and 14-3-3 zeta/delta in the inhibitory effects of heparin on PC-3M cell proliferation and B16-F10-luc-G5 cells metastasis. *Acta Pharmacol Sin* **33**: 798-808

Paul CP, Good PD, Winer I, Engelke DR (2002) Effective expression of small interfering RNA in human cells. *Nat Biotechnol* **20**: 505-508

Paul R, Cowan KH (1999) Drug resistance in breast cancer. In *Breast Cancer Molecular Genetics, Pathogenesis and Therapeutics*, Bowcock (ed), pp 481-517. Totowa: Humana Press

Persengiev SP, Zhu X, Green MR (2004) Nonspecific, concentration-dependent stimulation and repression of mammalian gene expression by small interfering RNAs (siRNAs). *RNA* **10**: 12-18

Pluen A, Boucher Y, Ramanujan S, McKee TD, Gohongi T, di Tomaso E, Brown EB, Izumi Y, Campbell RB, Berk DA, Jain RK (2001) Role of tumor-host interactions in interstitial diffusion of macromolecules: cranial vs. subcutaneous tumors. *Proc Natl Acad Sci U S A* **98**: 4628-4633

Rieger PT (2004) The biology of cancer genetics. *Semin Oncol Nurs* **20**: 145-154

Ross JS, Fletcher JA, Bloom KJ, Linette GP, Stec J, Symmans WF, Pusztai L, Hortobagyi GN (2004) Targeted therapy in breast cancer: the HER-2/neu gene and protein. *Mol Cell Proteomics* **3**: 379-398

Sarrio D, Rodriguez-Pinilla SM, Hardisson D, Cano A, Moreno-Bueno G, Palacios J (2008) Epithelial-mesenchymal transition in breast cancer relates to the basal-like phenotype. *Cancer Res* **68**: 989-997

Satelli A, Li S (2011) Vimentin in cancer and its potential as a molecular target for cancer therapy. *Cell Mol Life Sci* **68**: 3033-3046

Schuetz EG, Schinkel AH, Relling MV, Schuetz JD (1996) P-glycoprotein: a major determinant of rifampicin-inducible expression of cytochrome P4503A in mice and humans. *Proc Natl Acad Sci U S A* **93**: 4001-4005

Semizarov D, Frost L, Sarthy A, Kroeger P, Halbert DN, Fesik SW (2003) Specificity of short interfering RNA determined through gene expression signatures. *Proc Natl Acad Sci U S A* **100**: 6347-6352

Shankar P, Manjunath N, Lieberman J (2005) The prospect of silencing disease using RNA interference. *JAMA* **293**: 1367-1373

Shen DW, Goldenberg S, Pastan I, Gottesman MM (2000) Decreased accumulation of [14C]carboplatin in human cisplatin-resistant cells results from reduced energy-dependent uptake. *J Cell Physiol* **183**: 108-116

Shen F, Chu S, Bence AK, Bailey B, Xue X, Erickson PA, Montrose MH, Beck WT, Erickson LC (2008) Quantitation of doxorubicin uptake, efflux, and modulation of multidrug resistance (MDR) in MDR human cancer cells. *J Pharmacol Exp Ther* **324**: 95-102

Shen J, Valero V, Buchholz TA, Singletary SE, Ames FC, Ross MI, Cristofanilli M, Babiera GV, Meric-Bernstam F, Feig B, Hunt KK, Kuerer HM (2004) Effective local control and long-term survival in patients with T4 locally advanced breast cancer treated with breast conservation therapy. *Ann Surg Oncol* **11**: 854-860

Shtivelman E (1997) A link between metastasis and resistance to apoptosis of variant small cell lung carcinoma. *Oncogene* **14**: 2167-2173

Singhal SS, Singhal J, Sharma R, Singh SV, Zimniak P, Awasthi YC, Awasthi S (2003) Role of RLIP76 in lung cancer doxorubicin resistance: I. The ATPase activity of RLIP76 correlates with doxorubicin and 4-hydroxynonenal resistance in lung cancer cells. *Int J Oncol* **22**: 365-375

Sledz CA, Holko M, de Veer MJ, Silverman RH, Williams BR (2003) Activation of the interferon system by short-interfering RNAs. *Nat Cell Biol* **5**: 834-839

Sнове O, Jr., Holen T (2004) Many commonly used siRNAs risk off-target activity. *Biochem Biophys Res Commun* **319**: 256-263

Sнове O, Jr., Nedland M, Fjeldstad SH, Humberstet H, Birkeland OR, Grunfeld T, Saetrom P (2004) Designing effective siRNAs with off-target control. *Biochem Biophys Res Commun* **325**: 769-773

Sommers CL, Heckford SE, Skerker JM, Worland P, Torri JA, Thompson EW, Byers SW, Gelmann EP (1992) Loss of epithelial markers and acquisition of vimentin expression in adriamycin- and vinblastine-resistant human breast cancer cell lines. *Cancer Res* **52**: 5190-5197

Speelmans G, Staffhorst RW, de Kruijff B, de Wolf FA (1994) Transport studies of doxorubicin in model membranes indicate a difference in passive diffusion across and binding at the outer and inner leaflets of the plasma membrane. *Biochemistry* **33**: 13761-13768

Swain SM, Whaley FS, Gerber MC, Ewer MS, Bianchini JR, Gams RA (1997) Delayed administration of dexrazoxane provides cardioprotection for patients with advanced breast cancer treated with doxorubicin-containing therapy. *J Clin Oncol* **15**: 1333-1340

Swift LP, Rephaeli A, Nudelman A, Phillips DR, Cutts SM (2006) Doxorubicin-DNA adducts induce a non-topoisomerase II-mediated form of cell death. *Cancer Res* **66**: 4863-4871

Takeshita F, Ochiya T (2006) Therapeutic potential of RNA interference against cancer. *Cancer Sci* **97**: 689-696

Thiery JP (2002) Epithelial-mesenchymal transitions in tumour progression. *Nat Rev Cancer* **2**: 442-454

Thompson EW, Newgreen DF, Tarin D (2005) Carcinoma invasion and metastasis: a role for epithelial-mesenchymal transition? *Cancer Res* **65**: 5991-5995; discussion 5995

Thorn CF, Oshiro C, Marsh S, Hernandez-Boussard T, McLeod H, Klein TE, Altman RB (2011) Doxorubicin pathways: pharmacodynamics and adverse effects. *Pharmacogenet Genomics* **21**: 440-446

Toetsch S, Olwell P, Prina-Mello A, Volkov Y (2009) The evolution of chemotaxis assays from static models to physiologically relevant platforms. *Integr Biol (Camb)* **1**: 170-181

Triton TR, Yee G (1982) The anticancer agent adriamycin can be actively cytotoxic without entering cells. *Science* **217**: 248-250

Valque H, Gouyer V, Gottrand F, Desseyn JL (2012) MUC5B leads to aggressive behavior of breast cancer MCF7 cells. *PLoS One* **7**: e46699

Vuoriluoto K, Haugen H, Kiviluoto S, Mpindi JP, Nevo J, Gjerdrum C, Tiron C, Lorens JB, Ivaska J (2011) Vimentin regulates EMT induction by Slug and oncogenic H-Ras and migration by governing Axl expression in breast cancer. *Oncogene* **30**: 1436-1448

Wallace KB (2007) Adriamycin-induced interference with cardiac mitochondrial calcium homeostasis. *Cardiovasc Toxicol* **7**: 101-107

Wang S, Konorev EA, Kotamraju S, Joseph J, Kalivendi S, Kalyanaraman B (2004) Doxorubicin induces apoptosis in normal and tumor cells via distinctly different mechanisms. intermediacy of H(2)O(2)- and p53-dependent pathways. *J Biol Chem* **279**: 25535-25543

Wei J, Xu G, Wu M, Zhang Y, Li Q, Liu P, Zhu T, Song A, Zhao L, Han Z, Chen G, Wang S, Meng L, Zhou J, Lu Y, Ma D (2008) Overexpression of vimentin contributes to prostate cancer invasion and metastasis via src regulation. *Anticancer Res* **28**: 327-334

WHO Report. (2006). World Health Organization.

Wojnowski L, Kulle B, Schirmer M, Schluter G, Schmidt A, Rosenberger A, Vonhof S, Bickeboller H, Toliat MR, Suk EK, Tzvetkov M, Kruger A, Seifert S, Kloess M, Hahn H, Loeffler M, Nurnberg P, Pfreundschuh M, Trumper L, Brockmoller J, Hasenfuss G (2005) NAD(P)H oxidase and multidrug resistance protein genetic polymorphisms are associated with doxorubicin-induced cardiotoxicity. *Circulation* **112**: 3754-3762

Yao L, Zhang Y, Chen K, Hu X, Xu LX (2011) Discovery of IL-18 as a novel secreted protein contributing to doxorubicin resistance by comparative secretome analysis of MCF-7 and MCF-7/Dox. *PLoS One* **6**: e24684

Zhao Y, Yan Q, Long X, Chen X, Wang Y (2008) Vimentin affects the mobility and invasiveness of prostate cancer cells. *Cell Biochem Funct* **26**: 571-577

APPENDIX A

CELL CULTURE MEDIUM

Table A. 1 RPMI 1640 Medium formulation (in mg/L) (Thermo Scientific HyCLone).

NaCl	6000	L-methionine	15
KCl	400	L-phenylalanine	15
Na ₂ HPO ₄	1512	L-proline	20
MgSO ₄ .7H ₂ O	100	L-serine	30
Ca(NO ₃) ₂ .4H ₂ O	100	L-threonine	20
D-glucose	2000	L-tryptophane	5
Phenol red	5	L-tyrosine	20
NaHCO ₃	2000	L-valine	20
L-arginine	200	Glutathione	1
L-asparagine	50	Biotine	0.2
L-aspartic acid	20	Vitamin B12	0.005
L-cystine	50	D-Ca-pantothenate	0.025
L-glutamine	300	Choline chloride	3
L-glutamic acid	20	Folic acid	1
Glycine	10	Myo-inositol	35
L-histidine	15	Nicotinamide	1
L-hydroxyproline	20	p-amino-benzoic-acid	1
L-isoleucine	50	Pyridoxin.HCl	1
L-leucine	50	Riboflavin	0.2
L-lysine. HCl	40	Thiamine.HCl	1

APPENDIX B

BUFFERS AND SOLUTIONS

- Diethylpyrocarbonate (DEPC) treated dH₂O (1L):
1mL DEPC was added to 1 L dH₂O and mixed well. After overnight incubation, autoclavation was performed.
- 50X Tris-acetate-EDTA (TAE) buffer (1L):
Tris base (MW: 121.14) 242 g
Acetic Acid 57.1 mL
0.5 M EDTA disodium dihydrate (MW: 372.24) 100mL
Volume was completed to 1 L with dH₂O and pH was adjusted to 8.5. After autoclavation, solution was diluted to 1X with dH₂O.
- Ethidium bromide (EtBr) solution:
10 mg EtBr was dissolved in 1 mL dH₂O and stored in dark.
- 2 % (w/v) paraformaldehyde
2 g paraformaldehyde was added to 10 mL phosphate buffered saline (PBS) and heated at 70 °C until the color turns to transplant.
- 6X DNA Loading Dye (Fermentas)
10 mM Tris-HCl (pH 7.6) 0.03% bromophenol blue
0.03% xylene cyanol FF 60% glycerol
60mM EDTA

APPENDIX C

TRESHOLD CYCLE VALUES

Table C. 1 Threshold cycle values (C_T) of qPCR

	<i>VIM</i>	<i>β-actin</i>
No Treatment MCF-7/S	22.63	8.54
	21.62	8.56
	22.50	8.52
No Treatment MCF-7/Dox	13.39	7.96
	12.68	7.91
	12.72	7.96
Mock siRNA/48h	13.83	6.77
	13.88	6.78
	13.75	7.86
<i>VIM</i> siRNA/48h	17.05	6.63
	17.36	6.15
	16.86	6.61
Mock siRNA/72h	13.37	6.13
	13.30	6.18
	13.76	6.75
<i>VIM</i> siRNA/72h	16.63	6.26
	17.63	6.73
	16.77	6.74
	<i>VIM</i>	<i>β-actin</i>
No Treatment MCF-7/S	23.01	8.68
	22.86	8.54
	22.56	7.96
No Treatment MCF-7/Dox	12.89	7.81
	12.76	7.66
	11.92	7.13
Mock siRNA/48h	13.46	6.78
	13.86	6.54
	12.87	6.42
<i>VIM</i> siRNA/48h	18.09	7.12
	17.86	6.89
	17.65	6.44
Mock siRNA/72h	13.46	7.12
	13.87	6.74
	12.57	6.45
<i>VIM</i> siRNA/72h	16.88	6.32
	17.68	6.42
	17.89	6.77
	<i>VIM</i>	<i>β-actin</i>
No Treatment MCF-7/S	23.32	8.48
	22.64	8.03
	22.12	8.12
No Treatment MCF-7/Dox	13.01	7.19
	12.76	6.98
	11.98	7.13
Mock siRNA/48h	13.33	6.64
	13.88	6.44
	12.96	6.12
<i>VIM</i> siRNA/48h	17.46	7.24
	17.93	6.91
	17.44	7.02
Mock siRNA/72h	13.22	7.06
	13.98	6.46
	12.42	6.13
<i>VIM</i> siRNA/72h	17.44	6.31
	17.66	6.86
	17.46	7.14

APPENDIX D

MIGRATED AND INVADED CELL NUMBERS

Table D. 1 Number of migrated and invaded cell.

	Number of Migrated Cell	Number of Invaded Cell
No Treatment MCF-7/S	246	14
	202	26
	146	11
No Treatment MCF-7/Dox	1008	864
	1312	936
	912	748
Mock siRNA Treated MCF-7/Dox	504	328
	428	286
	602	357
VIM siRNA Treated MCF-7/Dox	192	82
	203	78
	286	116

APPENDIX E

FLOW CYTOMETRY HISTOGRAM GRAPHS

In order to visualize the control siRNA uptake values, following tables were prepared.

Tube: 1 CELL KONTROL			
Population	#Events	%Parent	%Total
■ All Events	15,225	###	100.0
■ P1	12,693	83.4	83.4
☒ P2	11	0.1	0.1
☒ Q1	34	0.3	0.2
☒ Q2	0	0.0	0.0
☒ Q3	12,659	99.7	83.1
☒ Q4	0	0.0	0.0
☒ Q1-1	27	0.2	0.2
☒ Q2-1	0	0.0	0.0
☒ Q3-1	12,666	99.8	83.2
☒ Q4-1	0	0.0	0.0
☒ P3	27	0.2	0.2

Figure E. 1 Flow cytometry analysis according to the gated area showing untransfected cell control results.

Tube: 1 NM			
Population	#Events	%Parent	%Total
■ All Events	10,000	###	100.0
■ P1	8,968	89.7	89.7
☒ Q1	215	2.4	2.2
☒ Q2	0	0.0	0.0
☒ Q3	8,753	97.6	87.5
☒ Q4	0	0.0	0.0
☒ Q1-1	606	6.8	6.1
☒ Q2-1	0	0.0	0.0
☒ Q3-1	8,362	93.2	83.6
☒ Q4-1	0	0.0	0.0
☒ P2	23	0.3	0.2
☒ P3	618	6.9	6.2

Figure E. 2 Flow cytometry analysis according to the gated area showing 1 nM fluorescein conjugated control siRNA transfected cell control results.

Tube: 3 NM

Population	#Events	%Parent	%Total
■ All Events	10,000	####	100.0
■ P1	9,193	91.9	91.9
☒ Q1-1	4,026	43.8	40.3
☒ Q2-1	0	0.0	0.0
☒ Q3-1	5,167	56.2	51.7
☒ Q4-1	0	0.0	0.0
☒ P3	4,090	44.5	40.9
☒ Q1	3,107	33.8	31.1
☒ Q2	0	0.0	0.0
☒ Q3	6,086	66.2	60.9
☒ Q4	0	0.0	0.0
☒ P2	1,379	15.0	13.8

Figure E. 3 Flow cytometry analysis according to the gated area showing 3 nM fluorescein conjugated control siRNA transfected cell control results.

Tube: 5 NM

Population	#Events	%Parent	%Total
■ All Events	10,000	####	100.0
■ P1	8,744	87.4	87.4
☒ Q1-1	5,127	58.6	51.3
☒ Q2-1	0	0.0	0.0
☒ Q3-1	3,617	41.4	36.2
☒ Q4-1	0	0.0	0.0
☒ P3	5,186	59.3	51.9
☒ Q1	4,411	50.4	44.1
☒ Q2	0	0.0	0.0
☒ Q3	4,333	49.6	43.3
☒ Q4	0	0.0	0.0
☒ P2	2,868	32.8	28.7

Figure E. 4 Flow cytometry analysis according to the gated area showing 5 nM fluorescein conjugated control siRNA transfected cell control results.

Tube: 8 NM			
Population	#Events	%Parent	%Total
■ All Events	10,000	###	100.0
■ P1	8,707	87.1	87.1
☒ P3	6,788	78.0	67.9
☒ Q1-1	6,760	77.6	67.6
☒ Q2-1	0	0.0	0.0
☒ Q3-1	1,947	22.4	19.5
☒ Q4-1	0	0.0	0.0
☒ Q1	6,391	73.4	63.9
☒ Q2	0	0.0	0.0
☒ Q3	2,316	26.6	23.2
☒ Q4	0	0.0	0.0
☒ P2	5,121	58.8	51.2

Figure E. 5 Flow cytometry analysis according to the gated area showing 8 nM fluorescein conjugated control siRNA transfected cell control results.

Tube: 10 NM			
Population	#Events	%Parent	%Total
■ All Events	10,000	###	100.0
■ P1	8,829	88.3	88.3
☒ Q1-1	6,696	75.8	67.0
☒ Q2-1	0	0.0	0.0
☒ Q3-1	2,133	24.2	21.3
☒ Q4-1	0	0.0	0.0
☒ P3	6,735	76.3	67.4
☒ Q1	6,328	71.7	63.3
☒ Q2	0	0.0	0.0
☒ Q3	2,501	28.3	25.0
☒ Q4	0	0.0	0.0
☒ P2	5,158	58.4	51.6

Figure E. 6 Flow cytometry analysis according to the gated area showing 10 nM fluorescein conjugated control siRNA transfected cell control results.

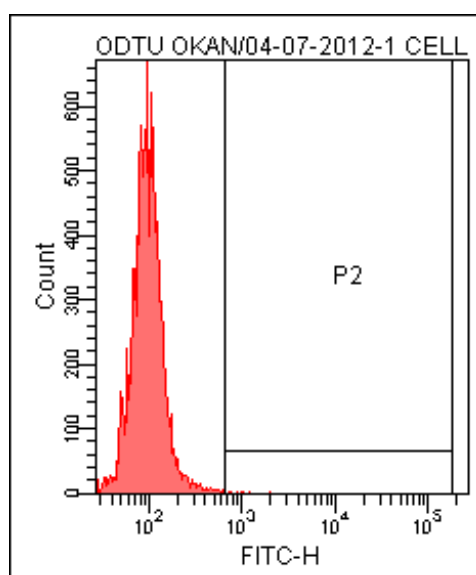


Figure E. 7 Flow cytometry analysis according to the gated area showing the FITC-H versus Cell Count histogram graph for untransfected cell control.

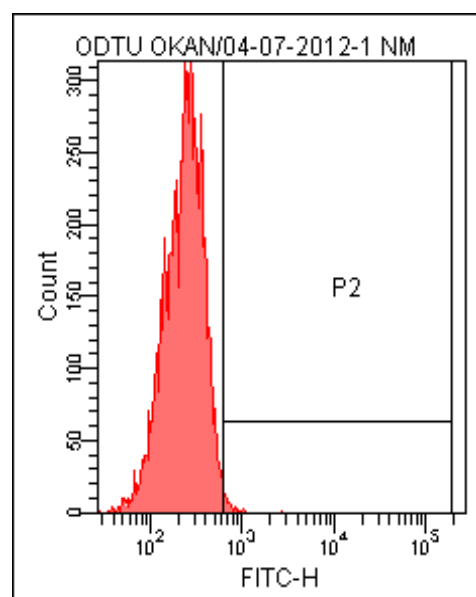


Figure E. 8 Flow cytometry analysis according to the gated area showing the FITC-H versus Cell Count histogram graph for 1 nM fluorescein conjugated control siRNA transfected cell results.

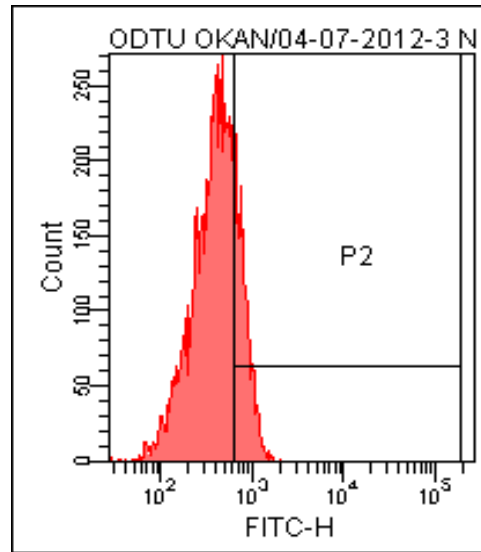


Figure E. 9 Flow cytometry analysis according to the gated area showing the FITC-H versus Cell Count histogram graph for 3 nM fluorescein conjugated control siRNA transfected cell results.

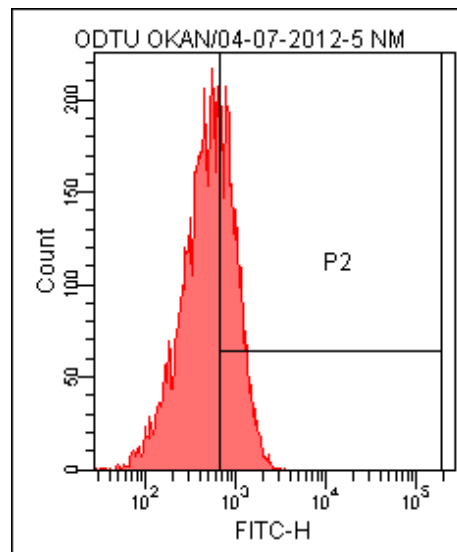


Figure E. 10 Flow cytometry analysis according to the gated area showing the FITC-H versus Cell Count histogram graph for 5 nM fluorescein conjugated control siRNA transfected cell results.

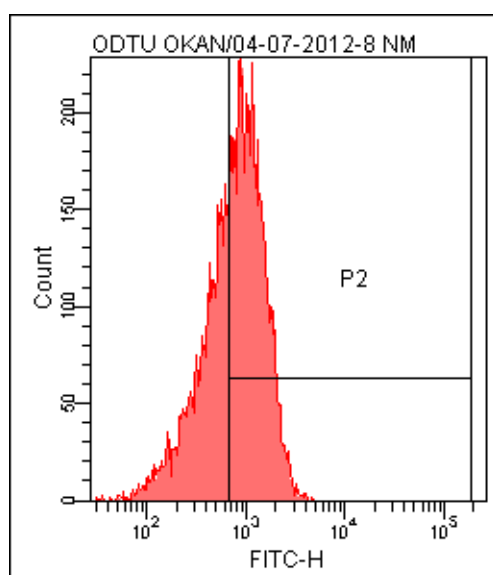


Figure E. 11 Flow cytometry analysis according to the gated area showing the FITC-H versus Cell Count histogram graph for 8 nM fluorescein conjugated control siRNA transfected cell results.

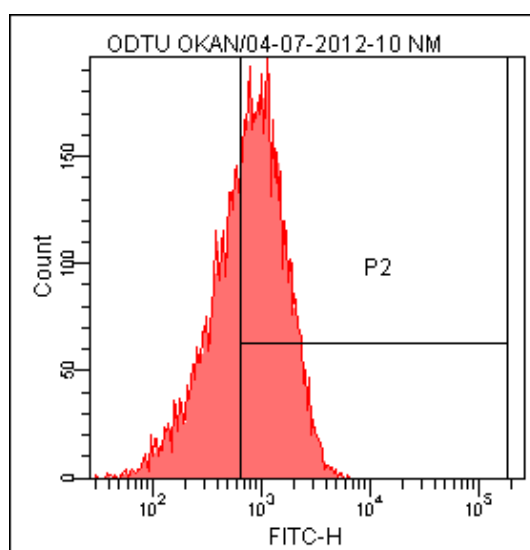


Figure E. 12 Flow cytometry analysis according to the gated area showing the FITC-H versus Cell Count histogram graph for 10 nM fluorescein conjugated control siRNA transfected cell results.